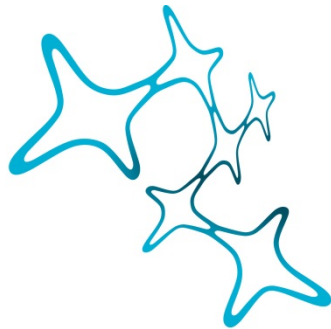


*IN VIVO* ANALYSIS OF DEMYELINATION  
AND REMYELINATION IN AN ANIMAL  
MODEL OF MULTIPLE SCLEROSIS

Aleksandra Barbara Meżydło



Graduate School of  
Systemic Neurosciences

LMU Munich



Dissertation at the  
Graduate School of Systemic Neurosciences  
Ludwig-Maximilians-Universität München

03.02.2020

Supervisor

Prof. Dr. Martin Kerschensteiner  
Institute of Clinical Neuroimmunology  
University Hospital and Biomedical Center of the  
Ludwig-Maximilians Universität München

First Reviewer: Prof. Dr. Martin Kerschensteiner

Second Reviewer: Prof. Dr. Thomas Misgeld

External Reviewer: Prof. Dr. med. Tanja Kuhlmann

Date of Submission: 03.02.2020

Date of Defense: 18.06.2020

To A. and M.  
*See you one day!*

*“Nothing in life is to be feared, it is only to be understood.  
Now is the time to understand more, so that we may fear less”*

Maria Skłodowska-Curie



## **Table of Contents**

<b>List of Abbreviations .....</b>	<b>9</b>
<b>Abstract.....</b>	<b>11</b>
<b>Zusammenfassung.....</b>	<b>13</b>
<b>Chapter I - Introduction.....</b>	<b>15</b>
1. Multiple Sclerosis .....	15
1.1. Epidemiology and etiology of MS.....	15
1.2. Pathology and pathophysiology of MS.....	16
1.2.1. White matter pathology .....	17
1.2.2. Grey matter pathology.....	19
1.3. Diagnostics and clinical course .....	21
1.4. Available treatment .....	23
1.5. Animal models of demyelination and remyelination.....	24
1.5.1. Experimental autoimmune encephalomyelitis .....	24
1.5.2. Cortical MS models .....	26
1.5.3. Toxin-induced lesions.....	26
2. Oligodendrocytes and Myelin in the Central Nervous System.....	27
2.1. Oligodendrocytes and myelin physiology.....	28
2.1.1. Oligodendrocyte lineage and development.....	28
2.1.2. Myelination and myelin structure.....	30
2.1.3. Myelin plasticity and remodeling.....	32
2.2. Oligodendrocytes pathology and demyelination.....	33
2.3. Oligodendrocytes recovery and remyelination.....	35
2.3.1. OPC-mediated remyelination .....	36
2.3.2. Involvement of pre-existing OLs.....	38
2.3.3. Remyelination failure and new trends in MS therapy.....	39
3. <i>In vivo</i> acute and chronic imaging of the oligodendrocytes and myelin .....	40
3.1. Two-photon excitation microscopy.....	40
3.2. Dynamic visualization of oligodendrocyte and myelin .....	41
<b>Chapter II – Aim of the study.....</b>	<b>45</b>
<b>Chapter III – Material and Methods .....</b>	<b>47</b>
1. Materials.....	47
1.1. Surgery procedures.....	47
1.2. Systemic and cortical EAE induction .....	49
1.3. Perfusion and immunohistochemistry.....	49
1.4. Viral labelling strategy .....	51
1.5. Electron microscopy .....	53
1.6. Imaging.....	54
1.7. Software.....	54
2. Experimental Animals .....	55
3. Methods .....	55
3.1. EAE induction .....	55
3.2. Cortical EAE induction.....	56

3.3. Immunofluorescence .....	56
3.4. Confocal microscopy .....	57
3.5. AAV vector generation and virus production .....	58
3.6. Single-cell labelling in the spinal cord .....	58
3.7. Ethidium bromide model .....	59
3.8. Single-cell labelling in the cortex .....	59
3.9. Cranial window surgery .....	60
3.10. <i>In vivo</i> 2PM imaging .....	60
3.10.1. Spinal cord .....	60
3.10.2. Cortex .....	61
3.11. Correlative light-to-electron microscopy .....	61
3.12. Image processing and analysis .....	62
3.13. Statistical analysis .....	64
<b>Chapter IV – Results .....</b>	<b>65</b>
1. Demyelination in the white matter of the spinal cord .....	65
1.1. Centripetal pattern of demyelination in EAE lesions .....	65
1.2. Centrifugal pattern of demyelination in EB-induced lesions .....	67
1.3. <i>In vivo</i> progression of oligodendrocyte damage in EAE .....	69
2. De- and remyelination in the cortical grey matter .....	70
2.1. Targeted MS model of cortical demyelination (c-MS) .....	71
2.2. Demyelination pattern and remyelination capacity in the cortical MS model .....	72
2.3. Characterization of the oligodendrocyte population in the cortical MS model .....	74
2.4. <i>In vivo</i> time-lapse imaging of oligodendrocyte turnover in cortical MS model .....	78
2.5. Compact myelin in remyelinated cortical lesion .....	80
2.6. <i>In vivo</i> imaging of mature, pre-existing oligodendrocytes in the cortical MS model .....	83
2.7. New approaches for spatiotemporal oligodendrocyte labelling .....	92
<b>Chapter V – Discussion .....</b>	<b>94</b>
1. Demyelination pattern and oligodendrocyte loss in the MS-like lesions .....	94
2. MS model of targeted cortical demyelination .....	97
3. Demyelination pattern and remyelination capacity in the cortical lesion .....	98
4. Myelin compaction in remyelinated cortical lesions .....	100
5. Chronic longitudinal imaging of the pre-existing oligodendrocytes in the cortical lesion .....	101
5. Concluding remarks .....	104
<b>Chapter VI – References .....</b>	<b>106</b>
<b>Acknowledgments .....</b>	<b>129</b>

## List of Abbreviations

2PEM	Two-Photon Excitation Microscopy (2PM)
AAV	Adeno-Associated Virus
Ab	Antibody
aCSF	Artificial Cerebrospinal Fluid
aOPC	Adult Oligodendrocyte Precursor Cell
APC	Antigen Presenting Cell
BBB	Blood-Brain Barrier
BSA	Bovine Albumin Serum
cEAE	Cortical Experimental Autoimmune Encephalomyelitis
CFA	Complete Freund's Adjuvant
CIS	Clinically Isolated Syndrome
CMC	Case Myelin Compound
c-MS	Cortical Multiple Sclerosis
CNP1	2', 3''-Cyclic-Nucleotide 3'-Phosphodiesterase
CNS	Central Nervous System
CSF	Cerebrospinal Fluid
DC	Dendritic Cell
DMEM	Dulbecco's Modified Eagle Medium
DMT	Disease-Modifying Treatment
DTA	Diphtheria Toxin A fragment
EAE	Experimental Autoimmune Encephalomyelitis
EB	Ethidium Bromide
EBV	Epstein - Barr virus
EM	Electron Microscopy
EMA	European Medicines Agency
EMS	Osmium tetroxide
ERK 1/2	Extracellular signal-Regulated Kinases 1 and 2
FBS	Fetal Bovine Serum
FDA	Food and Drug Administration (US)
GA	Glatiramer Acetate
GalC	Galactosylcerebroside
GC	Galactocerebroside
GM	Grey Matter
GWAS	Genome-wide Association Study
HBSS	Hank's Balanced Salt Solution
HLA	Human Leukocyte Antigen
IFN- $\beta$	Interferon- $\beta$
IFN- $\gamma$	Interferon- $\gamma$
IGF-1	Insulin-like Growth Factor 1
LFB	Luxol Fast Blue

LGE	Lateral Ganglionic Eminence
LPC	Lysolecithin
mAChR	Muscarinic Acetylcholine Receptor
MAG	Myelin-associated Glycoprotein
MAPK	Mitogen-Activated Protein Kinase
MBP	Myelin Basic Protein
MGE	Medial Ganglionic Eminence
MHC II	Major Histocompatibility Complex II
MOG	Myelin Oligodendrocyte Glycoprotein
MRI	Magnetic Resonance Imaging
MS	Multiple Sclerosis
NAGM	Normal-appearing Grey Matter
NAWM	Normal-appearing White Matter
NF155/186	Neurofascin 155/186
NIRB	Near-infrared Branding
NMO	Neuromyelitis Optica
OL	Oligodendrocyte
OPC	Oligodendrocyte Precursor Cell
PBS	Phosphate Buffered Saline
PDGF $\alpha$ R	Platelet-Derived Growth Factor- $\alpha$ Receptor
PEG	Polyethylene glycol
PEI	Polyethylenimine
PFA	Paraformaldehyde
PLP	Myelin Proteolipid Protein
PNS	Peripheral Nervous System
PPMS	Primary Progressive Multiple Sclerosis
PUMA	p53 Upregulated Modulator of Apoptosis
RIS	Radiologically Isolated Syndrome
RRMS	Relapsing-Remitting Multiple Sclerosis
SCoRe	Spectral Confocal Reflectance microscopy
SPMS	Secondary Progressive Multiple Sclerosis
SVZ	Subventricular Zone
T/B reg	Lymphocyte T/B regulatory
TFEB	Transcription Factor EB
Th	Lymphocyte T helper
TM	Tamoxifen
TNF- $\alpha$	Tumor Necrosis Factor- $\alpha$
VZ	Ventricular Zone
WHO	World Health Organization
WM	White Matter
XFP	'X' Fluorescent Protein

## Abstract

Multiple Sclerosis (MS) is a chronic, neuroinflammatory disease of the central nervous system (CNS) commonly diagnosed in young adults. Underlying histopathology, driven by activation and infiltration of immune cells, includes demyelinating lesions in white and grey matter of the CNS. Such widespread tissue damage results in not only different clinical phenotypes but also presents challenges for the efficient treatment.

Oligodendrocytes (OLs), the myelinating cells of the CNS, are believed to be the main target of the inflammatory reaction. However, the resulting demyelination can, at least to some extent, be restored by remyelination. The cellular processes that mediate myelin restoration in MS patients are still incompletely understood. The classical concept stipulates that remyelination is achieved by proliferation, differentiation and integration of OL precursors. Recent findings now challenge this concept and raise the question whether pre-existing, mature oligodendrocytes, which had survived the initial immune attack, might contribute to remyelination as well. My PhD project focused on understanding how OL damage spreads and determining the long-term fate of surviving OLs during the course of the disease. To address these questions, I applied confocal microscopy, intravital viral labeling as well as multiphoton *in vivo* imaging combined with ultrastructural electron microscopy analysis.

The first part of my study was focused on demyelination in the white matter of the spinal cord, induced in BiozziABH mice by MOG immunization. This strain, characterized by strong antibody response, develops a relapsing-remitting disease course, making it well suited to investigate OL and myelin damage and recovery. In this model, I contributed to the characterization of the cellular sequence of demyelinating events and OL morphology during the peak of the disease. My findings suggest that white matter oligodendrocytes can survive over longer periods in an *amputated* state characterized by extensive loss of their processes. This observation raised the question whether these affected cells may be able to undergo a healing process.

Therefore, my second part of the project aimed to understand myelin sheaths restoration. For this purpose, I used a new model of cortical MS pathology, induced in BiozziABH mice by combination of MOG immunization and intracerebral cytokines injection. I investigated the sequence of events during de- and

remyelination and imaged the same OLs over time - before cortical lesion, during the immune attack and in the recovery phase. Results demonstrate that *i*) OL damage follows a similar pattern in grey and white matter; *ii*) myelin sheaths are restored with high efficiency in grey matter lesions in young adult but not in aged mice and *iii*) pre-existing oligodendrocytes might contribute to remyelination since they are able to extend new primary processes. All of above expands current concepts of remyelination strategies and raises the possibilities for novel MS regenerative therapies, which specifically target mature OL.

## Zusammenfassung

Die Multiple Sklerose (MS) ist eine chronische neuroinflammatorische Erkrankung des zentralen Nervensystems (ZNS), die häufig bei jungen Erwachsenen diagnostiziert wird. Die zugrundeliegende Histopathologie, die durch die Aktivierung und Infiltration von Immunzellen bedingt ist, umfasst demyelinisierende Läsionen der weißen und grauen Substanz des ZNS. Die Gewebeschäden führen nicht nur zu unterschiedlichen klinischen Phänotypen, sondern stellen auch eine Herausforderung für die effiziente Behandlung dar.

Es wird angenommen, dass Oligodendrozyten (OLs), die myelinisierenden Zellen des ZNS, das Hauptziel der Entzündungsreaktion sind. Die resultierende Demyelinisierung kann jedoch zumindest teilweise durch Remyelinisierung wiederhergestellt werden. Nach dem klassischen Konzept erfolgt die Remyelinisierung durch die Proliferation, Differenzierung und Integration von OL-Vorläufern. Neuere Untersuchungen legen jetzt jedoch die Vermutung nahe, dass sich evtl. auch überlebende reife Oligodendrozyten, die die initiale Immunreaktion überstanden haben, an der Remyelinisierung beteiligt sein könnten. In meinem Promotionsprojekt ging es darum zu verstehen, wie sich die Oligodendrozytenschädigung ausbreitet und welches das langfristige Schicksal der überlebenden Oligodendrozyten im Verlauf der Krankheit ist. Um diese Fragestellungen zu beantworten, habe ich konfokale Mikroskopie, intravitale Virusmarkierung sowie Multiphotonen-In-vivo-Bildgebung in Kombination mit ultrastruktureller Elektronenmikroskopieanalyse angewandt.

Der erste Teil meiner Studie konzentrierte sich auf die Demyelinisierung der weißen Substanz des Rückenmarks, die bei BiozziABH-Mäusen durch MOG-Immunsierung induziert wurde. Dieser Mausstamm, der durch eine starke Antikörperantwort gekennzeichnet ist, entwickelt einen schubförmig-remittierenden Krankheitsverlauf und eignet sich daher gut zur Untersuchung von OL- bzw. Myelin-Schädigungen sowie –Wiederherstellung im Krankheitsverlauf. In diesem Modell habe ich die zelluläre Abfolge der Oligodendrozytenschädigung in akute entzündlichen Läsionen beobachtet. Meine Ergebnisse legen nahe, dass Oligodendrozyten der weißen Substanz über längere Zeiträume in einem amputierten Zustand, der durch den Verlust zahlreicher Prozesse gekennzeichnet ist, überleben können. Aus dieser

Beobachtung ergab sich die Frage, ob diese überlebenden Zellen einen Regenerierungsprozess durchlaufen können.

Im zweiten Teil meiner Promotion habe ich diese Frage in einem neuen Modell der kortikales MS-Pathologie untersucht, das in BiozziABH-Mäusen durch eine Kombination von MOG-Immunsierung und intrazerebraler Zytokininjektion induziert werden kann. In diesem Modell habe ich die morphologischen Veränderungen einzelner Oligodendrozyten über die Zeit verfolgt: vor der kortikalen Läsion, während des Immunangriffs und in der Erholungsphase. Die Ergebnisse zeigen, dass i) die Oligodendrozytenschädigung in grauer und weißer Substanz einem ähnlichen Muster folgt; ii) Myelinscheiden bei adulten, aber nicht bei gealterten Mäusen mit hoher Effizienz bei Läsionen der grauen Substanz wiederhergestellt werden können und iii) überlebende reife Oligodendrozyten möglicherweise zur Remyelinisierung beitragen können, da sie in der Lage sind, neue Primärfortsätze zu bilden. Diese Erkenntnisse erweitern unser Verständnis der Oligodendrozytenpathologie in entzündlichen Läsionen und eröffnen zudem die Möglichkeit für neuartige regenerative Therapieansätze, die gezielt die Erholung reifer Oligodendrozyten unterstützen können.

## Chapter I - Introduction

### 1. Multiple Sclerosis

Multiple Sclerosis (MS) originating from Latin *Sclerosis Multiplex* in literal translation means nothing more but hardening of the tissue - *sclerosis* at multiple sites - *multiplex* (Oxford University Press). According to the current medical definition, MS is a chronic autoimmune disease of the central nervous system (CNS) characterized by myelin destruction and axonal pathology. Such damage occurs in patches throughout the brain and the spinal cord interrupting the nerve tracks (Filippi et al., 2019). Extended disease duration leads to the lesions accumulation and further on to brain tissue atrophy. It translates into increasing neurological deficits, and can ultimately results in social exclusion and significant economic consequences (Jennum et al., 2012).

The oldest known document describing multiple sclerosis-like symptoms is a charter from 1421. It includes the case of young Lidwina van Schiedam, who suddenly became weak while ice-skating. After the onset of the disease, her condition progressively worsened over the next years until she lost the vision in her eyes, experienced paresis of arms and paralysis of both legs (Medaer, 1979). Although four centuries later two pathologists - Sir Robert Carswell and Jean Cruveilhier correctly described and illustrated CNS lesions (Carswell, 1838; Pearce, 2005), it was Dr. Jean-Martin Charcot who recognized multiple sclerosis as a new disease entity. In 1868, a French doctor successfully linked pathological structures in the brain, which he called '*sclérose en plaques*' with clinical manifestation of his patient (Lublin, 2005).

#### **1.1. Epidemiology and etiology of MS**

Multiple sclerosis is one of the most common causes of non-traumatic disability, comprising motor, sensory and cognitive deficits, among young people in their early 30s. The median survival time varies between 28 and 43 years after the onset of disease with life expectancy being reduced by, on average, 10 years (Brønnum-Hansen et al., 2004). According to World Health Organization, it affects more than 2.3 million people worldwide, placing also Germany within the nations with the highest prevalence i.e. 149/100.000 (WHO, MS Atlas 2008-2013). Female-to-male ratio has increased over the last 50 years and now exceeds 3:1 in most populations. This could be explained by gender-specific characteristics of the

immune or nervous systems caused by gonadal hormones as well as environmental and modern lifestyle differences (Orton et al., 2006; Greer and McCombe, 2011). Ethnicity and geography are the important factors in the MS global distribution. In general, multiple sclerosis is more commonly observed with increasing distance from equator in both, the northern and southern hemisphere. However, this rendition conceals disproportion of MS prevalence among certain ethnical groups such as Inuits, Yakutes and Australian Aborigines, who all have a low risk of developing the disease and on the contrary – Sardinians who over decades have shown increased MS risk (Browne et al., 2014; Pugliatti et al., 2001; Compston and Coles, 2008). Although the cause of multiple sclerosis remains unknown, there are several factors, which may enhance the likelihood of disease onset. Chief among environmental factors are smoking (Hernan et al., 2005); vitamin D deficiency and obesity, which also results in lower 25-hydroxyvitamin D, a biomarker for vitamin D nutritional status (Salzer et al., 2012; Munger et al., 2013); and infection with Epstein-Barr virus (EBV) (Levin et al., 2005).

Multiple sclerosis is not an inherited disorder; however, genetic factors are known to play a role in disease susceptibility. Genome-wide association studies (GWAS) identified more than 200 genes independently contributing to disease development (Lundmark et al., 2007; Sawcer et al., 2011; Beecham et al., 2013). The human leukocyte antigen (HLA) gene cluster is consistently considered as the strongest genetic locus for MS. HLA molecules are involved in immune regulation and response and are also taking part in self-nonsel self recognition, which points to an autoimmune origin of the disease. CNS-expressed candidate autoantigens, which recruit T and B cells, have been proposed but none of them has been finally confirmed (Sawcer et al., 2014, Hohlfeld et al., 2016). Despite the fact that multiple sclerosis is clinically and pathologically heterogeneous disease, etiological and epidemiological considerations in most cases consider MS as a uniform disease. Thus, one has to acknowledge the possibility that particular subtypes of MS might differ in their risk factors (Ascherio et al., 2016).

## **1.2. Pathology and pathophysiology of MS**

The key histopathological hallmark of MS is an extensive demyelination, which leads to axonal and neuronal damage. The emphasis given to the primary myelin loss is important since it distinguishes multiple sclerosis from other pathological conditions like i.e. Neuromyelitis Optica (NMO), where the initial steps are likely triggered by antibody-mediated astrocytes impairment (Misu et al., 2013; Lassmann,

2018). Multiple sclerosis has been classically considered as a white matter (WM) disease. Although there have been some histological evidences for grey matter (GM) pathology (Brownell and Hughes, 1962), its involvement in the disease progression was not fully acknowledged for decades (Geurts and Barkhof, 2008). In general, focal white matter lesions, driven by acute neuroinflammatory conditions, characterize early stages of the disease (Frischer et al., 2009). Grey matter pathology is considered as being associated with more progressive MS, however in some individuals it is a predominant form, starting from the disease onset (Lucchinetti et al., 2011). Up to date, the relationship between white and grey matter lesions remains largely unknown. It is believed that cortical lesions are, to some extent, independent from white matter lesions (Kutzelnigg et al., 2005; Bø et al., 2007; Trapp et al., 2018) and that they have a distinct underlying pathophysiology (Mahad et al., 2015). The major differences are found in the parenchyma lymphocyte infiltration, antibody deposition, complement activation and disruption of blood-brain barrier (BBB). Above components are abundant and frequently seen in the focal WM lesions, while in more diffused GM lesions they are rather at the lower levels (Lassmann et al., 2007, Brink et al., 2005, van Horsen et al., 2007). Therefore, pathology and pathophysiology as well as possible treatments will most likely vary in region-specific manner and should be discussed separately.

### **1.2.1. White matter pathology**

One of the possible early event in MS is the breakdown of the blood-brain barrier (BBB), which allows peripheral immune cells to access the brain parenchyma (Prat et al., 2002). BBB is a complex structure, composed of cerebral endothelial cells and pericytes, supported by astrocytes and perivascular macrophages that protects CNS microenvironment (Armulik et al., 2010). Barrier damage is observed in MS-WM lesions but also its increased permeability is detected in the periventricular normal appearing white matter (NAWM; Cramer et al., 2013). Both arms of the immune system - innate and adaptive - contribute to the MS development and progression (Hemmer et al., 2015). During the early phases of disease course, innate immune system cells - dendritic cells (DCs), microglia and infiltrating macrophages contribute to the inflammatory pathology by acting as antigen-presenting cells (APC) for autoreactive T cells. They also secrete the cytokines (i.e. TNF- $\alpha$ , IFN- $\gamma$  and different chemokines), which modulate adaptive immune responses (Weiner, 2008). The role of adaptive immune system has always been considered as central in multiple sclerosis pathogenesis. A wealth of immunological data suggests that

CD4+ T cells are inducers and drivers of the disease (Olsson et al., 1990; Zhang et al., 1994; Hohlfeld et al., 2016a). This hypothesis is strongly supported by the data obtained from experimental autoimmune encephalomyelitis (EAE) models (Fletcher et al., 2010). In this leading hypothesis, myelin-reactive CD4+ T cells migrate across the BBB into the unaffected CNS. In the parenchyma, these T cells become reactivated, which leads to a cascade of local immune responses, release of inflammatory mediators and migration of other immune cells into the central nervous system. CD8+ T cells have been shown to be oligoclonally expanded in the brain, blood and cerebrospinal fluid (CSF), suggesting that they also play an important role in the disease development (Skulina et al., 2004; Jacobsen et al., 2002, Beltrán et al., 2019). Furthermore, in comparison to CD4+ T cells, CD8+ T cells are more abundant in the inflamed plaques and their number correlates with the extent of axonal damage (Kuhlmann et al., 2002). B cells are also involved in MS pathogenesis and possibly act through different manners; they are professional APCs, which not only allows them to prime T cells in the CNS but also this interaction facilitates their differentiation into antibody-producing plasma cells. Furthermore, B cells can secrete pro-inflammatory cytokines modulating the inflamed CNS environment indirectly (Häusser-Kinzel and Weber, 2019). The interactions between different components of the immune system are still elusive. The emerging view on

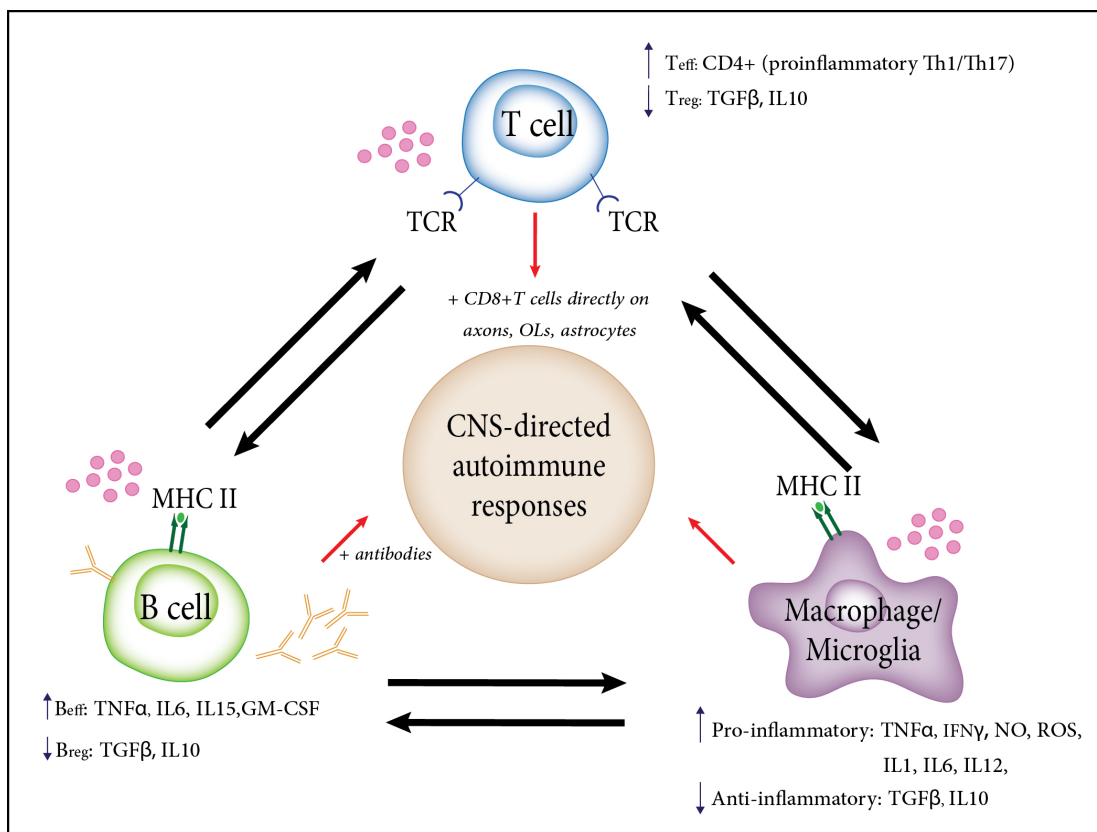


Figure 1. Emerging view on immune cells interaction in the early pathogenesis of MS. Inspired from Li, 2018.

the probable intercommunication of lymphocytes and phagocytes is shown in the Figure 1. Despite years of investigating, the question ‘what is the target antigen?’ remains without clear answer.

White matter histopathology is characterized by disseminated focal lesions, which consist of largely demyelinated areas some of which show partial remyelination (shadow plaques). Myelin breakdown is accompanied by extensive infiltration of lymphocytes and mononuclear phagocytes (Henderson et al., 2009). Actively demyelinating lesions show different pathological features; therefore, they have been classified into distinct patterns based on the myelin/oligodendrocyte destruction and main inflammatory pathways involved in this process. *Pattern I – ‘macrophages-mediated’* is associated with T lymphocytes and activated macrophages/microglia that produce compounds such as tumor necrosis factor- $\alpha$  (TNF- $\alpha$ ) and interferon- $\gamma$  (IFN- $\gamma$ ), which may induce myelin damage (Bitsch et al., 2000). Most frequently observed in MS samples, *Pattern II – ‘antibody-mediated’* is as well dominated by T cells and macrophages but it is distinguished from the previous pattern by antibody deposition and complement activation resulting in demyelination. *Pattern III – ‘distal oligodendroglialopathy’* has significantly lower levels of immune cells in comparison to the other patterns. It can be described as a dying-back model, where oligodendrocyte’s most distal processes are the primary sites of the destructive mechanism. Damage spreads back to the oligodendrocyte’s somata, which in a cascade manner leads to cells apoptosis. Interestingly, in this pattern, there is a preferential and selective loss of myelin-associated glycoprotein (MAG), while the other myelin components remain stable. The least common, *Pattern IV – ‘primary oligodendrocyte damage’* is associated with non-apoptotic oligodendrocyte death, followed by radially expanding secondary demyelination (Lucchinetti et al., 2000; Rosenberg, 2012).

### 1.2.2. Grey matter pathology

Cortical pathology is mainly characterized by widespread demyelination, persistent microglia activation and neuritic transection (Peterson et al., 2001). Importantly, neuronal cell bodies are in the relative proximity to inflammatory demyelination, which makes them a potential and direct target of immune responses (Stadelmann et al., 2008). Furthermore, one of the possible early hallmark of GM pathology is synapse loss, which is seen widespread in the demyelinated regions as well as in the normal-appearing grey matter (NAGM; Jürgens et al., 2016). Another important finding recently described by Schirmer *et al* is the cellular heterogeneity and vulnerability in cortical and subcortical MS. By employing single-cell

transcriptomic techniques, they revealed that the number of CUX2-expressing, excitatory neurons localized in upper cortical layers is selectively decreased in comparison to other cerebral neuronal subtypes in the cases of MS. Furthermore, such loss is frequently observed together with meningeal infiltration of plasma B cells (Schirmer et al., 2019). Leptomeningeal follicles-like structures containing B cells, T cells, plasma cells and dendritic cells are found in the patients with progressive MS (Magliozzi et al., 2007, 2010; Serfaini et al., 2004). This ectopic lymphoid tissue could represent a source of proinflammatory cytokines and immunoglobulins, which diffusing from cerebrospinal fluid may contribute to the damaging environment (Howell et al., 2011). Although B and T cells infiltrates might be also found in close proximity to the cortical lesions, their total number, even in mixed white-grey matter lesion, remains significantly lower in comparison to white matter pathology (Bø et al., 2003). Grey matter demyelinated areas are rather associated with activated microglia/macrophages. Activated microglia, with extended processes towards the neuronal cell body, dendrites and axons, are frequently detected in cortical lesions (Dutta and Trapp, 2007). Notably, they stay in a persistently activated shape, defined by processes projections, regardless of lesion activity status (Brink et al., 2005; van Horssen et al., 2007). Mononuclear phagocytes are mainly involved in myelin damage and removal, leaving the axons without trophic and metabolic support (Simons, Misgeld and Kerschensteiner, 2014).

A proposed classification system categorizes grey matter pathology with regards only to the area of distribution. *Leukocortical* Type I comprises deep layers of grey matter and adjacent white matter lesions. Three remaining patterns are composed of purely cortical lesions. *Intracortical* Type II is located entirely in the cortex reaching neither to the pial nor subcortical regions of the brain. Most commonly occurring cortical MS pathology is *subpial* Type III with lesions extending into the cortex from the pial surface. Subpial type can be further distinguish to rarely appearing Type IV, which is characterized by lesions placed in all cortical layers, involving several gyri (Peterson et al., 2001; Bø et al., 2003).

In the last years, GM pathology has gain more interest among researchers in part due to an improvement of the methods used to detect it. Demyelinated areas in the grey matter could be better visualized thanks to the new myelin staining techniques introduced at the turn of the millennium. Immunohistochemistry with anti-myelin basic protein (MBP) and anti-myelin proteolipid protein (PLP) had noticeable higher sensitivity in cortical lesions than classically used Luxol fast blue (LFB) (Bø et al., 2003). In addition,

improvements in the magnetic resonance imaging (MRI) allowed visualizing the demyelination and its extent. High-field scanners with a stronger magnetic field yield greater signal-to-noise ratio allowing to assess the damage in the grey matter and correlate it with the patient disability (Stadelmann et al., 2008; Nowogrodzki, 2018). GM pathology can explain cognitive decline, memory impairment and diminished mental processing occurring in about half of the patients. It can also contribute to progressive physical disability (Nielsen et al., 2013).

### 1.3. Diagnostics and clinical course

Multiple sclerosis still presents a challenge for diagnostics; a recent study showed that about 20% of the patients is misdiagnosed. This is mainly because MS is a disease with a very diverse course and it lacks a conclusive test, which ideally should have sufficient sensitivity and specificity for an accurate and quick detection (Kaisey et al., 2019). The most widely used diagnostic checklist-tool – *the McDonald Criteria*, integrates clinical, imaging and laboratory findings. Primary established in 2001 and recently revised, the newest 2017 version provides a step-by-step, simplified protocol for diagnosing different MS phenotypes. If the following criteria are fulfilled: *i*) number of clinical attacks, *ii*) number of lesions in distinct anatomical location; in which cortical lesions are equivalent to subcortical, *iii*) presence of CSF oligoclonal IgG bands and in addition, the symptoms cannot be attributed to any other disorder, the diagnosis is considered to be multiple sclerosis (Thompson et al., 2017).

The clinical course of MS is individual and unpredictable but depending on the frequency and intensity of relapses, the ‘International Advisory Committee on Clinical Trials of MS’ recognized four disease subtypes (updated in 2013). *Radiologically Isolated Syndrome* (RIS) is not considered as a distinct type of MS and identifies patients with MS-like demyelination plaques in the absence of clinical symptoms. However, follow-up studies showed that about 30% of the cases would convert into *Clinically Isolated Syndrome* (CIS), the first clinical manifestation of MS, which should last at least 24 hours in absence of fever and any signs of infection (Okuda et al., 2014; Figure 2A). If the primary symptoms coincide with abnormalities in the MRI, the chance of developing clinically definitive MS stands at 60 to 80% (Miller and Rhoades, 2012). The second subtype, *Relapsing-Remitting MS* (RRMS) is the most common phenotype and can be found in 85% of the patients. It is characterized by clear neurological deterioration periods (relapses) interspersed

with relative stable periods with complete or incomplete recovery (remissions; Figure 2B). Accumulation of disability over time will transition most of the RRMS affected individuals to the third phenotype, *Secondary Progressive MS* (SPMS). Patients experience progressive impairment with almost no recovery (Figure 2C). SPMS is not phenotypically uniform and since there is no available immunological marker, the diagnosis is often made retrospectively, based only on the clinical manifestation. Additionally, approximately 15% of the patients are diagnosed with *Primary Progressive MS* (PPMS) in which symptoms gradually get worse starting from the disease onset (Figure 2D). All of the above MS phenotypes can be further characterized by the presence or absence of new lesions in the MRI, referred to as active or not-active accordingly and with or without worsening/progression of disability (Lublin, 2014).

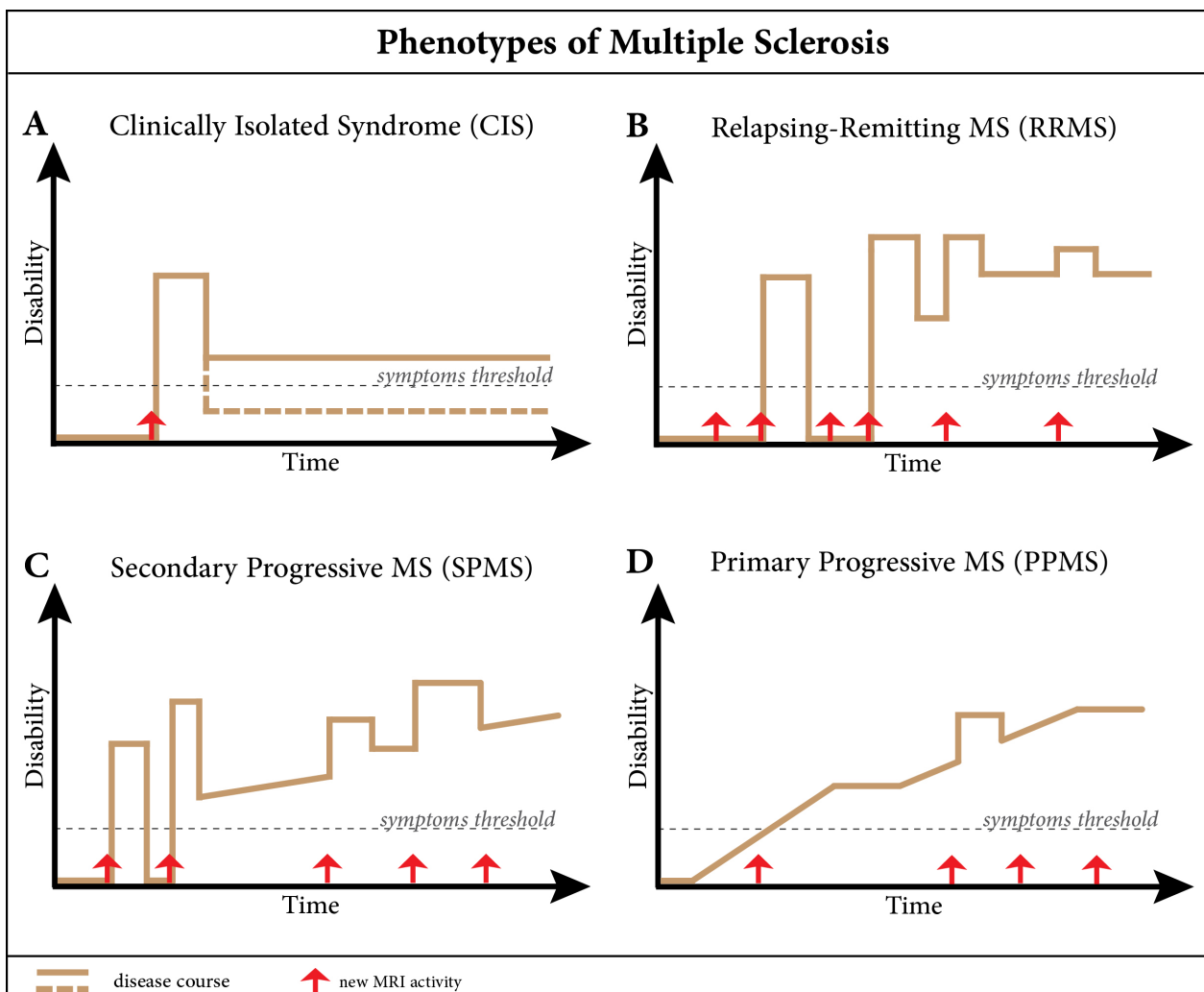


**Figure 2. Representative disease courses in MS.** (A) CIS with a complete (dashed-line) or partial (solid-line) remission of the symptoms. (B,C,D) Different disease courses with relapses and complete/incomplete remissions interspersed with potentially stable periods. New MRI activities with or without worsening indicated with red arrows. Inspired from [nationalmssociety.org](http://nationalmssociety.org) (Lublin, 2014; Thompson, 2017).

#### 1.4. Available treatment

The treatments, which finally modified the disease progression, started in the 90' with the approval of interferon- $\beta$  (IFN- $\beta$ ) (Paty and Li, 1993) and Glatiramer Acetate (GA) (Johnson et al., 1995); drugs that reduce antigen presentation and T cell proliferation. Since then, the US Food and Drug Administration (FDA) and the European Medicines Agency (EMA) have approved numerous disease-modifying treatments (DMTs) for patients with RRMS (Figure 3). Given the inflammatory nature of multiple sclerosis, the majority of the available drugs modulate or suppress immune responses. Unfortunately, up to now there is no curative treatment and modern therapy aims at balancing between reducing the number of MS attacks and avoiding the severe side effects of long-term immunomodulatory treatment (Tramacere et al., 2015). There are two therapeutic approaches – escalation strategy and induction strategy (Rieckmann, 2009). Escalation strategy recommends moderately effective medications (i.e. IFN- $\beta$ , GA, Dimethyl Fumarate, Teriflunomide) as a starting treatment and implementing more powerful, but also more toxic drugs as the symptoms progress. The more aggressive, induction approach is suggested for patients with highly active MS. Second-line therapy drugs include: *i*) humanized monoclonal antibodies like Natalizumab – preventing leukocyte migration across BBB (Rudick et al., 2006); Alemtuzumab - depleting circulating T and B-lymphocytes (Cohen et al., 2012); Ocrelizumab – depleting CD20+ B-cells (Salzer et al., 2016); *ii*) antagonist of sphingosine, Fingolimod – inhibiting lymphocytes migration from lymph nodes (Kappos et al., 2010); *iii*) synthetic adenosine analogue, Cladribine - depleting T and B cells (Cook et al., 2019) and *iv*) anti-cancer agent, Mitoxantrone – inhibiting proliferation of lymphocytes (Marriott and Miyasaki, 2010).

The above-mentioned drugs work relatively well in the relapsing-remitting MS but most of them show almost no effect in the progressive course of the disease. Up to date, the only available treatment for primary-progressive MS is Ocrelizumab, a second-generation anti CD20+ monoclonal antibody, which showed positive effects on MS activity, reflected in MRI signal (Montalban et al., 2017). Other encouraging results come from the clinical trials with Siponimod, acting similar to Fingolimod but with less side effects. In addition, Simvastatin, a cholesterol-lowering drug and Ibudilast, a neuroprotective agent, showed reduced progression of brain atrophy and reduced disability (Fox et al., 2018). Lastly, new trends in

therapy are focusing on promoting direct oligodendrocyte repair and remyelination and they will be further discussed in Chapter 2.3.3.

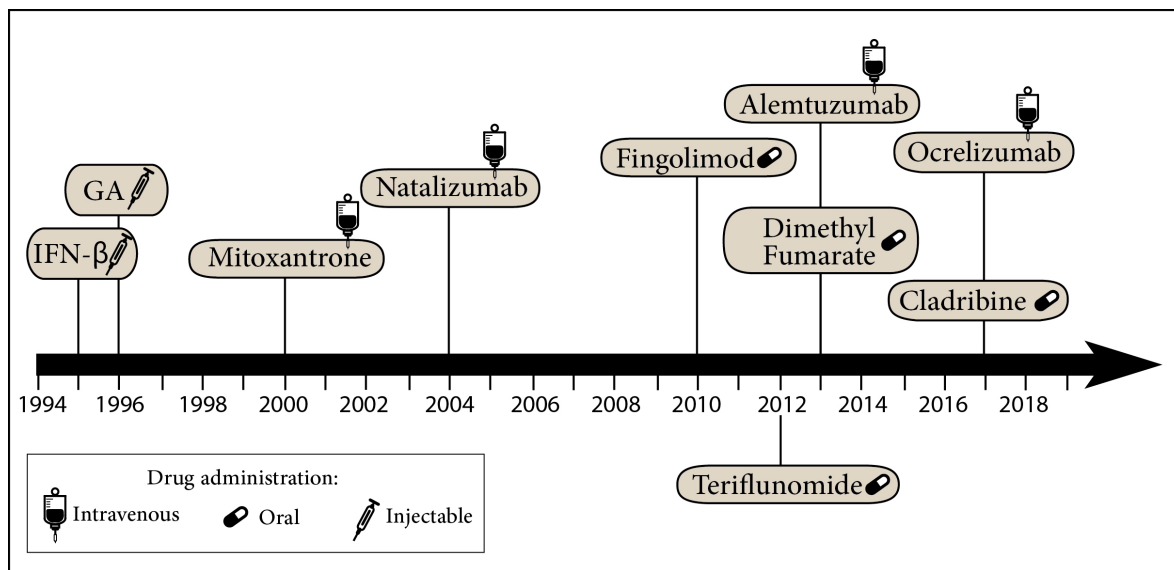


**Figure 3. Timeline of disease-modifying treatments for MS.** Their earliest FDA or EMA approval and way of administration. IFN- $\beta$  – interferon- $\beta$ ; GA – Glatiramer Acetate. Inspired from De Angelis et al.,2018.

## 1.5. Animal models of demyelination and remyelination

There is a broad selection of rodent models that are used to understand MS pathology. Among them experimental autoimmune encephalomyelitis (EAE) models help to investigate primary inflammatory mechanisms in the CNS followed by the demyelinating phase. In contrast toxin-induced models like cuprizone and lysolecithin (LPC)/ ethidium bromide (EB) are particularly useful to study remyelination processes.

### 1.5.1. Experimental autoimmune encephalomyelitis

Experimental autoimmune encephalomyelitis mimics many aspects of multiple sclerosis pathology. Predominant perivascular lesions develop in a similar cascade manner; starting from neuroinflammation, followed by demyelination, oligodendrocyte impairment and partial axonal degeneration along with debris clearing and limited remyelination. Originally introduced by *Rivers et al* in 1933, EAE is the most commonly used experimental model in MS research. Rivers' initial experiments performed on monkeys provided evidence that immunization against CSN antigens (in this study using rabbit brain extracts) leads to pathological changes in the brain (Rivers et al., 1933). Nowadays, numerous encephalitogenic factors

and induction methods are used in a variety of animal species and strains in order to target different aspects of the disease. Accordingly, the variability of EAE models can be used to describe a range of clinical features (Burrows et al., 2019). EAE can be actively induced by immunization with encephalitogenic myelin antigens including purified or recombinant myelin proteins or peptides such as MBP, PLP and MOG. Additionally, complete Freund's adjuvant (with mycobacterium tuberculosis) and pertussis toxin are used to boost the immune response (Billiau et al, 2001) and disrupt the blood-brain barrier (Linthicum and Frelinger, 1982), respectively. As a second approach, passive sensitization requires adoptive transfer of myelin specific CD4+ T cells, isolated from lymph nodes of previously immunized animals, into naïve recipients (Stromnes and Goverman, 2006a and 2006b). In both methods, the underlying pathways of pathological demyelination are, in principle, the same. Activated myelin specific peripheral CD4+ T cells cross the BBB and enter the central nervous system. They are then reactivated by residual and infiltrating APCs and secrete pro-inflammatory cytokines such as TNF- $\alpha$ , IFN- $\gamma$  or IL-17, which leads to further recruitment of microglia and macrophages. These events subsequently result in extensive myelin breakdown and increasing number of demyelinated plaques. Clinical features of CNS tissue damage are demonstrated in mouse by progressive paralysis of tails, hind- and forelimbs (Miller et al., 2007).

By acting through myelin specific CD4+ T cells, EAE models mimic pattern I and II of MS lesions characterized by *Lucchinetti et al* – macrophage/antibody mediated demyelination (Lucchinetti et al., 2000). Furthermore, specific mouse strains can resemble different MS disease courses. MOG<sub>1-125</sub>-induced EAE in C57BL/6 mice results in disease onset around day 12 post immunization. This strain is used to mirror relapsing-(no)remitting MS since neurological deficits and paralysis only marginally improve over the following months (Jones et al., 2008). A secondary progressive MS-like disease course is observed in another mice strain, BiozziABH. Due to the high antibody titers against specific antigens, BiozziABH mice are very susceptible to a low-dose MOG<sub>1-125</sub> induction of experimental autoimmune encephalomyelitis (Biozzi et al., 1972). After initial onset and partial remission of the symptoms, they enter a second, chronic relapse without clear improvement. This phase is marked by extensive demyelination, gliosis and neuronal and axonal loss (Hampton et al., 2008). Moreover, immunized with spinal cord homogenate, aged BiozziABH mice (12 months old) demonstrate a primary progressive disease from the onset and are

characterized by the increased number of microglia/macrophages and T cells in compare to animals at 3 months of age (Peferoen et al., 2016).

As there is no ideal model for MS, also EAE has some limitations. First, the MS trigger is still not known so it is difficult to investigate the disease initiating events in the EAE because primary demyelination is artificially induced with myelin antigens. Furthermore, because of the active EAE induction manner, CD8+ T cells and B cells play a smaller role in the initial steps of the modelled disease development, which might be contrary to the MS situation. Lastly, the majority of lesions is found in the white matter tracks of the spinal cord, leaving the cerebral cortex intact (Lassmann and Bradl, 2017).

### 1.5.2. Cortical MS models

Cortical demyelination is a key pathological hallmark of progressive MS. However, the number of experimental models mimicking this feature is very limited. A novel cortical MS (c-MS) mouse model, recently described by our group was developed by adapting previously published cortical models in rats (Merkler et al., 2006; Gardner et al., 2013). MOG-immunized mice on BiozziABH/C57Bl/6 background are stereotactically injected with TNF- $\alpha$  and IFN- $\gamma$  into the somatosensory cortex. This focal cortical EAE results in extensive subpial demyelination, phagocyte activation, infiltration of inflammatory cells and minimal axonal loss (Jafari et al., 2019). In addition, *Stadelmann and colleagues* recently reported another c-MS model characterized by cortical demyelination and monocyte infiltration. It is an anti-myelin antibody-dependent model induced in susceptible mice, genetically modified to produce high titers of autoantibodies against MOG. Interestingly, they have shown that autoantibodies contribute to cortical pathology in absence of classical complement activation pathway (Lagumersindez-Denis et al., 2017).

### 1.5.3. Toxin-induced lesions

Several agents can cause focal or more systemic demyelinating lesions in the CNS. Toxin-induced models resemble pathological hallmarks seen in pattern III and IV of MS lesions described in Lucchinetti -primary oligodendrocyte and/or myelin attack (Lucchinetti et al., 2000). Lysophosphatidylcholine and ethidium bromide are commonly used chemicals that are directly injected into a pre-defined location, commonly in white matter tracks. Injection of 1% of LPC causes myelin breakdown, oligodendrocytes loss, reactive astrogliosis, infiltration of macrophages and to some extent axonal degeneration in the lesion center

(Miron et al., 2013). Focally induced demyelination allows for precise control of the lesion site as well as the timeline of the occurring events. For example, these features provide the possibility to detect electrophysiological changes during the phase of demyelination and remyelination. By implementing electrodes above and below the lesion, one can compare axonal conductivity between different time points and selected treatment approaches (Smith et al., 1981).

Cuprizone intoxication leads to widespread demyelination in the corpus callosum and less frequently in the cortex (Skripuletz et al., 2008). In this model, damage is specifically targeted to oligodendrocytes but the mechanisms of this selective destruction are not fully understood. Cuprizone is a copper chelator and inhibits mitochondrial copper-dependent enzymes, which might disturb oligodendrocyte's energy metabolism resulting in cell apoptosis (Venturini, 1973; Matsushima et al., 2001; Torkildsen et al., 2008). The toxin is administered with the chow for 6 weeks leading to extensive myelin loss and subsequent remyelination occurs as early as 4 days after cuprizone withdrawal. This model allows precise investigation of the steps of myelin breakdown and restoration (Lindner et al., 2008).

## **2. Oligodendrocytes and Myelin in the Central Nervous System**

Oligodendrocytes (OLs) are neuroectodermally-derived glial cells, which constitute around 20% of all cells in the CNS (Valerio-Gomes et al., 2018; Allen and Lyons, 2018). The main role of the OLs is myelin production that spirally ensheaths neuronal axons providing them with electrical insulation. However, OL's function is not only limited to myelination as they are also responsible for trophic support. Oligodendrocyte-derived insulin-like growth factor (IGF-1) promotes neuronal survival and neurite outgrowth (Wilkins et al., 2001). Moreover, OLs provide axons with energy substrates and such metabolic support might be regionally heterogeneous. In the optic nerve, lactate and pyruvate are the main metabolites delivered by oligodendrocytes to the periaxonal space (Lee Y. et al., 2012); in the corpus callosum, it is primarily glucose necessary to maintain axonal functions (Meyer et al., 2018). Furthermore, OLs take part in extracellular potassium homeostasis in white matter; loss of OL's K<sup>+</sup> channels do not affect myelin but impairs neuronal activity (Larson et al., 2018).

The relationship between OLs and axons is based on their tight connection through myelin sheaths and by physically non-direct interaction. Therefore, impairment of oligodendrocytes and myelin loss, which is one of the central events in multiple sclerosis, is coupled with axonal and neuronal damage. Due to their importance, there has been a growing interest in OLs' physiology and pathophysiology and they are starting to be considered as a promising therapeutic target. Since most of the research has been done in animal models, in this chapter I will mainly refer to rodent (mouse) and human data.

## **2.1. Oligodendrocytes and myelin physiology**

### **2.1.1. Oligodendrocyte lineage and development**

Myelinating oligodendrocytes are the final product of the cell lineage, which underwent timed steps of proliferation, migration, differentiation and maturation. Spatiotemporal dynamics of OLs are reflected in the expression of specific markers, transcription factors and behavioral characteristics. They arise from glial progenitors called oligodendrocyte precursors cells (OPCs), which originate in waves from distinct areas in the spinal cord and the brain during development. The majority of OPCs in the spinal cord are derived from the ventral ventricular zone (VZ) at around embryonic day 12.5 (E12.5) in mice and E45 in humans (Hajihosseini et al., 1996; Lu et al., 2000). Shortly after, they proliferate and widely migrate to the white and grey matter. A second wave of OPCs originates in the dorsal VZ but contrary to the previous one, does not spread but enter the maturation pathway locally (Cai et al., 2005; Tripathi et al., 2011). In the rodent forebrain, OPCs appear first in the ventral VZ – earliest in the medial ganglionic eminence (MGE) and soon afterwards in the lateral ganglionic eminence (LGE). These progenitors spread through the brain and eventually they are complemented and partially replaced by the last OPCs wave, which comes from the cortical VZ (Kessaris et al., 2006). An analogous series of events happen in the developing human brain, following similar spatial and temporal resolution in OPCs production (Jakovcevski et al., 2009).

Developing oligodendrocytes consecutively express transcription factors, which define their fate and determine their temporal phenotype (Figure 4). The early stages of oligodendroglial lineage commitment require the transcription factor *Olig2*, which remains expressed during every further differentiation step, including mature OLs. Genetic ablation of this protein in mouse models results in the complete loss of OPCs and death at birth (Lu et al., 2002). Other essential factors required for lineage differentiation and

specification are Nkx2.2, Sox10 and Olig1 and their expression precedes expression of the platelet-derived growth factor- $\alpha$  receptor (PDGF $\alpha$ R) and NG2 proteoglycan (Nishiyama et al., 1999). PDGF $\alpha$ R<sup>+</sup> and NG2<sup>+</sup> are the classical markers for OPCs during development and adulthood in the human and mouse central nervous system (Sim et al., 2011). Oligodendrocyte precursor cells uniformly disperse throughout white and grey matter occupying non-overlapping territories and remain mitotically competent progenitors (Hughes et al., 2013). In fact, they are the most proliferating cells in the adult CNS (Dawson et al., 2003). Once they reach the destined location, OPCs can exit the cell cycle and start a maturation process. A large proportion of OPCs terminally differentiate initially into premyelinating OLs and soon become fully mature, myelinating OLs. At this stage, they continuously express high levels of myelin proteins such as MBP, PLP, CNP and the cytoplasmic marker APC (clone CC1; Marques et al., 2016). Recent findings identified also BCAS1, as a unique marker for oligodendrocytes in the early-active myelinating phase. In the healthy WM, BCAS1<sup>+</sup> OLs are present only in the early postnatal period, but they can be detected at later stages within MS lesions, thus allowing detection of ongoing remyelination (Fard et al., 2017).

OLs progenitors are functionally a homogenous population at the developmental stage and afterwards they separate into more specialized clusters. Over time and depending on the brain region, in which they are located (WM/GM), they selectively gain and lose expression of ion channels and these differences in their electrophysiological properties, change as well their sensitivity to neuronal activity (Spitzer et al., 2019). In addition, grey matter NG2<sup>+</sup> OLs proliferate at a very low level in comparison to white matter progenitors and generate lower number of mature OLs, reaching ~11% in GM versus more than 40% in WM (Dimou et al., 2008). These findings are very important when considering the relative lack of sufficient remyelination within cortical MS. Moreover, PDGF $\alpha$ R<sup>-</sup>/NG2<sup>-</sup> oligodendrocytes are as well a heterogeneous population in terms of *i*) morphological differences (Murtie et al., 2007), *ii*) myelin sheath length (Bechler et al., 2015) and *iii*) transcriptional characteristics revealed by single-cell RNA sequencing (Marques et al., 2016; Falcão et al., 2018). Based on the transcriptomic data, different regions of the adult brain are occupied by oligodendrocytes of diverse characteristics. Analyzed CNS regions are differently and preferentially enriched by subclasses of: differentiation-committed oligodendrocyte precursors, newly formed oligodendrocytes, myelin-forming oligodendrocytes and mature oligodendrocytes (Marques et al., 2016).

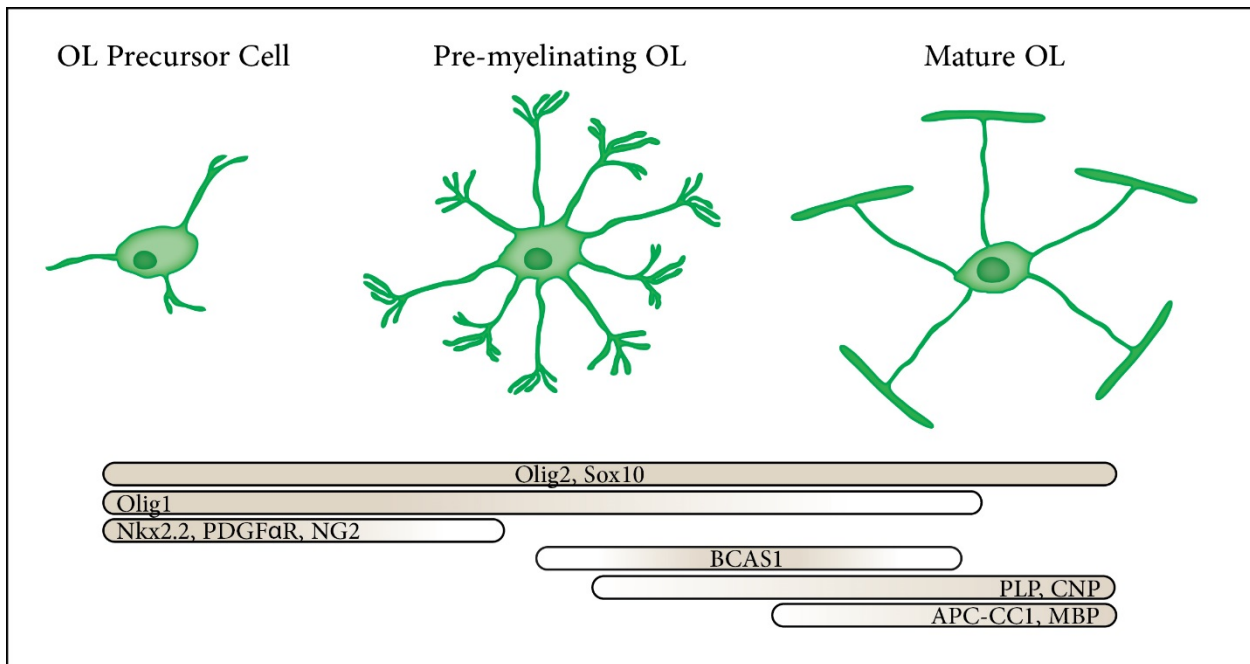


**Figure 4.** Developmental stages of the oligodendrocyte lineage. Morphological features and stage-specific markers of OPCs, pre-myelinating and mature OLs.

### 2.1.2. Myelination and myelin structure

Axonal myelination is a crucial step in CNS development allowing faster action potential transmission. In humans, myelin production starts in the second trimester of fetal development, reaching its peak in early childhood to slow down in late adolescence (Fields, 2008). However, adaptive myelination of cerebral cortex and experience-dependent myelin remodeling are now recognized to take place throughout life (discussed further in Chapter 2.1.3).

Myelinogenesis includes several, precisely controlled steps; radial processes extension, axon ensheathment, longitudinal myelin growth and myelin compaction (Snaidero et al., 2014). Pre-myelinating OLs radially extend processes in search for the axons; in general, the higher the axon diameter the higher the chance that it will be myelinated. Axons ensheathment begins when some of extended processes eventually set up a stable ‘*connection*’, while those that did not are retracted. OLs seem to have a precisely defined time window, in which they can complete the myelination process (Czopka et al., 2010). Once the axoglial contact is defined, the myelin inner tongue acting as a leading edge consecutively wraps around the axon. Subsequently, the outer myelin layer extends laterally forming the internodal segment. Depending on the region in which it resides, a single oligodendrocyte can form up to 80 myelin sheaths on distinct axons (Snaidero et al., 2014). Additionally, to develop the broad myelination pattern, half of

the pre-myelinating OLs undergo programmed cell death during the developmental phase in order to eliminate OLs from regions that should remain unmyelinated (Raff et al., 1993). More recently, Sun *et al.* showed that this intrinsic control pathway is regulated by the OL's transcription factor EB (TFEB), which induces pro-apoptotic protein 'p53 upregulated modulator of apoptosis' (PUMA) and further directs pre-myelinating OLs to Bax-Bak dependent cell death (Sun et al., 2018).

Until now, the mechanisms controlling myelination of selective axonal targets remains elusive. One hypothesis is that developing OLs sense neuronal activities and can respond to their needs. Cells from the OL lineage express ligand-gated channels for the excitatory neurotransmitter glutamate such as NMDA (Karadottir et al., 2005) or AMPA/kainate receptor (Bergles et al., 2000). Signaling through NMDA receptors directly enhance myelination (Saab et al., 2016) while the role of AMPA receptor-mediated signaling seems to be more supportive for the pre-OL survival without affecting myelin *per se* (Kougioumtzidou et al., 2017). Furthermore, *in vivo* experimental models show that release of neuronal factors encourages pre-OLs to start the ensheathment of active axons (Gibson et al., 2014; Hines et al., 2015). On the other hand, *in vitro* data shows that oligodendrocytes can wrap myelin sheaths also on artificial nanofibers and they produce all myelin proteins resembling the *in vivo* situation. These findings suggest that axonal signaling acts as a modulator of myelination rather than process initiator (Lee S. et al., 2012). Moreover, neuronal regulation of myelination is not always stringent enough to secure correct myelin targeting. When myelin production exceeds axonal needs, oligodendrocytes can misdirect process outgrowth and myelinate neuronal cell bodies (Almeida et al., 2018).

The myelin sheath has a characteristic periodic structure of ~12nm, in which major dense lines alternate with intraperiod lines; electron-dense and light layers, respectively. Myelin is composed 70% of lipids, mainly enriched with cholesterol and glycosphingolipids (i.e. galactosylcerebroside, GalC) and 30% of proteins, which are rather specific for this structure. The most abundant myelin protein is proteolipid protein (PLP) and its isoform DM20 and they are responsible for intraperiod line stabilization (Klugmann et al., 1997). An essential protein for myelin compaction is myelin basic protein (MBP). MBP is localized between two lipid bilayers, which facilitates its adhesive role. Another component, 2', 3''-cyclic-nucleotide 3'-phosphodiesterase (CNP1) by its direct association with actin cytoskeleton, forms cytoplasm-rich compartments, therefore opposing the MBP-tightening effects (Snaidero and Simons, 2017). Two other

proteins, myelin oligodendrocyte glycoprotein (MOG) and myelin associated glycoprotein (MAG), members of immunoglobulin super family of cell adhesion molecules are found in the most inner (MAG) and outer surface (MOG). MOG localization on the most external lamellae makes it an accessible target for antibodies attack (Figure 5).

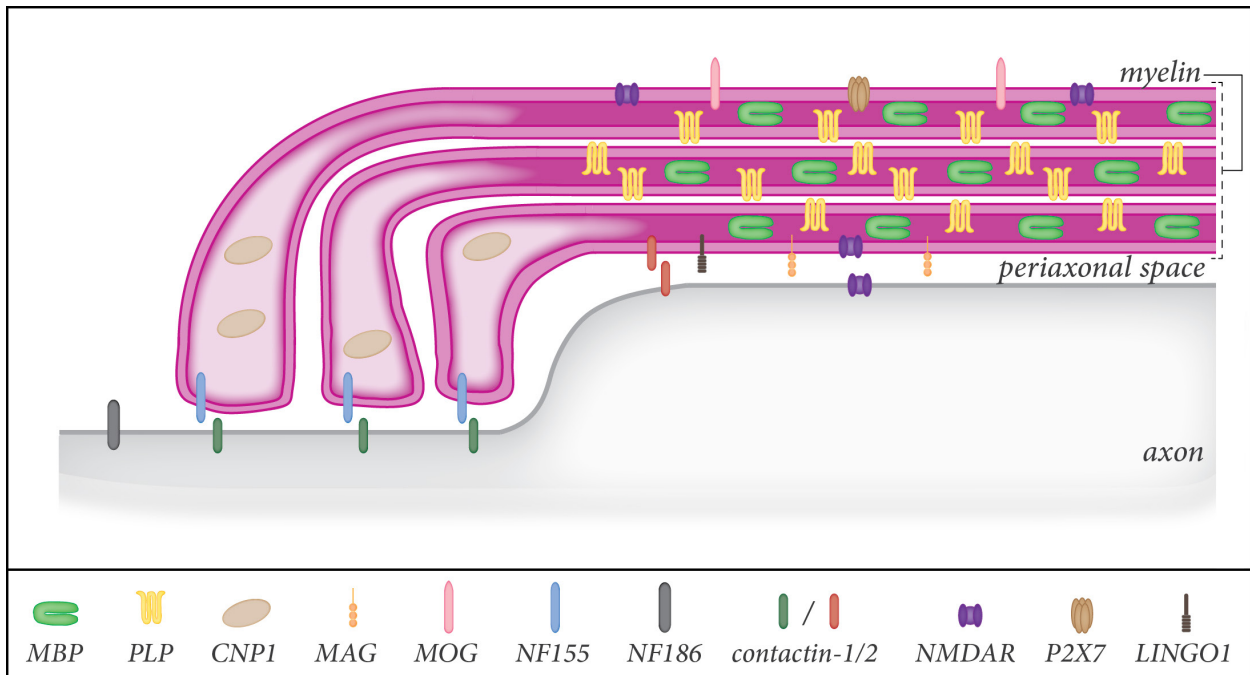


**Figure 5. Myelin sheath in longitudinal view.** Compact myelin (dark magenta) includes mainly MBP and PLP proteins; CNP1 is found in less compact myelin (light magenta). MAG and MOG proteins are localized on the most inner and outer surface of myelin sheaths, respectively.

Additionally, myelin surface proteins like NF155, contactins and LINGO1, which are localized in the close proximity to the axon, are the possible targets of immune attack. Glutamate (NMDAR) and ATP (P2X7) receptors, involved in extracellular space-oligodendrocyte signaling, are found on the outer myelin surface. Moreover, NMDAR localized on the inner surface, take part in axon-oligodendrocyte signaling.

### 2.1.3. Myelin plasticity and remodeling

Myelination of white matter axonal tracks and optic nerve is established relatively early during development because it is important to achieve maximal conduction velocity. Despite of the fact that there is little place for potential myelin plasticity, evidences from human MRI (diffusion tensor imaging) point to WM changes promoted by visuo-motor skill learning in adulthood (Scholz et al., 2009). Contrary to WM, grey matter myelination pattern largely depends on the additional, postnatal input. Longitudinal imaging of mouse cortex revealed that only half of the internodes are established in early life and the rest is added during the adulthood in an experience-dependent manner (Hill et al., 2018; Hughes et al., 2018).

Adaptive myelination manifests itself as formation of new internodes or re-shaping the existing ones. It is still debated to what extent oligodendrocyte progenitors and/or mature OLs can contribute to this process. In mouse cortex, OPCs continue to proliferate and generate myelin-forming OLs in the adulthood, but only one fifth on these newly born cells successfully integrates and form internodes (Hughes et al., 2018). *In vivo* and labelling techniques allowed to observed that newly formed internodes are added up to the existing pattern of myelin sheaths rather than acting as their substitutions (Young et al., 2013). Analysis of oligodendrocytes dynamics in rodents revealed that OLs continuously exchange myelin over the lifetime. Their cell-survival rate is up to 90%, depending on the CNS region suggesting that adult-born OLs are mainly responsible for adaptive myelination rather than myelin homeostasis (Tripathi et al., 2017). Studies in mice indicate that OLs remain stable and do not retract nor add new myelin sheaths, however individual internodes can adjust their length over time (Hill et al., 2018). Furthermore, it has been observed using the zebrafish model that white matter myelin sheaths are able to respond to local signals and compensate the loss of an adjacent internode by increasing their own length. Moreover, once remyelination has occurred, the myelin sheath can shrink back to its original form (Auer et al., 2018). Myelin modulation carried out by pre-existing oligodendrocytes rather than *de novo* differentiated ones, is believed to also take place in humans. Carbon-14 dating of human CNS cells shows that OLs maturation reaches a plateau around 9 years of age with a minimal annual turnover, while myelin is exchanged at a high rate during the whole adulthood (Yeung et al., 2014).

## 2.2. Oligodendrocytes pathology and demyelination

Oligodendrocytes and myelin damage are the early pathological hallmarks of MS, although the initial sites and mechanisms driving this process are still not entirely known. Axonal pathology can occur independently of myelin damage. In the EAE model, focal axonal swellings, which may lead to axonal degeneration, are present even when they are wrapped by intact-appearing myelin (Nikić et al., 2011). Furthermore, organelle transport deficiencies, detected in normal-appearing axons within the lesion area, seem to take place before any other axonal abnormalities become detectable (Sorbara et al., 2014). On the contrary, EM analysis of several demyelinating models revealed that the earliest event is primary loss of MBP, which decreases myelin compaction, subsequently causing myelin breakdown leaving axons initially

unscathed (Weil et al., 2016). Nevertheless, considering axon and myelin as a tightly connected unit, the aforementioned events might take place simultaneously, both being the cause as well as the effect. Moreover, these findings suggest that demyelination can occur in a dying-back manner starting at the distal OL's processes and spreading back to the OL's soma. This 'outside-in' hypothesis would be consistent with the MS lesions *Patterns I-II*, in which myelin is a direct or indirect primary target (Lucchinetti et al., 2000). Such a chain of events also occurs in cuprizone models, where the earliest oligodendrocytes changes are detected in the myelin inner cytoplasmic tongues weeks before OL soma degeneration (Ludwin and Johnson, 1981). In addition, bulb-like structures called 'myelinosomes' are observed in MS autopsy samples and in the EAE model, representing an early stage of myelin pathology. These out-foldings, possibly induced by the loss of myelin compaction, are surrounded by phagocytes, which facilitate further myelin removal (Romanelli et al., 2016). Relatively accessible internodal myelin proteins, which can act as antigens, can also support the outside-in mechanism of autoinflammatory demyelination. This feature is broadly used in autoimmune encephalomyelitis models of MS. Paranodal loops at the internodes edges might also be the site of immune cells attack as there are evidences of autoantibodies against extracellular domains of neurofascin (NF) isoforms in MS patients - NF186, localized at the node of Ranvier and paranodal, OL-specific NF155 (Mathey et al., 2007). In addition, juxtaparanodal, myelin-anchoring protein, contactin-2 (mouse TAG-1) specific T cells are also present in the MS samples (Derfuss et al., 2009; Figure 5).

Alternatively, the 'inside-out' hypothesis, assumes that the oligodendrocyte's cell body is the initial target and further damage spreads towards the myelin sheaths resembling MS *Pattern IV* (Lucchinetti et al., 2000). Histopathological data indicates that oligodendrocyte apoptosis can occur only in the presence of activated microglia, without evident signs of lymphocytes involvement nor myelin phagocytosis (Barnett and Prineas, 2004). Mature OLs can be selectively eliminated in transgenic mice carrying tamoxifen-inducible diphtheria toxin fragment A (Plp1-CreER<sup>T</sup>;ROSA26-eGFP-DTA). Using this model, it was shown that OLs death and eventual myelin breakdown results in autoreactivity against myelin proteins and can lead to a secondary CD4<sup>+</sup> T cells attack in the CNS (Traka et al., 2015).

Oligodendrocytes are very susceptible to extracellular toxicity making them a possible target of 'bystander damage'. They are particularly vulnerable to excessive signaling of glutamate, a neurotransmitter released

at high levels by microglia/macrophages and dendritic cells in the inflamed human CNS (Macrez et al., 2016). Prolonged overactivation of AMPA/kainate and NMDA receptors leads to calcium ion influx through  $\text{Ca}^{2+}$ -permeable AMPA/kainate channels. Similar calcium accumulation can also be caused by overexpression of oligodendroglial ATP receptor, P2X7 (Matute et al., 2007; Figure 5). Increased intracellular  $\text{Ca}^{2+}$  concentration impairs mitochondrial functions resulting in oxygen radicals' production (Matute et al., 2006). Because OLs contain low levels of glutathione antioxidant they are defenseless against oxidative damage (Thorburne and Juurlink, 2002).

Recent evidence suggests that OLs play a more active role in MS instead of being just a passive immune target. Disease-specific OLs and their precursors have been identified in the human MS brains and EAE spinal cords. In response to the lymphocyte-derived interferon- $\gamma$  stimulation, a subset of OLs lineage cells express key genes involved in MHC-I and MHC-II mediated immune response. In line with these findings, OPCs are not only detected to be able to phagocytose myelin but also they can trigger CD4+T cell proliferation and further cytokines secretion (Falcão et al., 2018).

### 2.3. Oligodendrocytes recovery and remyelination

Remyelination is a CNS regenerative process, during which myelin sheaths are restored in previously demyelinated sites. Although the new sheaths are abnormally thinner and shorter, they are able to ensure axonal conduction properties and secure axoglia relationships (Smith, 1979). Furthermore, based on the long-lived experimental models, such thin myelin sheaths preserve and remain stable over time (Duncan et al., 2017). One of the methods, allowing the assessment of the myelination status is the g-ratio, determined by the inner axonal diameter divided by the total outer diameter of the axon-myelin unit. Under healthy conditions, myelinated axons have g-ratio of ~0.6. However, recent imaging improvements revealed that a single intact axon can have different g-ratio values at the given internode location (local g-ratio ranges from 0.4 to 0.8; Gao et al., 2019). Typically, the g-ratio of remyelinated axons is increased because of their thinner myelin and oscillates around 0.8-1.0 (Duncan et al., 2017). Fully or partially remyelinated areas, referred to as *shadow plaques*, are detected in MS autopsies regardless of the disease course and duration (Patrikios et al., 2006). Unfortunately, remyelination, which is very efficient in animal experimental models, frequently fails in MS affected individuals. A hostile environment for OPCs

maturation and oligodendrocytes survival could contribute to the limited lesion recovery. Classically, remyelination is believed to be driven purely by OL precursors' proliferation, differentiation and myelin integration; however, recent findings suggest that mature, pre-existing oligodendrocytes may also contribute to this process (Nave and Ehrenreich, 2019; Figure 6).

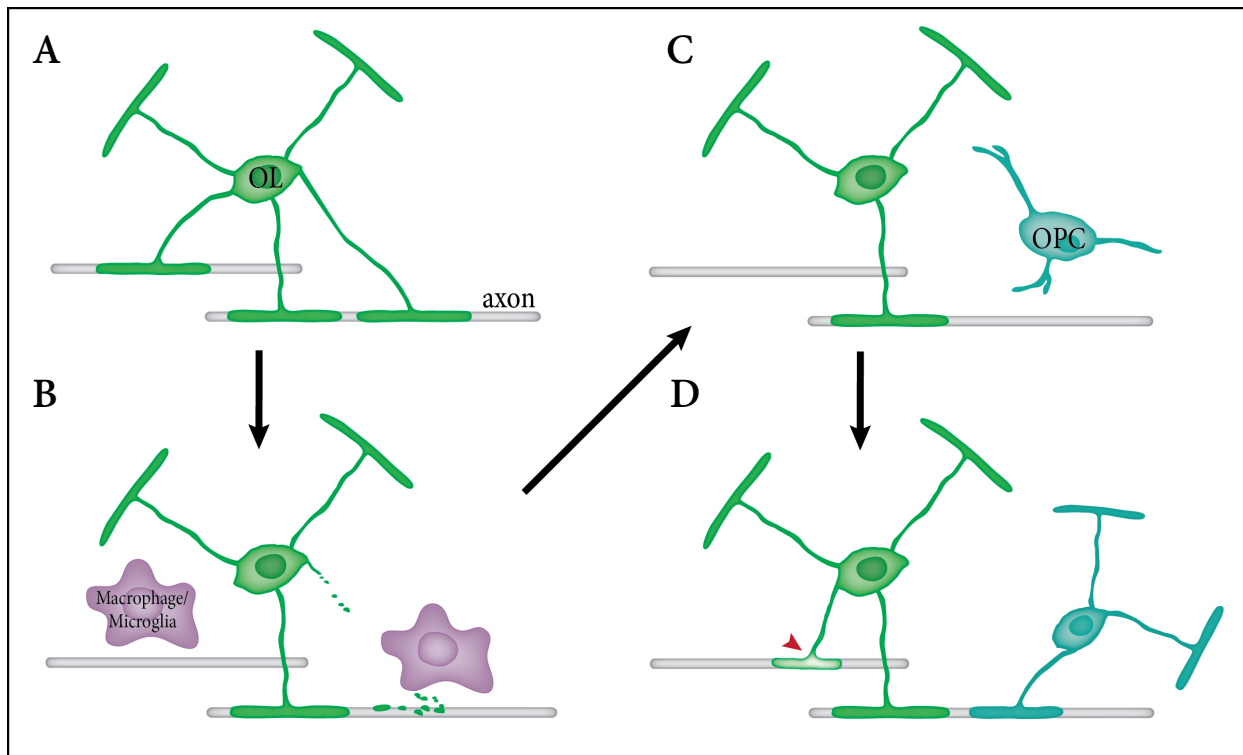


**Figure 6 – Hypothetical sequence of events in remyelinating lesion.** (A) Unaffected oligodendrocyte partially loses its processes and internodes. (B) Myelin debris are cleared by phagocytes. (C) OPC starts proliferation and migration to the lesion area; amputated-state oligodendrocyte survives the initial demyelination attack. (D) OPC differentiates into mature OL and extends processes forming new internodes; pre-existing OL restore some processes also forming new internodes - both events possibly contribute to remyelination.

### 2.3.1. OPC-mediated remyelination

Remyelination driven by re-activated oligodendrocytes precursor cells requires their migration, proliferation and differentiation as well as the successful integration of their newly synthesized myelin. Although from *in vitro*/transplantation studies it was known for a long time that OPCs take part in myelin restoration (Groves et al., 1993), the cellular origin of these newly myelinated oligodendrocytes, in the damaged CNS, was revealed by fate-mapping techniques two decades later. Labelling certain progenitor populations revealed that adult OPCs are the predominant source of new OLs but SVZ progenitors might also give rise to myelinating cells, if the damage is located within a small distance i.e. corpus callosum

(Zawadzka et al., 2010; Xing et al., 2014). Adult OPCs (aOPC), developmental precursors that persisted into adulthood, are equally distributed throughout the central nervous system. Similar to neonatal progenitors, aOPCs express NG2, PDGF $\alpha$ R, Olig1 and Olig2 markers and they maintain their developmental properties such as proliferation and migration. They represent 8% of the white matter and 2% of the grey matter cells (Dimou et al., 2008; Dawson et al., 2003). Adult NG2<sup>+</sup> cells are very dynamic in the mouse cortex, they scan local environment with filopodia, extend *growth cones* and migrate within the unique territories. In case of precursor cell death, the adjacent NG2<sup>+</sup> cell proliferates to maintain the desired density and fulfill the empty non-occupied space (Hughes et al., 2013).

In response to tissue damage, quiescent aOPCs become activated and starts proliferating and migrating into the lesions. These steps are tightly controlled by cell cycle regulators, such as p27 or Cdk2 (Crockett et al., 2005; Caillava et al., 2011) and migratory regulators including semaphorins (Williams et al., 2007). A recruitment phase is followed by a differentiation phase during which, progenitors have to exit the cell cycle and start extending processes around the axons. This step also requires intrinsic and extrinsic factors, acting both as positive and negative regulators. Among others, the transcription factor Olig2 plays a crucial role in OPCs differentiation and its overexpression correlates with MS lesion activity (Wegener et al., 2015). Extrinsic factors like chemokines and hormones (estrogen, progesterone, and thyroid hormones) are believed to boost remyelination by promoting OL differentiation (Crawford et al., 2010). Innate immune components also take an active role in this process. Anti-inflammatory phagocytes-derived activin-A promotes OPCs maturation and prevents their apoptosis (Miron et al., 2013). Leucin-rich repeat and immunoglobulin-like-domain-containing nogo receptor-interacting protein 1 (LINGO1) is an extensively studied negative regulator of OPC differentiation. Inhibition of this transmembrane glycoprotein promotes axonal integrity and remyelination in the EAE model (Mi et al., 2007). Secondly, astrocytes-expressed Jagged1 is potentially another maturation inhibitor since it is abundant in MS lesions failing to remyelinate. Jagged1 mediates canonical Notch signaling pathway in OPCs and thus inhibits their further differentiation (John et al., 2002). In rodents, remyelination takes place because differentiated, pre-myelinating oligodendrocytes extend their processes, contact the axons and wrap the new myelin around them. However, this process is not as efficient in the MS patients.

### 2.3.2. Involvement of pre-existing OLs

There are important differences in oligodendrocyte and myelin dynamics between the animal models and humans, both under healthy and disease conditions (Yeung, et al. 2014, 2019). Relatively high OLs turnover and effective remyelination driven by OPCs in EAE rodents might not be comparable with MS patients. Indeed, repetitive induction of cortical EAE in rats does not result in permanent reduction of Olig2<sup>+</sup> cells suggesting that the CNS maintains its recovery capacity. As a comparison, human OPCs-driven reparative processes are significantly decreased in chronic subpial demyelination areas with still partial remyelination (Rodriguez et al., 2014). Based on these observations, an alternative pathway was recently suggested, where the surviving adult oligodendrocytes could participate in myelin repair. Firstly, by utilizing a carbon-14 birth-dating technique, it was revealed that the majority of mature OLs from the WM shadow plaques of MS autopsies, were born in the early postnatal life. Data shows that in MS individuals, born before 1955 (peak of the ‘cold war’) who had an onset of disease after that year, the OLs’ carbon-14 levels are as low as never after the cold war, suggesting almost no oligodendrocyte turnover. It is however possible that new oligodendrocytes were generated but not successfully integrated (Yeung et al., 2019). Secondly, oligodendrocyte heterogeneity in MS has been recently described. A study identifies sub-clusters of OLs, which are present only in MS patients as compared to healthy controls. Furthermore, in NAWM and lesions, single-cell analysis of mature oligodendrocytes shows increased upregulation of several genes involved in active myelination in compare to control brains. These findings suggest that pre-existing OLs might contribute to the remyelination process (Jäkel et al., 2019).

Mimicking this hypothesis in animal models can be challenging. Lysolecithin-induced demyelination in the mice spinal cord exposed that pre-existing oligodendrocytes do not participate in myelin restoration (Crawford et al., 2014). As a remark, this model is characterized by substantial oligodendrocyte death in the lesion center. There is however, evidences from cats demyelinating models that, the damaged, mature oligodendrocytes might be able to undergo a healing process and extend processes to set up new myelin sheaths. Electron microscopy pictures highlight single OLs and their internodes, which differ in g-ratio, indicating that a fraction of them was remyelinated while the others survived the initial immune attack (Duncan et al., 2018). Moreover, sustained genetic overexpression of OL’s extracellular signal-regulated kinases 1 and 2 (ERK1/2) in mice results in extending new myelin sheaths in toxin-induced lesion (Jeffries

et al., 2016). Injured oligodendrocytes are able to rescue the pathological pathway and re-extend their processes *in vitro*, possibly restoring functional myelin sheaths (Cui et al., 2017). Furthermore, amputated-state oligodendrocytes remain stable and survive over time in the white matter of EAE mice (Romanelli, 2016). Amputated OLs are found in the MS autopsies, primarily in lesions that are more recent but as well in chronic demyelinated sites (Wolswijk, 2000). These would leave the possibility that remyelination can occur as long as the OLs are not lost.

### 2.3.3. Remyelination failure and new trends in MS therapy

Several elements may contribute to remyelination failure. A hostile environment with outnumbered extrinsic inhibitors and the lack of sufficient pro-regenerative factors can lead to impaired remyelination at the levels of OPC recruitment, differentiation and compact myelin restoration (Wolswijk, 1998; Chang et al., 2002; Kirby et al., 2019). Similar lesion components might prevent recovery of amputated-state oligodendrocytes. Impaired remyelination may also be caused by myelin itself, which under physiological condition acts as a OPCs inhibitor i.e. through ephrinB3. Ineffective myelin debris clearance and phagocytic overload in the lesion prevent precursor cells to migrate and differentiate (Syed et al., 2016). Furthermore, studies in both human and animals show that remyelination dynamics decline with aging (Shields et al., 1999; Kuhlmann et al., 2008). One of the reasons for age-dependent failure is the decreased capacity of myelin removal by phagocytes. In aged, toxin-induced demyelination models, it was recently shown that myelin debris accumulated in the phagocytic cells, leading to toxic cholesterol overload and further cell membrane rupture, which results in infiltration of immune cells and failure of self-resolving inflammation (Cantuti-Castelvetri et al., 2018).

There are two strategies to enhance remyelination, either by supporting the pro-regenerative factors or by removing the inhibitors. Preclinical, functional screening of small molecules led to the selection of remyelination-promoting drug candidates. Micropillar arrays with stem cell-derived OPCs provide a platform, which can be used to identify factors enhancing different steps in OPCs maturation and OL myelination (Mei et al., 2013). Such extensive screening yielded drugs (some already FDA-approved), which are now being investigated in pre-clinical or clinical trials for their pro-remyelinating properties. The most promising compounds in clinical phase II include antagonists of muscarinic acetylcholine (M1) receptor Clemastine fumarate (Green et al., 2017) and histamine (H1/H3) receptor GSK239512

(Schwartzbach et al., 2017). Furthermore, animal data from other selected candidates provide a rationale for testing remyelination enhancement in patients: Miconazole, acting on mitogen-activated protein kinase (MAPK) and ERK1/2 signaling pathway; Clobetasol, activating nuclear glucocorticoid receptors (Najm et al., 2015); Benzotropine, antagonist of mAChR, already approved for Parkinson treatment (Deshmukh et al., 2013). Lastly, thyroid receptor agonist GC1 is believed to stimulate myelination but not cell proliferation and differentiation, a feature that could be utilized in boosting myelination of pre-existing oligodendrocytes within the lesion (Baxi et al., 2014; Preston et al., 2019). Promoting remyelination by actively acting on oligodendrocytes and their precursors is an uprising trend in novel therapy approaches. Overcoming immune-mediated inhibitors, enhancing myelin repair and rejuvenating aged-impaired remyelination is a potential treatment pathway also in the progressive stage of MS.

### **3. In vivo acute and chronic imaging of the oligodendrocytes and myelin**

#### **3.1. Two-photon excitation microscopy**

Introduced for the first time in the early nineties, two-photon excitation microscopy (2PEM) is a major technical advancement in the field of neurobiology, as it allows observing changes in the CNS in the real time *in vivo*. As a type of fluorescent microscopy, 2PEM also utilizes a well-known physical phenomenon of excitation and emission. The technique is based on the principle that two lower energy photons by almost simultaneous absorption, cause fluorophore ('X'FP) excitation and light emission. This combined effect is comparable to that of a single photon with higher energy, as it is in the case of confocal microscopy. 2PEM titanium-sapphire laser emits near-infrared waves in the tunable range of 700-1200nm. Infrared radiation penetrates the tissue up to 1mm, which is a significant difference in compare UV/blue-green light and its penetration limited to 0.1mm. Furthermore, the two-photon excitation volume in the tissue is strictly defined in  $x,y,z$  eliminating the out-of-focus problem and decreasing photobleaching and phototoxicity (Denk et al., 1990; Svoboda et al., 2006).

### 3.2. Dynamic visualization of oligodendrocyte and myelin

*In vivo* imaging of the central nervous system requires physical access to the exposed tissue and selection of labeling tools to visualize cells, structures, organelle and molecules. Several methods have been developed for chronic and acute imaging of the brain and the spinal cord. Imaging the brain involves either thinning the skull bone or implantation of a cranial window that replaces the piece of bone but leaves the dura matter intact. Such windows remain clear for several weeks to months, which provides the possibility of chronic imaging, thus allowing i.e. longitudinal observation of de- and remyelination in the same cortical area (Trachtenberg et al., 2002; Grutzendler et al., 2002). Laminectomy-dependent imaging of the spinal cord is most commonly a single-time point experiment. By using specially designed mouse holders, it facilitates stable time-lapse imaging over several hours (Davalos et al., 2008; Farrar et al., 2012).

Oligodendrocytes and myelination status can be observed with the use of transgenic animals, *in vivo* staining and label-free reflectance microscopy. There are several transgenic mouse models, in which fluorescent tags (cyan [CFP], green [GFP], yellow [YFP], red [RFP] and their variants) are fused to specific proteins or added to 3'UTR end. Mice expressing fluorescent proteins under desired oligodendrocyte promoter are used for cell-fate mapping, OL population heterogeneity assessment or de- and remyelination evaluation. Another powerful tool in transgenic mouse generation is the *Cre/lox* system, which enables not only cell tracking but also cell-specific modification. Transgenic mice carrying *Cre* recombinase under OL lineage promoter can be crossed with reporter mice i.e. Rosa26-Confetti to obtain multicolor cell population (Livet, 2007; Snippert et al., 2010). Its modification; via an *inducible-Cre/lox* system requires additional exogenous ligand like tamoxifen (TM). Such manipulation enables control of *knock-outs* and fluorescence expression activation in place and time. Some of the most common oligodendrocyte reporter mouse lines are shown in the Table 1.

Target	Promoter	Fluorophore	Cre+/-	Reference
OPCs	NG2	mGFP	-	Hughes et al., 2013
	NG2	XFP	+ (TM-inducible)	Zhu et al., 2011
	PDGF $\alpha$ R	XFP	+ (TM-inducible)	Kang et al., 2011
Oligodendrocyte lineage	Olig1	XFP	+	Lu et al., 2002
	Olig2	XFP	+ (TM-inducible)	Dimou et al., 2008
	Olig2	GFP	-	Zhou et al., 2002
	Sox10	XFP	+ (TM-inducible)	Simon et al., 2012
	Sox10	Venus (YFP)	-	Shibata et al., 2010
Mature OLs/ myelin	PLP	eGFP	-	Mallon et al., 2002
	PLP	eGFP	-	Spassky et al., 1998
	PLP	XFP	+ (TM-inducible)*	Doerflinger et al., 2003
	MBP	XFP	+ (TM-inducible)*	Crawford et al., 2016
	Opalin	XFP	+ (TM-inducible)	Crawford et al., 2016
	Opalin	XFP	+ (TM-inducible)	Tripathi et al., 2017
	Opalin	mGFP	+ (TM-inducible)	Tripathi et al., 2017
	CNP	XFP	+	Lappe-Siefke et al., 2003

**Table 1. Transgenic mouse lines.** Common transgenic mouse lines targeting oligodendrocyte precursor cells (OPCs); mature oligodendrocyte (OLs) and myelin; or the whole oligodendrocyte lineage. Fluorophore: XFP – crossing to any reporter mice possible; mGFP – membrane-targeted GFP; eGFP – enhanced GFP. Available variant with *Cre/lox* system indicated as +; additionally, *inducible-Cre/lox* indicated as + (TM-inducible); TM-tamoxifen. \* confirmed non-tamoxifen dependent *Cre* expression.

Another strategy to label cells of interest is a direct gene transfer to the CNS with the help of viruses like adeno-associated viruses (AAVs). Non-pathogenic AAV serves as a vector for transgene delivery and expression *in vivo*. Different AAV serotypes have specific CNS transduction capacity and together with unique promoters can secure cellular specificity of transgene expression. For example, viral construct with a fluorescent protein of choice, under the *Mbp* or *Mag* promoter, targets oligodendrocytes and results in production of fluorescently tagged myelin proteins as early as 14 days after virus administration (von Jonquieres et al., 2016).

Myelin can be detected *in vivo* by applying a specific excitable dye, FluoroMyelin Red/Green<sup>TM</sup> on the exposed brain and spinal cord. This is a water-soluble, lipophilic fluorescent agent with selectivity for myelin due to its high lipid content. Another dye, case myelin compound (CMC), a coumarin derivative, can be administrated in mice with a single intravenous injection into the tail vein. CMC was shown to stain myelin sheaths in the peripheral nervous system but also by crossing the BBB in the central nervous system. However, studies with CMC suggests that this dye does not stain the cortical grey matter (Wang et al., 2010). Lastly, spectral confocal reflectance microscopy (SCoRe) is a high resolution imaging technique which allows *in vivo* assessment of myelination status in the PNS and CNS. It is a label-free, relative easy to implement method, which utilizes the high refractive index of lipid-rich myelin. Myelin is visualized by merging simultaneous light reflection of myelin sheaths generated by confocal laser beams of three different wavelengths (Schain et al., 2014).



## Chapter II – Aim of the study

Demyelination, followed by remyelination, is the key pathological feature of the central nervous system in multiple sclerosis. However, the dynamics of oligodendrocytes and myelin damage and their survival as well as recovery capabilities remain elusive. Moreover, based on the recent findings (Nave and Ehrenreich, 2019), it is debated if and to what extent restored myelin can be derived from pre-existing OLs, which underwent the healing process. Giving the above, the overall aim of my PhD project was to investigate the fate of surviving oligodendrocytes under inflammatory conditions by utilizing multiphoton and confocal microscopy and single-cell OL viral labeling techniques.

The first part of my project was focused on characterization demyelinating lesions in the white matter of the spinal cord. This part aimed to answer the following questions:

- What is the sequence of myelin damage in EB and EAE models?
- What is the fate of affected oligodendrocytes? Are they immediately stepping towards the cell death pathway?

The obtained results provided the basis for the second part of the project, which investigated demyelination and remyelination dynamics at both, population and single-cell level, in the inflamed cortical grey matter. This part aimed to answer the following questions:

- Is the sequence of demyelinating events in grey matter similar to white matter? Does age influence remyelination efficiency?
- What are the oligodendrocyte population characteristics during the course of the disease?

By using longitudinal *in vivo* imaging techniques we further asked:

- What is the remyelination efficiency at the population level of the defined areas? Further, what is oligodendrocyte turnover and can amputated-state oligodendrocytes survive over time?

- Is the restored myelin compact?
- How to visualize oligodendrocyte and its myelin with a single-cell resolution?
- What is the contribution of pre-existing oligodendrocytes in remyelination?

The results from the first part of the project are published in a peer-reviewed journal (Romanelli, Merkler, **Mezydło**, (...) Misgeld & Kerschensteiner, *Nature Communications*, 2016). Single-cell oligodendrocyte's viral labelling approaches are included in manuscript (Snaidero, Schifferer, **Mezydło**, Kerschensteiner & Misgeld, BioRxiv: 2019.12.16.877597, 2019). *In vivo* cortical remyelination results from the second project are included in manuscript, which is currently in preparation (**Mezydło** et al., 2020; manuscript in preparation).

## Chapter III – Material and Methods

### 1. Materials

#### 1.1. Surgery procedures

Medication and reagents		
<i>KX anesthesia</i>	Ketamine 10% (Ketamine hydrochloride)	Bela-Pharm GmbH, Vechta, Germany
	Xylazin 20mg (Xylazine)	Serumwerk Bernburg AG, Bernburg, Germany
<i>ISO anesthesia</i>	Isofluran CP (Isoflurane)	CP-pharma GmbH, Burgdorf, Germany
<i>MMF anesthesia</i>	Fentanyl 0.05mg	B.Braun AG, Melsungen, Germany Ratiopharm GmbH, Ulm, Germany
	Midazolam 5mg	
	Cepetor 1mg (Medetomidine hydrochloride)	CP-pharma GmbH, Burgdorf, Germany
<i>Anesthesia antagonist</i>	Revertor 5mg (Atipamezole hydrochloride)	CP-pharma GmbH, Burgdorf, Germany
	Naloxon 0.4mg (Naloxone hydrochloride)	B.Braun AG, Melsungen, Germany
	Flumazenil 0.1mg	Hameln GmbH, Hameln, Germany
<i>Analgesia</i>	Temgesic 0.324mg (Buprenorphine hydrochloride)	Reckitt Benckiser GmbH, Heidelberg, Germany
	Xylocain 2% (Lidocaine hydrochloride)	Aspen GmbH, Munich, Germany
<i>Antibiotics</i>	Baytril 2.5% (Enrofloxacin)	Bayer AG, Leverkusen, Germany
<i>Sterile artificial mouse cerebrospinal fluid (aCSF) (Solution A and B in 1:1 ratio)</i>	Solution A: 8,66 g NaCl	(Merck)
	0,224 g KCl	(Merck)
	0,206 g CaCl <sub>2</sub> · 2H <sub>2</sub> O	(Sigma-Aldrich)
	0,163 g MgCl <sub>2</sub> · 6H <sub>2</sub> O	(Sigma-Aldrich)
	Solution B: 0,214 g Na <sub>2</sub> HPO <sub>4</sub> · 7H <sub>2</sub> O	(Merck)
	0,027 g NaH <sub>2</sub> PO <sub>4</sub> · H <sub>2</sub> O dH <sub>2</sub> O ad 500 ml	(Merck)
<i>Other</i>	Agarose	Sigma-Aldrich Chemie GmbH, Taufkirchen, Germany
	Ethidium Bromide solution 10mg/ml	
<i>Hydration solution</i>	Ringerlösung Fresenius (Ringer's solution) Glucose 5% Saline (NaCl 0.9%)	B.Braun AG, Melsungen, Germany

<b>Skin and eye protection /disinfection</b>	Bepanthen Augen- und Nasensalbe 5 g (eye ointment)	Bayer AG, Leverkusen, Germany
	Cutasept Lösung 250 ml (antiseptic spray)	Bode Chemie GmbH & Co, Hamburg, Germany
	Braunovidon Salbe 10% (Povidon iod)	B.Braun AG, Melsungen, Germany
	Ethanol 70%	CLN GmbH, Niederhummel, Germany
<b>Cortical window</b>	Paladur (Dental cement set)	Kulzer GmbH, Hanau, Germany
	Histoacryl (Topical skin adhesive)	B.Braun AG, Melsungen, Germany

<b>Tools and materials</b>		
<b>Syringes and needles</b>	Syringe 3pc 3 and 5ml Omnifix luer slip	B.Braun AG, Melsungen, Germany
	BD Plastipak Hypodermic luer slip syringe 1ml	Becton, Dickinson&Co, Franklin Lakes, USA
	Hypodermic Needles BD Microlance 3 30 Gauge (0,3 mm, yellow)	
<b>Tissue exposure tools</b>	Feather blade, surgical scalpel	Pfm medical AG, Cologne, Germany
	Noyes Spring Scissors (big)	
	Vannas-Tübingen Spring Scissors (small)	FST GmbH, Heidelberg, Germany
	Dumont Mini Forceps Inox Style 3 (big)	
	Dumont Mini Forceps Inox Style 5 (small)	
<b>Wound closure</b>	Ethicon Ethilon monofil 6-0 size (skin)	Johnson&Johnson Medical GmbH, Norderstedt, Germany
	Ethicon Vicryl 4-0 size (internal)	
	AutoClip system	FST GmbH, Heidelberg, Germany
<b>Cranial window</b>	4mm Ø coverslip for cranial window	Warner Instruments, Hamden, USA
	Metal head bar	Hager&Meisinger GmbH, Neuss, Germany
	Stainless Steel Burs 1 HP 0.5mm	
<b>Other</b>	Blaubrand intraMark micropipettes (Ultrathin pulled glass pipette)	Brand GmbH & Co KG, Wertheim, Germany
	Sugi	Kettenbach GmbH&Co KG, Eschenburg, Germany

<b>Devices</b>		
<b>Microscope</b>	Olympus KL 1500 LCD (light source for stereomicroscopy)	Olympus Deutschland GmbH, Hamburg, Germany
	Olympus Stereo Microscope SZ51	(Headquarter in Japan)
<b>Sterilizer</b>	FST 250 Hot Bead Sterilizer	FST GmbH, Heidelberg, Germany

<i>Other</i>	T/Pump Heating Pad Hammer MicroMotor Kit 0-25000	Gaymar Industries, NY, USA Foredom Electric Co. Connecticut, USA
--------------	---	--

### 1.2. Systemic and cortical EAE induction

Reagents		
<i>MOG emulsion</i>	Purified recombinant MOG (N1-125, from E. Coli)  Mycobacterium Tuberculosis H37 RA Incomplete Freund's adjuvant (IFA) Pertussis toxin from Bordetella pertussis, inactivated Acetate buffer 20mM pH 3.0	Stock solution, produced by laboratory of Doron Merkler (University of Geneva) and by laboratory of Martin Kerschensteiner  Sigma-Aldrich Chemie GmbH, Taufkirchen, Germany
<i>Cortical EAE</i>	TNF-alpha IFN-gamma  Bovine Albumin Serum (BSA) Fraction V	R&D System, Minneapolis, USA Peprotech GmbH, Hamburg, Germany Sigma-Aldrich Chemie GmbH, Taufkirchen, Germany

Tools and materials		
	Hamilton 10 ml syringes Hypodermic Needles BD Microlance 3 23 Gauge (0,6 mm, blue)	Hamilton Becton, Dickinson&Co, Franklin Lakes, USA

### 1.3. Perfusion and immunohistochemistry

Reagents		
<i>Perfusion / microdissection</i>	PFA 4% (paraformaldehyde) in PBS pH 7.4, ready-to-use; stored in 4 °C for max 2 weeks Sucrose 30%  Sodium azide 0.1% in PBS 1x  Heparin-Natrium 25.000IE (Heparin sodium)	Morphisto GmbH, Frankfurt a.M, Germany Sigma-Aldrich Chemie GmbH, Taufkirchen, Germany Sigma-Aldrich Chemie GmbH, Taufkirchen, Germany Ratiopharm GmbH, Ulm, Germany

<i>IHC/IF</i>	PBS 10x (phosphate buffered saline) pH 7.4 Triton X-100 Sodium Citrate Buffer 10mM pH 8.5 Methanol 100% Gibco goat serum  Tissue-Tek O.C.T (Cryoprotection) Vectashield Mounting Medium	Sigma-Aldrich Chemie GmbH, Taufkirchen, Germany  Invitrogen GmbH, Darmstadt, Germany Sakura Fintek Ltd, Tokyo, Japan Vector Laboratories Inc., Burlingame, USA
---------------	--	---

<b>Antibodies, dyes and tracers</b>		
<i>Primary antibodies</i>	Anti-APC/CC1 monoclonal mouse; #OP80  Anti-MBP polyclonal rabbit; #A0623  Anti-PDGF $\alpha$ R polyclonal rabbit; #3164  Anti-Olig2 polyclonal rabbit; #AB9610  Anti-NG2 polyclonal rabbit; # AB5320	Calibochem; Merck Millipore, Darmstadt, Germany Dako/Agilent Tech, Santa Clara, USA  Cell Signaling Tech, Danvers, USA  Merck Millipore, Darmstadt, Germany Merck Millipore, Darmstadt,
<i>Secondary antibodies</i>	Goat-anti-rabbit AlexaFluor 594 Goat-anti-mouse AlexaFluor 594 Goat-anti-rabbit AlexaFluor 647	Invitrogen GmbH, Darmstadt, Germany
<i>Dyes / Tracers</i>	DAPI NeuroTrace 640/660 fluorescent Nissl FluoroMyelin 488 fluorescent myelin stain	Invitrogen GmbH, Darmstadt, Germany

<b>Tools and materials</b>		
<i>IHC/IF</i>	Microscope slides 76x26 mm Microscope cover slips 24x60 mm  12-well cell culture  15 and 50ml centrifuge tubes  Pipettes, pipette tips and tubes (0.5, 1.5, 2 ml)	Gerhard Menzel Glasbearbeitungswerk GmbH, Braunschweig, Germany Becton, Dickinson and Company, Franklin Lakes, USA Greiner Bio-One GmbH, Frickenhausen, Germany Eppendorf AG, Hamburg, Germany

Devices		
<i>Perfusion</i>	Ismatec IP high precision multichannel pump	ISMATEC SA, Labortechnik - Analytik, Glattbrugg, Switzerland
<i>IHC/IF</i>	Leica CM1850 (cryostat)	Leica Microsystems GmbH, Wetzlar, Germany
	Vortex-Genie 2 (vortex)	Scientific Industries Inc., Bohemia, USA
	Polymax 1040 (shaker)	Heidolph Instruments GmbH, Schwabach, Germany

#### 1.4. Viral labelling strategy

Viruses		
<i>Rabies</i>	Rabies virus SAD $\Delta$ G (CVS G) mcherry	Provided by K-K. Conzelmann, GeneCenter LMU, Munich
<i>AAV</i>	AAV- <i>Mbp</i> :mem-tdTomato	in-house made
	AAV- <i>Mbp</i> :mem-tdTomato-2A-paEGFP	Custom-made by Vector BioLab, Malvern, USA
	AAV- <i>Mbp</i> :DIOfem-tdTomato	
	AAV- <i>Mbp</i> :CreERT2	

Cloning strategy		
<i>DNA</i>	Vector with <i>Mbp</i> promoter (first 1.3kB of the promoter region)	DNA synthesized by Metabion AG, Planegg, Germany
	Membrane tag sequence (5' TGCTGTGCTGCATCAGAAGAACTAA ACCGGTTGAGAAGAATGAAGAGGCCGA TCAGGAGCTGCAGTCGACGGTACCGCG GGCCCGGGATCCACCGGTCGCCACC)	
<i>Plasmid</i>	AAV- <i>Cmv</i> :mem-tdTomato	Provided by F. Bareyre, BMC, Munich
	AAV- <i>Mbp</i>	In-house made
<i>DNA extraction</i>	Qiagen Plasmid Maxi Kit #12165	Qiagen GmbH, Hilden, Germany
<i>Restriction enzymes / cloning kit</i>	AgeI-HF, BmtI-HF SalI-HF, MluI-HF	New England Biolabs Ltd, Ipswich, USA
	CutSmart buffer	
	dNTPs	
	DNA polymerase I (Klenow)	Invitrogen GmbH, Darmstadt,
	T4 Ligase, Ligase buffer	
	Electrocompetent cells + S.O.C. kit	

<b>Virus production</b>		
<b>Chemicals</b>	Polyethylenimine (PEI) 1mg/mL pH 7.0 Polyethylene glycol (PEG) 8000 40% pH 7.4 Benzonase Iodixanol 60% Phenol Red	Sigma-Aldrich Chemie GmbH, Taufkirchen, Germany
<b>Buffers</b>	<u>NaCl/PBS-MK 1M (filtered)</u> 5,84 g NaCl 0,026.3 g MgCl <sub>2</sub> 0,01491 g KCl add PBS 1x 100mL  <u>PBS-MK 1M (filtered)</u> 0,026.3 g MgCl <sub>2</sub> 0,01491 g KCl add PBS 1x 100mL  <u>100X Pluronic F-68</u> Stock A – 0.1% P-F68 Stock B – 0.01% P-F68 Stock C – 0.001% P-F68 + NaCl 200mM Formulation Buffer: Pluronic-F68 0.001%  <u>Lysis buffer pH 8.5</u> NaCl 150mM Tris-HCl 50mM	Sigma-Aldrich Chemie GmbH, Taufkirchen, Germany  Sigma-Aldrich Chemie GmbH, Taufkirchen, Germany  Invitrogen GmbH, Darmstadt, Germany  Sigma-Aldrich Chemie GmbH, Taufkirchen, Germany
<b>Cell culture</b>	Dulbecco's Modified Eagle Medium (DMEM) Fetal Bovine Serum (FBS) Penicillin/Streptomycin 10.000U  HEK-293 cells  pAD-Helper AAV-Capsid Advanced Roswell Park Memorial Institute (aRPMI) Transfection Medium	Invitrogen GmbH, Darmstadt, Germany Invitrogen Sigma-Aldrich Chemie GmbH, Taufkirchen, Germany Provided by M. Goetz, BMC, Munich University of Pennsylvania, Philadelphia, USA Invitrogen GmbH, Darmstadt, Germany
<b>Materials</b>	Membrane filters 0.22 µm Membrane filters 0.45 µm Conical tubes 50mL	Merck Millipore, Darmstadt, Germany

	Petri-dish plates Ø15cm Quick-Seal polypropylene tube  Hypodermic Needle-Pro 18G  Amicon Ultra Centrifugal filter	Falcon, ThermoFisher Scientific, Waltham, USA Beckman Coulter Inc., Brea, USA B.Braun AG, Melsungen, Germany Merck Millipore, Darmstadt, Germany
<b>Devices</b>	Heraeus Multifuge XCR  Optima L-90K UltraCentrifuge	ThermoFisher Scientific, Waltham, USA Beckman Coulter Inc., Brea, USA

### 1.5. Electron microscopy

<b>Reagents</b>		
<b>Perfusion / post-fixation</b>	Hank's Balanced Salt Solution (HBSS) Glutaraldehyde 50% Formaldehyde 16% Osmium tetroxide 2% (EMS) in sodium cacodylate buffer 0.1M pH 7.4 Potassium ferricyanide 2%	Invitrogen GmbH, Darmstadt, Germany Electron Microscopy Sciences, Hatfield, USA Science Services GmbH, Munich, Germany
<b>preparation</b>	LX112  Epon- embedding	LADD Research Industries Inc. Williston, USA Serva Electrophoresis GmbH, Heidelberg, Germany

#### Tools, materials, devices

<b>Microscope</b>	Crossbeam Gemini 340 SEM	Carl Zeiss AG, Oberkochen, Germany
<b>Other</b>	TRIM90 diamond knife Ultra diamond knife ATUMtome Powertome, RMC  Plasma-treated, carbon-coated Kapton tape Carbon tape  Silicon wafers (4-inch)	Diatome AG, Nidau, Switzerland Science Services GmbH, Munich, Germany In-house made Science Services GmbH, Munich, Germany Siegert Wafer GmbH, Aachen, Germany

## 1.6. Imaging

Devices		
<b>Microscopes and objectives</b>	<p><u>FV1000 confocal system mounted on an upright BX61 microscope;</u> <i>Equipped with an y10/0.4 water immersion objective and x20/0.85 and x60/1.42 oil immersion objectives</i></p> <p><u>Olympus FV1000 MPE multiphoton microscope;</u> <i>Equipped with X25/1,05 water immersion objective; femtosecond-pulsed Ti:Sapphire laser (Mai Tai HP, Newport/Spectra Physics) and opto-electrical intensity regulation</i></p> <p><u>Olympus FV 1200 MPE-RS multiphoton microscope;</u> <i>Equipped with X25/1,05 water immersion objective; femtosecond-pulsed Ti:Sapphire laser (Mai Tai HP-DS, Newport/Spectra Physics) and opto-electrical intensity regulation</i></p>	Olympus Deutschland GmbH, Hamburg, Germany (Headquarter in Japan)
<b>Clamping devices</b>	<p>Spinal clamping device (spinal adaptor for a stereotaxic frame)</p> <p>Head-fix device</p>	Narishige Inc., NY, USA
<b>Tracheotomy</b>	<p>Small animal ventilator</p> <p>Intratracheal cannula (1.0mm OD, 13 mm length )</p>	Harvard apparatus Ltd, Cambridge, USA

## 1.7. Software

Data analysis		
<b>Image processing</b>	<p>Adobe Creative Suite CS6 (Photoshop, Illustrator)</p> <p>ImageJ</p> <p>IMOD (EM reconstruction)</p>	<p>Adobe Systems, Inc., San Jose, California, USA</p> <p>General Public License <a href="http://rsbweb.nih.gov">http://rsbweb.nih.gov</a></p>

	Berger's Vast lite (EM reconstruction)	General Public License, D. Mastronarde. UColorado <a href="https://bio3d.colorado.edu/imod">https://bio3d.colorado.edu/imod</a>  Developed by Seung (MIT) and Lichtman (Harvard) <a href="https://software.rc.fas.harvard.edu/lichtman/vast/">https://software.rc.fas.harvard.edu/lichtman/vast/</a>
<b>Statistics</b>	Microsoft Office Excel  GraphPad Prism 7.0	Microsoft Corporation, Redmond, USA  GraphPad Software, La Jolla, USA

## **2. Experimental Animals**

Experiments were performed on young adult mice of both sexes from 3 to 5 months of age and, where indicated, 9 to 11 months of age (so-called 'aged' animals). Female and male were equally distributed into control and experimental groups. All animals were bred in our animal facilities and uniformly housed under standard conditions (12h light/dark cycle; maximum 5 mice/cage; autoclaved food and water supplied *ad libitum*). Animals with F1 background of C57BL/6 (strain designation C57BL/6J, Jackson Laboratories) and BiozziABH (strain designation BiozziABH/RijHsd, Harlan Laboratories) were used in the different project's parts. To assess myelin and OL's processes pathology at the population level, I used *Plp:eGFP* (Mallon et al., 2002) x BiozziABH. For viral labelling of single OLs, either *Plp:eGFP/BiozziABH* or C57BL/6 / BiozziABH were used.

All animal experiments were performed in accordance with regulations of the relevant animal welfare acts and protocols approved by the respective regulatory bodies (Regierung von Oberbayern).

## **3. Methods**

### **3.1. EAE induction**

Systemic EAE was induced in young adult (3 to 5 months) and aged (9 to 11 months) mice as previously described (Romanelli et al., 2016). Briefly, *Plp:eGFP/BiozziABH* and C57BL6J/BiozziABH animals were immunized subcutaneously with a total volume of 250µl of an emulsion, which contains 50µg of purified

recombinant myelin oligodendrocyte glycoprotein (MOG, N1-125, expressed in *E. coli*) and complete Freund's adjuvant (supplemented with 10 mg/mL *Mycobacterium Tuberculosis* H37Ra). Immunization was repeated one week later. Additionally, pertussis toxin (100ng) was injected intraperitoneal at day 0 and 1 for both immunizations.

Animals were weighted daily and classified by an EAE scoring system according to the severity of neurological deficits: 0 – no detectable clinical signs; 0.5 – partial tail weakness; 1 – complete tail paralysis; 1.5 – gait instability; 2 – hind limb paresis; 2.5 – hind limb paresis with partial dragging; 3 – complete hind limb paralysis; 3.5 – complete hind limb paralysis and forelimb paresis; 4 – hind and fore limb paralysis; 5 – death.

### 3.2. Cortical EAE induction

*Plp:eGFP/BiozziABH* and *C57BL6J/BiozziABH* mice with a clinical EAE score were used to induce the cortical lesions. Cortical EAE induction was performed 21 days after initial systemic EAE immunization. Animals, anesthetized with MMF (Medetomidine (0.5 mg/kg), Midazolam (5 mg/kg) and Fentanyl (0.05 mg/kg)) were given stereotaxic intracerebral injection of 2µl of cytokine mix - 0.25µg/µl TNF-alpha and 750U/µl IFN-gamma in PBS/0.1% BSA. Surgery procedures as follows; after opening of the disinfected scalp, a fine hole was drilled into the skull with 0.4mm stainless drill head; coordinates - 1.2 mm lateral, 0.6 mm caudal to Bregma. A glass capillary (Ø 25µm) containing cytokines was inserted into the cortex at the depth of 0.8mm and the volume was injected over 15 minutes. After the surgery, animals were injected with 250µl of saline/glucose 5% solution for rehydration and anesthesia antagonist (Naloxone (1.2 mg/kg), Flumazenil (0.5 mg/kg), Atipamezole (2.5 mg/kg)). Analgesia (buprenorphine 0.1 mg/kg) was applied every 12 hours on the days following surgery.

### 3.3. Immunofluorescence

Animals were lethally anesthetized with Isoflurane and perfused transcardially with 15-20mL Heparin-1xPBS followed by 25mL of 4% paraformaldehyde in phosphate buffered saline using peristaltic pump, velocity 6 mL/min. Tissue was post-fixed for 12-24 hours in 4% PFA, isolated and cryoprotected in 30% sucrose for 48-72 hours. Samples were embedded in Tissue-Tek O.C.T., froze down in -20°C and cut in 40µm-50µm thick longitudinal (spinal cord) / coronal (brain) sections using cryostat. A free-floating

staining method was used to visualize selected markers. Sections were rinsed with 1xPBS at room temperature and blocked for 1 hour with 10% goat serum (GS) in 0.5% Triton X-100/1xPBS. An antigen retrieval step was necessary to unmask anti-NG2 and anti-PDGFR. Sections were treated with pre-heated 10mM sodium citrate buffer pH 8.5 for 25 min at 85°C and further rinsed with 1xPBS before proceeding to the blocking step. Methanol treatment was needed to obtain crisp MBP staining. Sections were incubated in cold methanol for 20 min in -20°C and further rinsed with 1xPBS before proceeding to blocking step.

Sections were incubated overnight at 4°C (shaking) with the following primary antibodies: mouse anti-APC/CC1 (1:150); rabbit anti-NG2 (1:250); rabbit anti-PDGFR (1:200); rabbit anti-MBP (1:200); rabbit anti-Olig2 (1:250) in 1% GS in 0.5% Triton X-100/1xPBS. Sections were washed with 1xPBS and incubated overnight at 4°C with (1:1000) AlexaFluor-conjugated goat anti-mouse 594 (APC/CC1); goat anti-rabbit 594 (PDGFR, MBP, Olig2); goat anti-rabbit 647 (NG2) antibodies. Samples were counterstained with Nissl-like NeuroTrace 640/660 (1:500) or DAPI (1:10 000) and later mounted with Vectashield.

### 3.4. Confocal microscopy

Immunofluorescently stained samples were imaged with upright Olympus Fv1000 confocal microscopy system equipped with x10/0.4 air, x20/0.85 and x60/1.42 oil immersion objectives. To assess oligodendrocytes and myelin damage in the WM of the spinal cord in *Plp:eGFP/BiozziABH*, high magnification images were taken with x60/1.42 oil objective with digital zoom of 4.0, z-spacing 200nm and pixel resolution 0.082 $\mu\text{m}$  pixel<sup>-1</sup>. To define oligodendrocyte populations and myelin recovery in GW of the cortex in *Plp:eGFP/BiozziABH*, images were taken with x60/1.42 oil objective, z-spacing 300nm and pixel resolution 0.267 $\mu\text{m}$  pixel<sup>-1</sup>. Images were obtained using standard filter sets and processed with ImageJ or Adobe Photoshop software.

*SCoRe*: Overall cortical myelin status in C57BL6J/BiozziABH (injected with AAV-*Mbp*:mem-tdTomato) was assessed by spectral confocal reflectance microscopy (SCoRe) as previously described (Schain et al., 2014). Briefly, 3 fixed wavelengths lasers -488, 539, 633 were used to generate the SCoRe signal within the first 50 $\mu\text{m}$  of the *in vivo* imaged somatosensory cortex. After the last *in vivo* imaging session (in details in 3.10.2 *in vivo* 2PM imaging, cortex) mice were perfused, intact brains were placed under the confocal

microscope and SCoRe was performed on the areas of interest containing 2PM-imaged mem-tdTomato+ OLs.

### 3.5. AAV vector generation and virus production

AAV-mem-tdTomato plasmid in which reporter gene expression was controlled under *Mbp* promoter (AAV-*Mbp*:mem-tdTomato) was generated by replacing the *Cmv* promoter in AAV backbone plasmid (AAV-*Cmv*:mem-tdTomato) with the first 1.3 kb of *Mbp* promoter. In short, AAV-*Cmv*:mem-tdTomato containing bovine growth hormone polyadenylation sequence (bGHpolyA) flanked by AAV2 inverted terminal repeats, was digested with AgeI-HF/BmtI-HF to replace the *Cmv* promoter with 1.3kb *Mbp* gene excised with Sall-HF/MluI-HF from AAV-*Mbp*. Both, the backbone and the insert were blunted with DNA polymerase I (Klenow) and dNTPs for 10 min in room temperature and further ligated by T4 Ligase in T4 Ligase buffer for 2 days in 16°C. Construct with correctly orientated insert (checked by PCR size) was introduced to competent cells through electroporation and the DNA-Bacteria Mix was left for overnight incubation at 37°C. Plasmid purification was performed with Qiagen Plasmid Maxi Kit accordingly to the attached protocol.

AAV vector packaging was performed using human embryonic kidney 293 (HEK 293) cells. Briefly, HEK 293 cells were transfected with pAD-Helper, AAV-Capsid and AAV-Construct (molar ratio 3:2:5) by RPMI:PEI incubation protocol. AAV vector was harvested from the supernatant (with PEG solution) and the pellet. Freeze/thaw cycles were utilized to lyse the cells. Any residual DNA from the packaging process was degraded with benzonase before proceeding to purification step. Vectors were purified using iodixanol gradient ultracentrifugation and concentrated by subsequent incubation/centrifugation with formulation buffer (Pluronic-F68 0.001%). Obtained ~300µl of the virus was stored in small aliquots in -80°C. Genomic titers was ~2.5 x 10<sup>13</sup>.

### 3.6. Single-cell labelling in the spinal cord

At the day 4 to 6 post immunization, *Plp*:eGFP/BiozziABH animals anesthetized with KX (Ketamine (87 mg/kg), Xylazine (13 mg/kg)) were given stereotaxic injection of 0.5µl of undiluted rabies virus SAD ΔG mcherry into the white matter of the spinal cord. The dorsal spinal cord was exposed as previously described (Romanelli et al., 2013). Briefly, laminectomy was performed in the lumbar region; dorsal half

of one vertebra was removed while the dura matter remained untouched. Glass capillary ( $\varnothing$  25 $\mu$ m) containing virus was inserted into the white matter at the depth of 0.2-0.4mm and the volume was injected over 15 minutes. Each mouse received two equal injections. After the procedure, muscles were sutured at first, followed by skin closure. Animals were injected with 250 $\mu$ l of saline/glucose 5% solution for rehydration. Analgesia (buprenorphine 0.1 mg/kg) was applied every 12 hours on the days following surgery.

Animals were kept for maximum of 9 days. For 2PM time-lapse experiment, mice were imaged at weight loss, at the onset of the disease and 1 or 2 days after the onset. Each time, mice were sacrificed after the imaging session.

### 3.7. Ethidium bromide model

Toxin-induced demyelination was performed as previously described (Fushimi and Shirabe, 2002) in *Plp:eGFP/BiozziABH* animals. Anesthesia, laminectomy and post-surgery treatment was performed as described above (3.6. Single-cell labelling in the spinal cord). Glass capillary ( $\varnothing$  25 $\mu$ m) containing 0.5 $\mu$ l of ethidium bromide (1mg/ml) was inserted into the ventral funiculus of the lumbar spinal cord at the depth of 1.2mm and the volume was injected over 15 minutes. Control animals were injected with 0.5 $\mu$ l of saline using the same protocol. Mice were sacrificed 4 days after the surgery.

### 3.8. Single-cell labelling in the cortex

At the day of initial immunization or 21 days before first imaging session in control (non-immunized, cytokines injected) animals, C57BL6J/BiozziABH received a single intracerebral injection of the AAV-*Mbp:mem-tdTomato*. Anesthesia, skull-hole generation and post-surgery treatment was performed as described above (3.2. Cortical EAE induction). For the vital labelling of OLs, 1 $\mu$ l of the virus was stereotactically injected into the somatosensory cortex; coordinates - 2 mm lateral, 2 mm caudal to Bregma, depth 0.1-0.2 mm. For 2PM longitudinal myelination analysis, mice were imaged before cortical EAE induction, 3 days after the cortical EAE induction (peak of demyelination) and 14 to 16 days after cortical EAE induction (remyelination phase). Mice were sacrificed after the last imaging session.

### 3.9. Cranial window surgery

To gain optical access to the animal cortex for monitoring myelin status and oligodendrocyte recovery over time, I have performed a craniotomy and implanted a cranial window above the somatosensory cortex of the *Plp:eGFP/BiozziABH* and *C57BL6J/BiozziABH* (injected with AAV-*Mbp:mem-tdTomato*) animals as previously described (Holtmaat et al., 2009). In short, animals anesthetized with MMF (Medetomidine (0.5 mg/kg), Midazolam (5 mg/kg) and Fentanyl (0.05 mg/kg)) were head-fixed in the stereotaxic frame and the head skin was disinfected. Craniotomy was performed with 0.5 mm stainless steel drill head and the skull loss was substituted with Ø 4mm cover glass which was sealed using histoacryl glue and the dental cement. After the surgery, animals were injected with 250 µl of saline/glucose 5% solution for rehydration and anesthesia antagonist (Naloxone (1.2 mg/kg), Flumazenil (0.5 mg/kg), Atipamezole (2.5 mg/kg)). Analgesia (buprenorphine 0.1 mg/kg) and antibiotic's treatment (Baytril 2.5%) was applied every 12 hours on the days following surgery. Cranial window was implanted on the day of first imaging session.

### 3.10. *In vivo* 2PM imaging

#### 3.10.1. Spinal cord

For acute *in vivo* imaging of the sequence of myelin damage, *Plp:eGFP/BiozziABH* (injected with rabies virus SAD ΔG mcherry) animals were used. Mice anesthetized with KX (Ketamine (87 mg/kg), Xylazine (13 mg/kg)) were imaged using Olympus FV1200 MPE equipped with femto-second pulsed Ti:Sapphire lasers (tuned at 840 nm for eGFP-oligodendrocytes, and 910nm for viral-induced expression of mcherry) with maximum power of 30mW at the back focal plan, 25x/1.25 water-immersion Olympus objective; digital zoom of 3.0, pixel resolution 165nm pixel<sup>-1</sup>, z-spacing 500nm, dwell time of 2µs. Single oligodendrocytes were imaged for 270-330 min. Control animals (healthy) with or without rabies virus SADΔG mcherry injection were performed in order to exclude phototoxicity, virus-induced damage or anesthesia and surgery related disturbances. No signs of oligodendrocyte and myelin damage were detected (n=5 mice, 270-330min).

Dorsal spinal cord was exposed as previously described (Nikić et al., 2011). Briefly, skin was disinfected and cut along the spinal cord. Dorsal half of 3 vertebrae were removed and the opening was kept hydrated

with artificial cerebrospinal fluid (aCSF). Vertebral column was position-fixed by spinal clamping device allowing controlled movement in x, y, z directions during imaging session. A 4% agarose well was built up around the spinal opening and filled with aCSF. Tracheotomy and intubation was performed to minimize breathing artefacts. Mice were sacrificed after the imaging session.

### 3.10.2. Cortex

For chronic *in vivo* imaging of oligodendrocyte and myelin recovery in the cortical lesions, *Plp:eGFP/BiozziABH* or *C57BL6J/BiozziABH* (injected with the *AAV-Mbp:mem-tdTomato*) animals were used. Cranial windows were implanted on the day of first imaging session as described above (3.9. Cranial window surgery). The same areas were imaged over the course of the disease: before cEAE induction (baseline), at 3 days after cEAE induction and in the recovery phase (day 14 to 16 after cEAE induction). Accordingly, control non-immunized animals were imaged before cytokines injection (baseline), 3 and 14 days after the cytokines injection. Animals with decreased cranial window quality throughout the imaging course were excluded from analysis. No phototoxicity in control and cEAE animals was observed.

Animals were anesthetized with MMF (Medetomidine (0.5 mg/kg), Midazolam (5 mg/kg) and Fentanyl (0.05 mg/kg)) and placed on the microscope imaging stage with head-fix device. Imaging was performed on 3 to 5 areas of interest of layer 1 somatosensory cortex at 15Hz with Olympus MPE-RS resonant scanner using a femto-second pulsed Ti:Sapphire laser (tuned at 1040nm for viral-induced expression of mem-tdTomato in oligodendrocytes and their processes) with maximum power of 20mW at the back focal plan, 25x/1.25 water-immersion Olympus objective; digital zoom of 3.0, pixel resolution 165nm pixel<sup>-1</sup>, z-spacing 500nm, dwell time of 4μs. After each imaging session, animals were injected with 250μl of saline/glucose 5% solution for rehydration and anesthesia antagonist (Naloxone (1.2 mg/kg), Flumazenil (0.5 mg/kg), Atipamezole (2.5 mg/kg))

### 3.11. Correlative light-to-electron microscopy

*C57BL6J/BiozziABH*, injected with *AAV-Mbp:mem-tdTomato*, were lethally anesthetized with isoflurane and perfused transcardially with 5mL HBSS followed by 30mL of EM-fixative (2.5% glutaraldehyde, 4% paraformaldehyde in phosphate buffered saline) using peristaltic pump. Tissue was extracted and post-

fixed for 8 hours at 4°C in EM-fixative. After post-fixation, brains were positioned back under the 2P microscope so the area of interest could be found. Asymmetric near-infrared brandings (NIRB) were performed around previously imaged area (1.0/1.0 mm) in order to enable further identification of specific oligodendrocytes with EM. Tissue was sequentially treated, first with 2% osmium tetroxide (EMS) in sodium cacodylate buffer pH 7.4 and later with 1.5% potassium ferricyanide in the same buffer; each treatment lasted for 2x45 min. Dehydrated by ethanol and infiltrated with LX112, samples were sectioned. Consecutive 50nm thick sections were generated with a 35° ultra-diamond knife and collected on plasma-treated, carbon-coated Kapton tape. EM of larger, pre-defined area of interest (based on venous architecture and NIRB marks) was obtained on a Zeiss Crossbeam Gemini 340 SEM with a four-quadrant backscatter detector at 8kV. At first, the overview low-resolution images (5000nm pixel<sup>-1</sup>) were taken to more precisely define area of interest. Then, smaller selected region was imaged at 200 x 200 nm<sup>2</sup> and after additional selection, final ROI was imaged at 50x50 nm<sup>2</sup>. EM image acquisition was performed in Electron Microscopy Hub, German Center for Neurodegenerative Diseases, Munich, Germany.

EM images stacks were further aligned by automatic and manual processing in ImageJ (Fiji) TrakEM. 3-D reconstructions were processed in IMOD and VAST software.

### 3.12. Image processing and analysis

*Spinal cord fixed-tissue analysis:* *Plp:eGFP/BiozziABH* with EB-induced demyelination were perfused at the day 4 after the EB injection. Control animals injected with saline were treated the same as EB-injected. *Plp:eGFP/BiozziABH* mice were immunized and perfused at weight loss, onset of clinical symptoms, two days after the onset and 40 days after the onset (20 days after the second relapse of clinical symptoms). Longitudinal sections of lumbar spinal cord were cut and stained with anti-MBP antibody and NeuroTrace 640/660 as described. For each animal, three examples of consecutive regions were imaged (lesion center, rim of the lesion and adjacent NAWM). ImageJ (Fiji) plugins were used for processing and quantification: ‘cell counter’ to count OLs somata number and number of nuclei, ‘freehand line tracing tool’ to mark and measure the length of myelin.

*Cortical fixed-tissue analysis:* *Plp:eGFP/BiozziABH* mice were immunized, induced with cortical lesion and perfused 3 and 14 days after cytokines injection (additionally 7d, 21d, 4w and 6w in screening experiment). Aged-matched healthy controls were treated the same as experimental animals. Coronal

sections of the brain were cut ( $\pm 200 \mu\text{m}$  anterior/posterior from the injection site) and stained with anti-MBP / anti-CC1 / anti-NG2 / anti-PDGFR $\alpha$  / anti-Olig2 antibody and DAPI as described. For each animal, three examples of cortical layer 1 and 2 were imaged  $\sim 300 \mu\text{m}$  laterally to the injection site. ImageJ (Fiji) plugins were used for processing and quantification: 'cell counter' to count OLs somata number (*Plp:eGFP*) as well as CC1, NG2, PDGFR $\alpha$  positive cells, 'freehand line tracing tool' to mark and measure the length of myelin (MBP).

*Spinal cord 'in vivo' analysis:* To analyze the sequence of demyelinating events, *Plp:eGFP/BiozziABH* were injected with rabies virus SAD  $\Delta\text{G}$  mcherry to obtain single-cell resolution. Animals were prepared as described above (*In vivo* imaging, spinal cord). Single OLs were imaged with 60 min intervals, with the last time point between 270-330 min. ImageJ (Fiji) was used for images processing. Maximum z-projections from individual OL's time points were compared in term of processes loss. OL's processes were traced with 'freehand line tracing tool' plugin.

*Cortical 'In vivo' analysis:* *Plp:eGFP/BiozziABH* mice were immunized, induced with cortical lesion and imaged at the day 3 and 14/16 after the cytokines injection. 2PM images were processed with ImageJ(Fiji), oligodendrocytes were compared in between time points and marked with 'cell counter' as 'remain' for the ones that stayed over time; 'lost' which were present at day 3 and not detected at day 14/16; 'new' which were only present at the day 14/16 and not day 3. Total oligodendrocyte processes length was marked and measured with 'freehand line tracing tool' at both time points. Aged-matched healthy controls were imaged at day 0 and 12/13 later and further images processing and quantification was done as for the experimental animals.

C57BL6J/*BiozziABH* (injected with the AAV-*Mbp:mem-tdTomato*) were immunized and imaged before cortical lesion induction, 3 and 14/16 days after the cytokines injection. 2PM images were processed with ImageJ(Fiji) and single oligodendrocytes were selected for further single cell reconstruction with 'simple neurite tracing' plugin. While comparing 3 time points (before cEAE, cEAE day3, cEAE d14/16) lost and new OL processes and myelin segments were marked at the level of individual oligodendrocyte. AAV-*Mbp:mem-tdTomato*, aged-matched non-immunized, cytokines injected controls were imaged at the same time points as the experimental animals.

*SCoRe analysis:* To assess the status of new myelin compaction, C57BL6J/BiozziABH (injected with the AAV-*Mbp*:mem-tdTomato) were immunized and imaged at the day 3 and 14/16 after the cytokines injection. 2PM images were processed with ImageJ(Fiji) and analysis of reconstructed single OL was performed as described above. SCoRe signal was overlaid on mem-tdTomato signal from day14/16; new internodes with SCoRe signal were marked. To check the accuracy of the method, reference internodes included 3 randomly assigned internodes from the same OL, which were present during both time points (remaining internodes).

### 3.13. Statistical analysis

Microsoft Excel software was used for data collection and preliminary analysis. Results are given as mean  $\pm$  s.e.m. Statistical significance was analyzed with GraphPad Prism 7.0. For samples where normal distribution was confirmed with Pearson test: for two samples comparison, *t*-test was used; for more than 2 samples, one-way ANOVA followed by Tukey's multiple comparison test was used. In non-normally distributed samples: for two samples comparison, nonparametric Mann-Whitney U-test was used; for more than 2 samples Kruskal-Wallis followed by Dunn's multiple comparison test were used. Obtained p-values were stated as significance levels in the figure legends (\*\*\*\*  $P < 0.0001$ , \*\*\*  $P < 0.001$ ; \*\*  $P < 0.01$ ; \*  $P < 0.05$ ).

---

## Chapter IV – Results

### 1. Demyelination in the white matter of the spinal cord

My main interest in this part of the project was to study the spread of oligodendrocyte damage in inflammatory white matter lesions and follow the fate of oligodendrocytes during the course of the disease. As reviewed in the introduction (Chapter I - Introduction, section 1.5.) there are different mouse models that mimic distinct aspects of MS pathology. Therefore as a first step, I investigated the cellular sequence of demyelination in EAE (an inflammatory model of demyelination) and EB-induced demyelination (toxic model of myelin loss). I performed all experiments using F1 hybrids, obtained from crossing *Plp:eGFP/C57BL6* with BiozziABH mice. These animals are characterized by GFP expression under the *Plp* promoter, allowing visualization of OLs somata and their processes with two-photon and confocal microscopy.

#### 1.1. Centripetal pattern of demyelination in EAE lesions

I induced EAE in *Plp:eGFP/C57BL6* x BiozziABH mice by low-dose MOG<sub>1-125</sub> active immunization (as described in Methods Chapter). Due to the strong antibody response and the relapsing-remitting course of the disease, the BiozziABH strain is particularly useful to study myelin damage and following remyelinating events. Detailed histopathological and clinical course analysis did not reveal any significant differences between wild-type BiozziABH and F1 hybrids, showing that mixed-background offsprings maintained the peculiar properties of the pure BiozziABH mice (Romanelli et al., 2016).

Immunized animals showed first clinical symptoms around twelve days after the initial MOG<sub>1-125</sub> administration. In order to determine to what extent oligodendrocytes and myelin are affected at the different stages of the EAE course, I perfused the animals at the weight loss, onset of the disease, and two days after the onset (peak of the disease); the corresponding analysis of chronic time-points, included in *Romanelli et al 2016*, was performed by Dr. Romanelli (Fig. 7A).

Based on the number of infiltrating cells, I first identified the lesion areas in the lumbar part of the spinal cord. The density of cells, detected by nuclear staining, was high in the lesion center and decreased with the distance towards the rim of the lesion, being relatively low in NAWM. In such defined lesion areas, I

quantified the number of OL cell bodies (PLP-GFP+ cells) and total myelin length (MBP+). The results showed that during the course of the disease myelin loss exceeded loss of oligodendrocytes. Even at the initial, weight loss stage, near half of the myelin was already gone, while the number of oligodendrocytes somata remained unchanged (Fig. 7B).

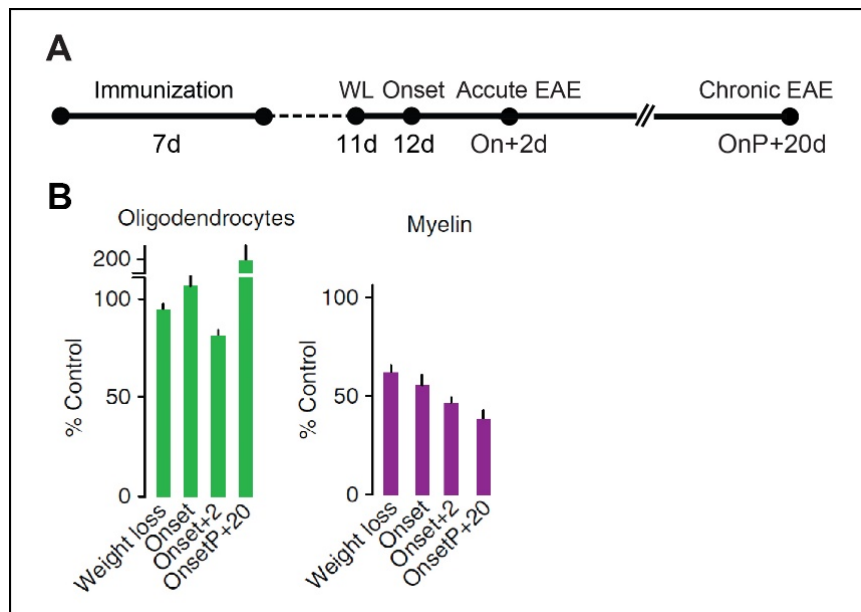


**Figure 7. Sequence of demyelination in EAE.** (A) Scheme of the experimental setup to investigate OLs and myelin loss during the EAE course. (B) Quantification of OLs number (green, left) and myelin length (magenta, right) performed at the different EAE stages. All values are normalized to healthy controls; n=3 mice for weight loss, onset, onsetP+20 (onset of progression +20 days) and n=6 mice for onset+2 analysis.

Detailed analysis of OLs and myelin density at the peak of the disease (onset +2; Fig. 8A) demonstrated that myelin was almost entirely lost in the lesion center, while over half of the oligodendrocytes were present. Moreover, at the border of the lesion, defined by a medium and low density of infiltrating cells, the number of OLs was nearly identical in comparison to healthy animals, while myelin length was decreased by 50% (Fig. 8B-D).

The centripetal pattern of oligodendrocyte damage was further confirmed by the 3-D reconstruction of single-OL. Intravital labelling with low concentration rabies virus SAD ΔG mCherry (Wickersham et al., 2007) resulted in sparse labelling of mCherry+ OLs (see Fig. 10). Confocal microscopy analysis of single OLs morphology in EAE lesion revealed that they preserved fewer and shorter processes with visible signs of damage (Romanelli et al., 2016).

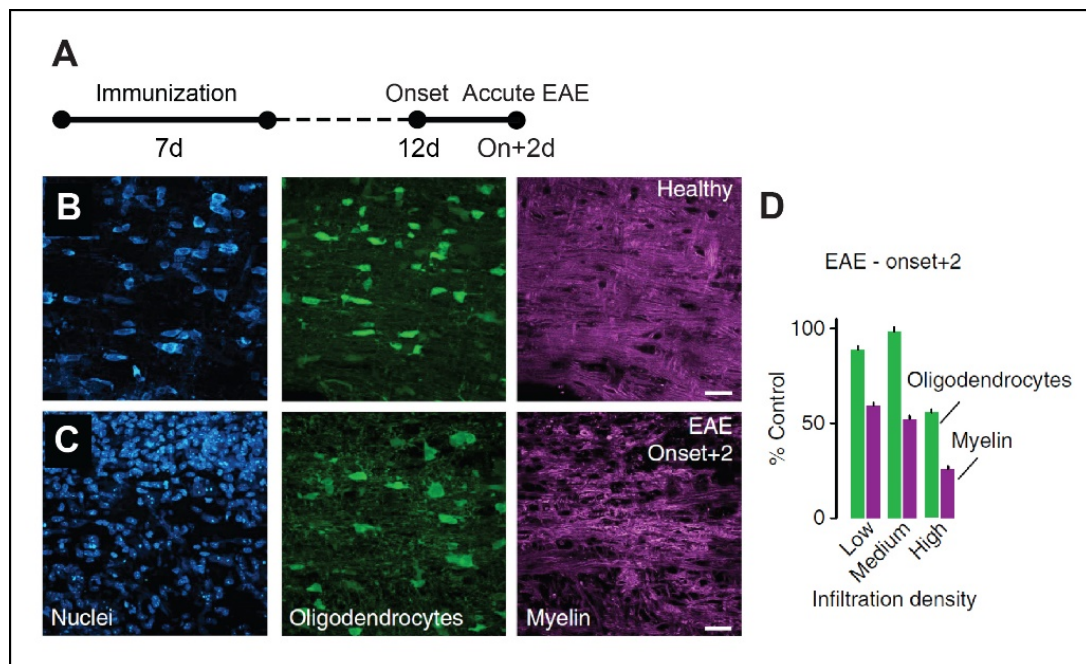


**Figure 8. Demyelination pattern in EAE lesion area at the peak of the disease.** (A) Experimental time line to study OLs and myelin loss during the peak of the disease (onset+2). (B,C) Low magnification, overview images of the *Plp:eGFP/C57BL6* x *BiozziABH* mice lumbar spinal cord in healthy control (B) and EAE lesion area (C). Infiltrating cells are visualized by staining with nuclear dye NeuroTrace (cyan), myelin with MBP staining (magenta) and OLs are transgenically labeled with GFP (green). Panel B represents uninflamed conditions with intact myelin in healthy animal, while panel C shows high density of infiltrating cells, myelin damage and myelin debris in the center and at the rim of the lesion. (D) Quantification of the OLs number and myelin length at the peak of the disease with regards to lesion area; lesion center (high infiltration), rim of the lesion (medium infiltration) and further from the lesion (low infiltration). All values are normalized to healthy controls. EAE n=6, healthy control n=3. Scale bars in B,C, 25 $\mu$ m.

## 1.2. Centrifugal pattern of demyelination in EB-induced lesions

To further investigate the patterns of oligodendrocyte damage, we also utilized another animal model of MS, in which demyelination is caused by ethidium bromide administration. Toxin-induced models are frequently used to model OLs pathology due to the relative simplicity of their experimental design. They also provide a paradigm for a primary damage to oligodendrocytes. Therefore, I investigated the sequence of demyelinating events in ethidium bromide injected *Plp:eGFP/C57BL6* x *BiozziABH* mice. I injected 0.5 $\mu$ g EB into the lumbar part of the spinal cord and perfused animals 4 days later, at the peak of demyelination (Fig. 9A). Similar to the lesion characterization in the EAE settings, I quantified the number of OLs and myelin length in the EB-lesion area. Analysis of the lesion border, which was characterized by comparable cell infiltration to the rim of the lesion in the EAE onset+2 samples (Fig. 8), showed an unaltered myelin length and decreased number of OLs by around 30% in comparison to saline-injected

controls. Furthermore, there was almost no PLP-GFP signal present in the lesion center, suggesting near complete loss of oligodendrocyte somata while half of the myelin was preserved (Fig. 9B-D). These results are consistent with the previous findings indicating that myelin can survive for a few weeks even without OL support (Locatelli et al., 2012).

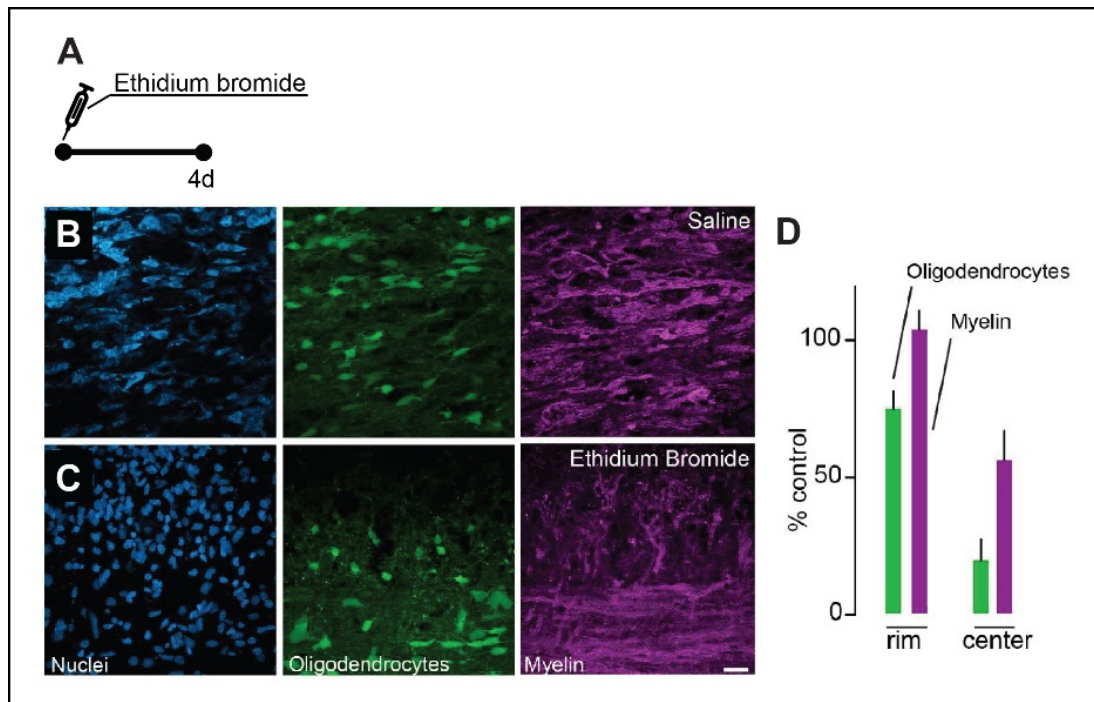


**Figure 9. Demyelination pattern in EB lesion area.** (A) Experimental time line to study OLs and myelin loss during the peak of the demyelination. (B,C) Overview images of the lumbar spinal cord from *Plp:eGFP/C57BL6* x *BiozziABH* mice injected with saline (B) and ethidium bromide (C). Sections stained with nuclear dye NeuroTrace (cyan) and myelin marker MBP (magenta); oligodendrocytes are visualized by transgenic labeling with GFP (green). Representative images of the rim of the lesion show oligodendrocyte loss increasing towards to lesion center with still present myelin (C, image upper part). (D) Quantification of oligodendrocyte number and myelin length at the rim (left) and in the lesion center (right). All values are normalized to controls. Saline-injected mice  $n=3$ , EB-injected mice  $n=3$ ). Scale bars in B,C, 25 $\mu$ m.

The above results indicate that EB-induced demyelination is characterized by a centrifugal pattern of oligodendrocyte pathology, which is observed in rarely occurring MS *Pattern IV*. Most commonly occurring OL damage follows outside to inside mechanisms – from distal internodal parts towards the cell body (*Patterns I-II*; Lucchinetti et al., 2000). Moreover, these amputated-state OLs are detected in chronic MS lesions suggesting that they persist for longer period (Wolswijk, 2000). Consequently, although the EB model presented defined lesion site along with minimal waiting, the almost immediate OLs death at lesion site made it unsuitable to study the fate of affected oligodendrocytes during the course of the disease. For these reasons, *in vivo* progression of OL damage was performed in the neuroinflammatory EAE conditions.

### 1.3. *In vivo* progression of oligodendrocyte damage in EAE

I used the single-cell labelling approach (Romanelli et al., 2016) to follow the morphological changes of surviving oligodendrocytes in neuroinflammatory lesions. Such analysis is not possible in *Plp:eGFP/C57BL6* strain because the density of PLP-GFP+ oligodendrocytes is too high for the reconstruction of individual cells. I therefore induced EAE in *Plp:eGFP/C57BL6* x BiozziABH mice as described above (Chapter IV - Results, section 1.1.). Four to six days post immunization animals received two injections of a low concentration rabies virus SAD ΔG mCherry into the lumbar dorsal white matter of the spinal cord. Based on the co-expression of GFP and mCherry, selected oligodendrocytes were imaged at different stages of the disease course; weight loss, onset of the disease, 1 and 2 days after the onset (Fig. 10A). Again, an outside-to-inside pattern of oligodendrocyte damage was confirmed as OLs presented shorter and fewer processes when compare to healthy controls from the early stages of the disease. These numbers decreased with the disease duration (Fig. 10B). Notably, several hours of time-lapse imaging unveiled OLs stability since almost no changes were detected during each single session of 2PM recordings. Furthermore, affected OLs can survive longer periods in neuroinflammatory conditions as no cell death was observed during the entire time-lapse experiment, even among the cells displaying a severely amputated morphology (Fig. 10B, lowest panel). Of the note, I also did not observe any increase in cell apoptosis at the OL population level (detected by immunostaining for activated death protease Caspase 3+/OL).

All of above suggests that in neuroinflammatory conditions, myelin loss takes place before oligodendrocyte death and that amputated oligodendrocytes are not immediately stepping towards cell death. This raises the question as to what happen to these affected OLs at the later stages during the remyelination phase of the disease (do they remain unchanged, undergo healing process, contribute to the remyelination or decrease its efficiency?). To answer this question, I used a newly adapted model of cortical MS pathology since – due to the comparably sparser density of OLs in the grey matter – this model allowed me to use multiphoton microscopy to follow the same group of oligodendrocytes over extended periods of time.

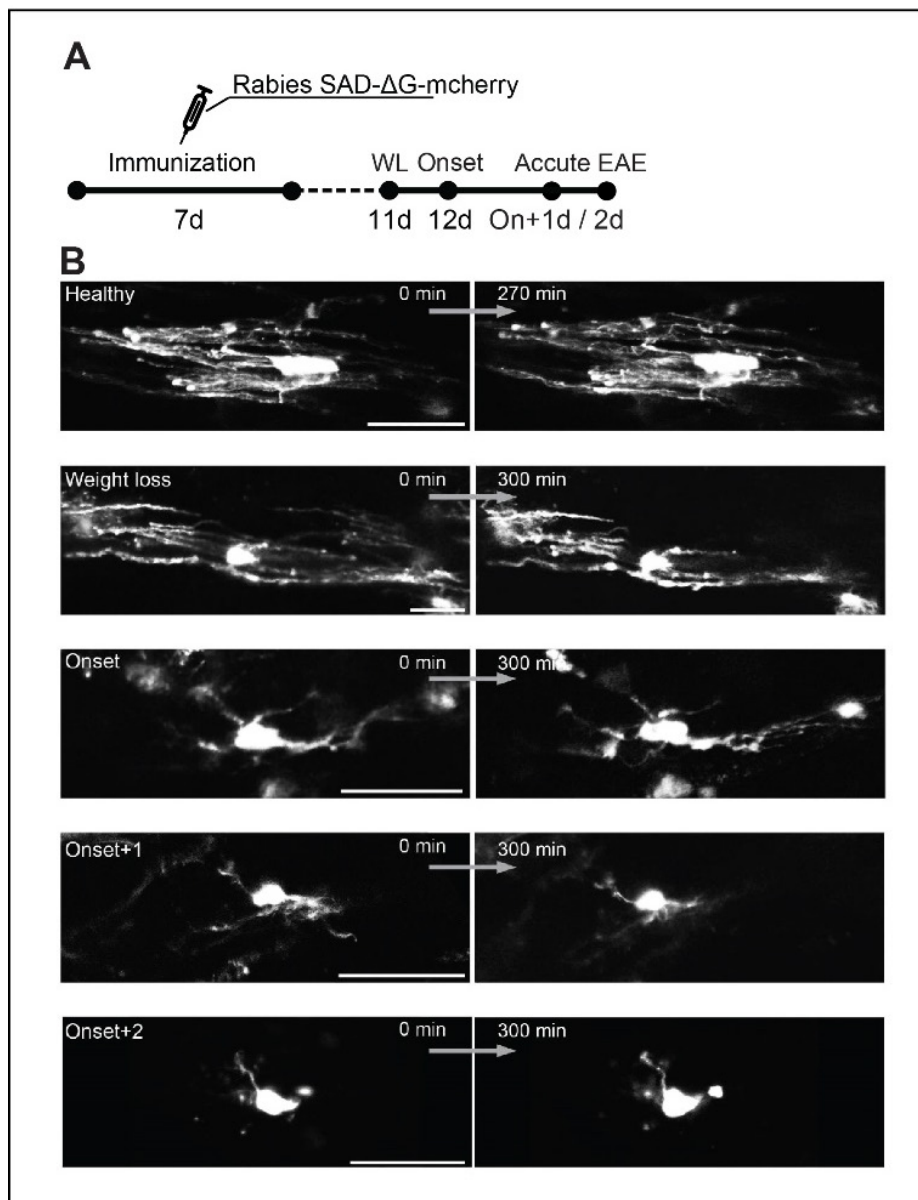


**Figure 10.** Time-lapse imaging of the amputated-state oligodendrocyte in the EAE lesion. (A) Experimental design time line to investigate fate of amputated-state oligodendrocytes. (B) Time-lapse imaging of single oligodendrocytes during different EAE stages (weight loss, onset of the disease, onset+1, onset +2). Each OL was imaged for up to 5 hours; total 100 hours of imaging of 20 OLs in 18 mice. Scale bars in B 50 $\mu$ m.

## 2. De- and remyelination in the cortical grey matter

Although cortical lesions are increasingly recognized as a hallmark of MS pathology, comparably little is known about mechanisms of oligodendrocyte and myelin damage in the cerebral grey matter. Moreover, knowledge about GM remyelination characteristics and its efficiency also remains at least partly elusive (Peterson et al., 2001; Bø et al., 2003; Chang et al., 2012; Trapp et al., 2018). Therefore, my second project aimed to understand how this remyelination occurs and how pre-existing OL are involved in this process.

## 2.1. Targeted MS model of cortical demyelination (c-MS)

To study de- and remyelination in the GM, I induced a cortical MS model by low-dose MOG<sub>1-125</sub> active immunization in *Plp:eGFP/C57BL6* x BiozziABH mice. Animals received an injection of intracortical cytokines (TNF- $\alpha$ /IFN- $\gamma$ ), which led to the widespread demyelination in the somatosensory cortex. Topologically, these demyelinating lesions were mainly localized in the subpial areas with the extent of demyelination decreasing towards the deeper cortical layers (Fig. 12B). These lesions spread also laterally to both hemispheres resembling Type III grey matter cortical lesions observed in MS patients (Peterson et al., 2001). In order to establish the most informative time points for the analysis of demyelination as well as remyelination, mice were perfused three, seven, twenty-one days and four and six weeks after the cortical lesion induction. I assessed the myelination status based on the MBP-stained sections (ipsilateral, 300 $\mu$ m from the injection site), in which I quantified the number of myelinated fibers crossing a 100 $\mu$ m reference line, positioned perpendicularly to the pial surface. Findings from the screening experiment indicates that the peak of the demyelination occurred three days after the cytokines injection and remyelination started slowly from day seven, reaching more than 65% of the original myelin density six weeks later (Fig. 11).

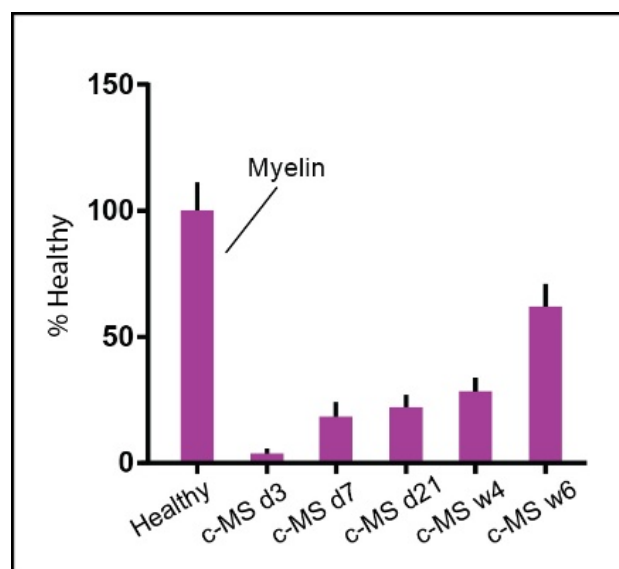


**Figure 11. Myelin time-course analysis in cortical MS model.** Quantification of myelinated fibers (MBP+) in subpial area at indicated time points revealed cortical demyelination at 3 days followed by partial remyelination. All values are normalized to healthy controls. EAE n=3 mice (n=2 for c-MS d7), healthy control n=3 mice.

## 2.2. Demyelination pattern and remyelination capacity in the cortical MS model

Next, I wanted to investigate if, under neuroinflammatory conditions, oligodendrocytes localized in the cortical grey matter demonstrate a similar pattern of damage as observed in the EAE white matter of the spinal cord. Therefore, I analyzed OLs number and myelin density during the peak of the demyelination in the cortical lesions. However, since I also aimed to study remyelination capacity in these lesions, I also investigated changes at the OL population and myelin level during the remyelination phase. Although the remyelination starts as early as day seven after the lesion induction (**Fig. 11**), inflammation only completely resolves another week later (Jafari et al., 2019). Thus, I designed an experimental setup, in which immunized *Plp:eGFP/C57BL6* x BiozziABH young adult mice were perfused three days after the cytokines injection, as the stage of maximal myelin loss and fourteen days later as the recovery phase (**Fig. 12A**). For the given time points, I quantified the number of OL cell bodies (PLP-GFP+ cells) and the total myelin length (MBP+) in the subpial area localized 300 $\mu$ m laterally from the injection site.

First, in comparison to healthy controls, myelin density at c-MS d3 was significantly decreased while the number of the OLs, which were characterized by shorter and fewer processes, remained unchanged. Additionally, substantially reduced myelin length, calculated per OL, indicated that the damage spread from the most distal internodal parts towards the cell body (**Fig. 12B left/middle, C-D**). These results suggest that, under neuroinflammatory conditions, grey matter demyelination follows a centripetal pattern of oligodendrocyte damage as detected in the white matter pathology of the spinal cord in the EAE (**Fig. 8**).

Secondly, our analysis demonstrated that in the cortical MS model, oligodendrocyte cell bodies persisted stably over time, while myelin, which was almost entirely lost during the peak of demyelination (c-MS d3) was restored to 80% near two weeks later (c-MS d14). Furthermore, myelin length per oligodendrocyte was also significantly increased when comparing these two time points. These findings indicate that the cortical lesions can be remyelinated with relatively high efficiency in young adult mice (**Fig. 12B-D**).

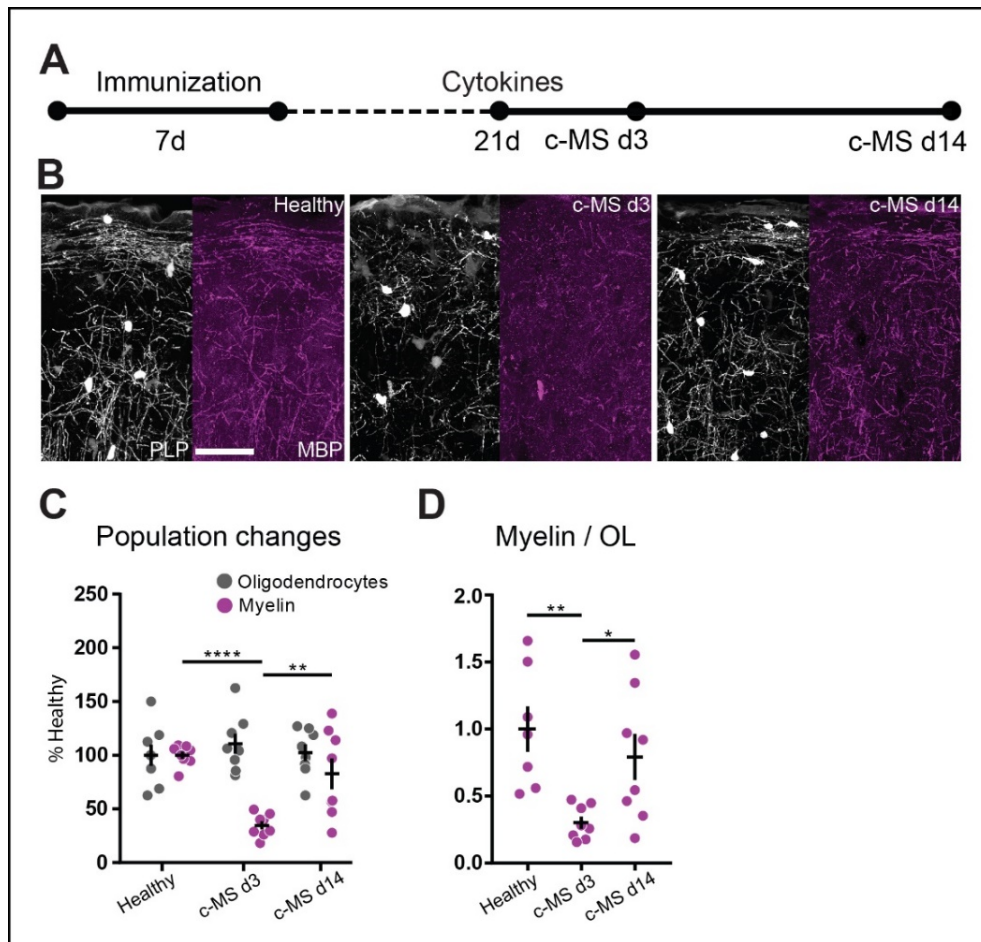


**Figure 12. Remyelination capability in c-MS lesions in young adult mice.** (A) Experimental time line to study OLs and myelin changes in the cortical MS model. (B) Overview images of the *Plp:eGFP/C57BL6* x *BiozziABH* adult mice somatosensory cortex, 300 $\mu$ m laterally from the injection site; healthy control (left), 3 days (middle) and 14 days (right) after cortical lesion induction. Myelin is visualized by staining with MBP staining (magenta) and OLs are transgenically labeled with GFP (grey). (C) Quantification of the OLs number and myelin density at the population level during the course of disease. (D) Quantification of the myelin length per oligodendrocyte at the different c-MS time points. All values are normalized to healthy controls. c-MS d3 n=8, c-MS d14 n=7, healthy control n=7 mice. Adult mice: 3-5 months of age. Scale bar in **B** 100 $\mu$ m. One-way ANOVA followed by Tukey's multiple comparisons test has been performed in **C** and **D**. \*\*\*\*P<0.0001, \*\*P<0.01, \*P<0.05.

MS pathology is often characterized by lesion regions, which fail to remyelinate (Kuhlmann et al., 2008). Due to the chronic nature of the disease, ageing can be considered as one of the limiting factors in efficient regenerative processes (Rist and Franklin, 2008; Crawford et al., 2016a; Cantuti-Castelvetri et al., 2018). To investigate the effect of age on the remyelination capacity of grey matter, I induced the cortical MS model in C57BL6 x BiozziABH mice at the age of 9 to 11 months and perfused them at the same time points as the cohort of young adult mice with a supplementary late time point, 28 days after the cytokines injection (Fig. 13A). I quantified the total myelin length (MBP+) using the same criteria as specified in c-

MS young adult mice analysis. Our findings showed that remyelination capacity was lower in aged animals and they could not restore myelin sheaths within the same period as observed in young adult mice. Even at the extended, late time point, myelin density was significantly decreased in comparison to age-matched healthy controls (Fig. 13B-C).

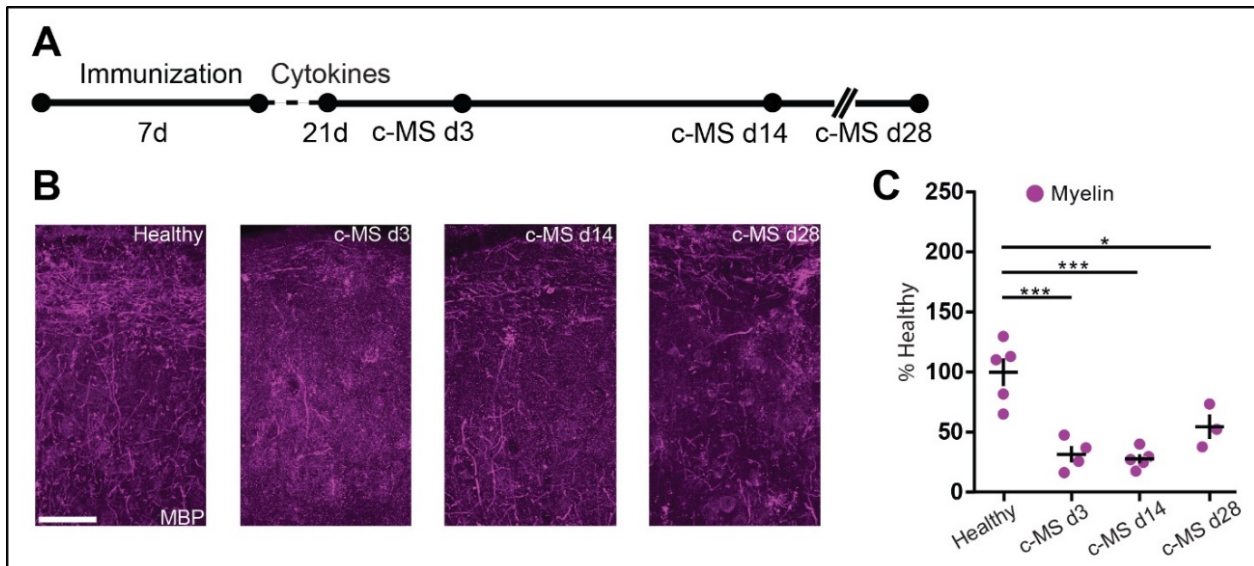


**Figure 13. Remyelination capability in c-MS lesions in aged mice.** (A) Experimental time line to study myelin changes in the cortical MS model in aged mice. (B) Overview images of the C57BL6 x BiozziABH aged mice somatosensory cortex, 300 $\mu$ m laterally from the injection site stained for myelin marker MBP (magenta); aged-matched healthy control (left), 3 days (middle left), 14 days (middle right) and 28 days (right) after cortical lesion induction. (C) Quantification of the myelin density during the course of the disease. All values are normalized to aged-matched healthy controls. c-MS d3 n=4, c-MS d14 n=5, c-MS d28 n=3, healthy n=5 mice. Aged mice: 9-11 months of age. Scale bar in B 100 $\mu$ m. Kruskal-Wallis followed by Dunn's multiple comparisons test has been performed in C and D. \*\*\*P<0.001, \*P<0.05.

### 2.3. Characterization of the oligodendrocyte population in the cortical MS model

Due to the high stability of oligodendrocytes in the c-MS induced in young adult mice, I further aimed to characterize these cells population in healthy cortex and in the GM lesion area. Differences in intensity of the GFP signals in labelled OLs were noticeable in the *Plp:eGFP/C57BL6 x BiozziABH* mice even under healthy conditions. In this strain, green fluorescent protein expression is driven by the *Plp* promoter, which increases its activity with the OL's maturation. In order to determine if dim GFP<sup>+</sup> OLs are less mature than bright GFP<sup>+</sup> cells, I co-stained cortical sections from aforementioned healthy animals with NG2, a marker of oligodendrocyte progenitors and CC1, a marker of mature oligodendrocytes (Fig. 14A). Quantification revealed that the dim GFP<sup>+</sup> OL population was rather equally composed of OPCs and

mature OLs, with few percent of the cells staining positive for both markers. In contrast, the second OL population was more homogenous; a vast majority of bright GFP+ cells could be classified as mature OLs and no double positive NG2/CC1 cells were detected in this population (Fig. 14B).

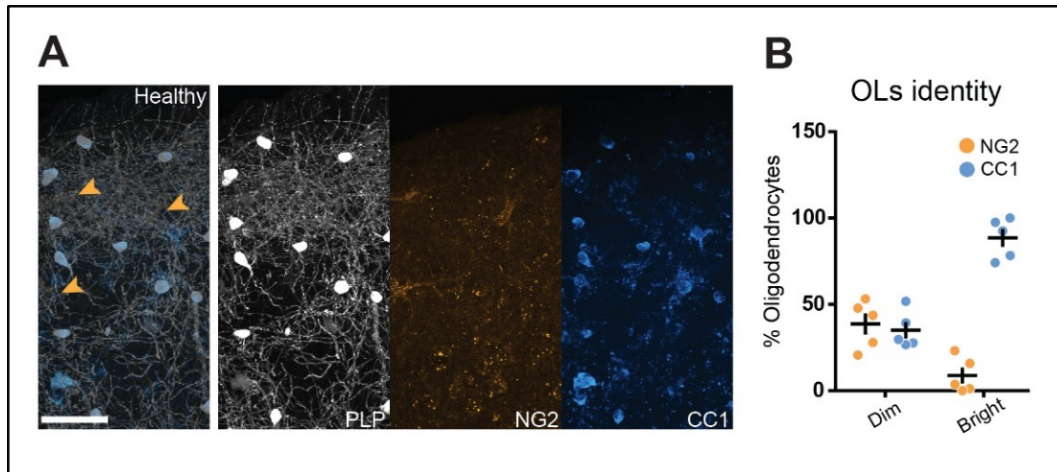


**Figure 14. Identity of GFP+ oligodendrocyte.** (A) Low magnification images of subpial cortical area of healthy *Plp:eGFP/C57BL6* x *BiozziABH* mice. Sections are co-stained for OPC marker - NG2 (orange) and mature OL marker - CC1 (cyan), Overlay image (right) shows co-localization of selected markers with dim and bright GFP+ OLs; the orange arrowhead points to the NG2+ OL. (B) Quantification of the OL's markers detected in the dim and bright GFP+ cell population; n = 5 mice. Scale bar in A 100 $\mu$ m.

Next, since GFP intensity can be a first-line indicator of oligodendrocyte developmental stage, I assessed the proportion of the dim and bright GFP+ OLs in the cortical lesions induced in the *Plp:eGFP/C57BL6* x *BiozziABH* mice. As shown before (Fig. 12), the number of OLs remained stable over the course of the disease; however, changes in the proportion of the dim/bright cells populations can indicate their different maturation status. I quantified the total number of oligodendrocytes, number of dim GFP+ OLs and bright GFP+ OLs. Both populations were almost equally abundant, with a minor predominance of the dim cells, regardless of the stage of the grey matter pathology. During the different time points, there was no shift detected in the distribution of the OL populations (Fig. 15).

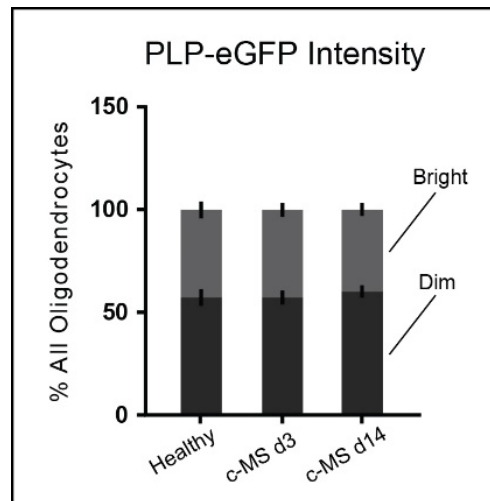


**Figure 15. Proportion of dim and bright GFP+ OL in c-MS model.** Percentage composition of the total oligodendrocyte population quantified in *Plp:eGFP/C57BL6* x *BiozziABH* mice somatosensory cortex, 300 $\mu$ m laterally from the injection site, 3 and 14 days after cortical lesion induction. c-MS d3 n=11, c-MS d14 n=12, healthy control n=12 mice.

To further characterize the total oligodendrocyte population in the cortical lesions during the course of the disease, I stained the sections for different OLs markers. NG2 and PDGF $\alpha$ R were used to label OPCs, Olig2 to mark the OL lineage cells and CC1 to detect mature oligodendrocytes (**Fig. 15A**). The marker positive GFP+ OL were quantified in healthy controls, and on day 3 and 14 after cytokines injections. The results showed no substantial differences in the OPC density nor in the number of OL lineage cells. The CC1+/GFP+ OL population seemed to be declined on the c-MS d3, yet the difference was not statistically significant and might result from the technical challenges of staining the inflamed tissue with mouse CC1 antibody (**Fig. 15B**). Our findings indicate oligodendrocyte population stability as no significant differences were detected in the number of OPCs nor mature OLs over the course of the disease.

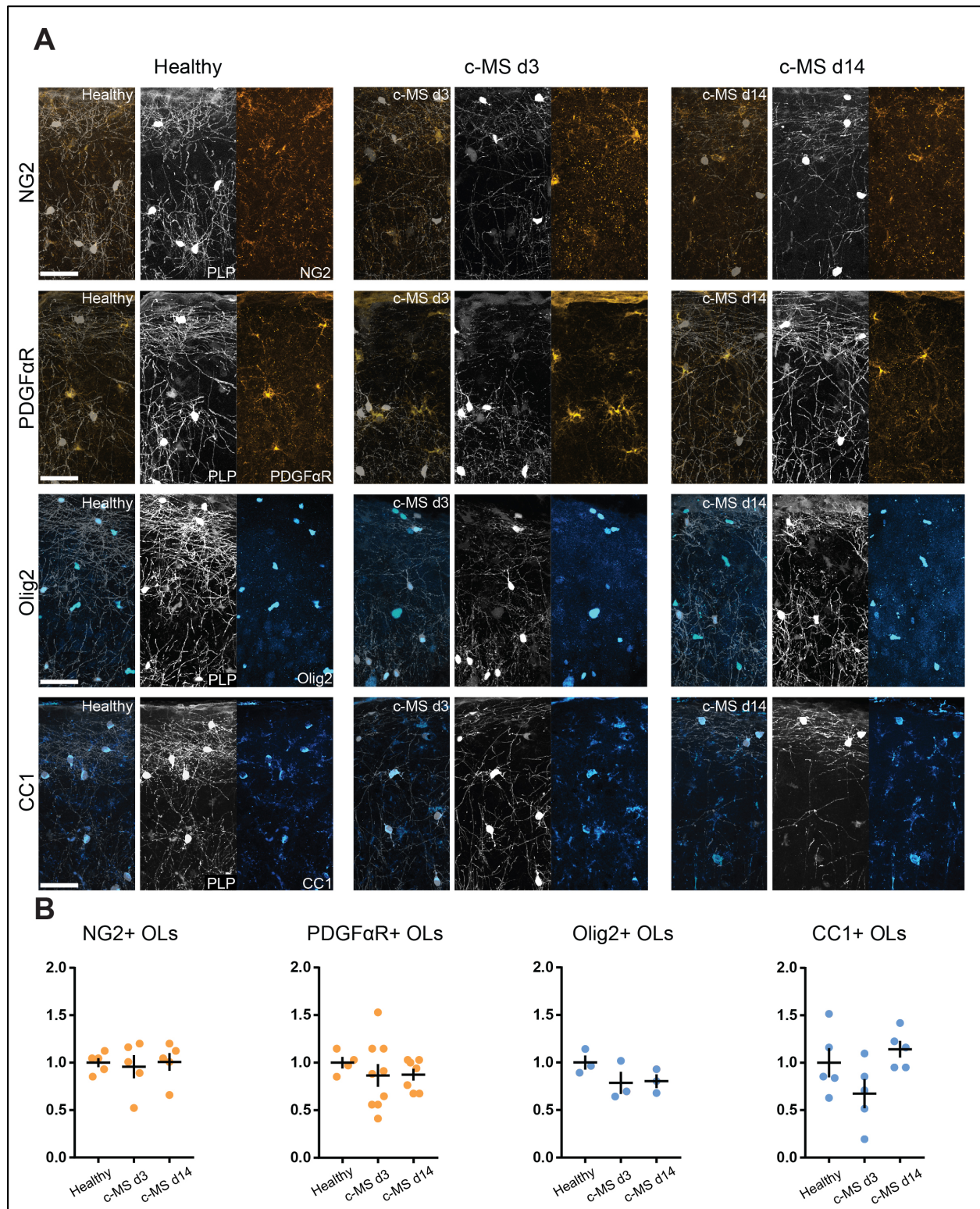


**Figure 16. Oligodendrocyte population characterization in c-MS model.** (A) Representative images of the *Plp:eGFP/C57BL6 x BiozziABH* adult mice somatosensory cortex, 300 $\mu$ m laterally from the injection site; healthy control (left panel), 3 days (middle panel) and 14 days (right panel) after cortical lesion induction. Sections are stained for OPC markers: NG2 (orange, upper panel) and PDGF $\alpha$ R (orange, upper middle panel); OL lineage detected by Olig2 (cyan, lower middle panel), mature OL visualized by CC1 (cyan, lower panel); OLs are transgenically labeled with GFP (grey). Overlay images (left, for each time point) shows co-localization of selected markers with OLs. (B) Quantification of the selected markers co-localized with GFP+ OLs, no statistically significant differences were detected in OL populations. All

values are normalized to healthy controls. NG2: n=5 mice/group; PDGF $\alpha$ R: c-MS d3 n=9, c-MS d14 n=7, healthy control n=4 mice; Olig2: n=3 mice/group; CC1: n=5 mice/group. Scale bars in **B** 100 $\mu$ m. One-way ANOVA followed by Tukey's multiple comparisons test has been performed in **C** for NG2 and CC1 and Kruskal-Wallis followed by Dunn's multiple comparisons test has been performed for PDGF $\alpha$ R and Olig2 analysis.

#### 2.4. *In vivo* time-lapse imaging of oligodendrocyte turnover in cortical MS model

As the *ex vivo* findings suggest that mature oligodendrocytes remain at unchanged levels during the course of the cortical MS model while myelin sheaths are restored with high efficiency, I next investigated OLs turnover and remyelination capacity in the individually tracked areas in *Plp:eGFP/C57BL6* x *BiozziABH* mice. Employing *in vivo* imaging approach allowed to me to record the same, mature oligodendrocytes at different time points. I utilized 2P microscopy for the intravital imaging through a cranial window, placed above the somatosensory cortex, 3 days after the cortical lesion induction. Selected areas of the top 80 $\mu$ m of the cortical layer 1, localized up to 1mm from the cytokines injection site, were imaged on c-MS d3 immediately after window implantation. Based on the cortical venous angioarchitecture in each mouse, the same areas were found back and imaged again two weeks later (**Fig. 17A-B**). Using this approach, I investigated the turnover of oligodendrocytes between the two time points. Because mature OLs demonstrate individually unique morphology and do not migrate, I identified and quantified the number of OLs that remained stable or survived the initial immune attack, the number of lost OLs, i.e. present on the c-MS d3 and not detected later and the number of new OLs, which were only observed on the c-MS d16 (**Fig. 17B**; yellow– remaining, red – lost, green – new OLs). Analysis of the oligodendrocyte turnover suggested that the vast majority of these cells remained from the initial demyelination period to the recovery phase, c-MS d3 and c-MS d16 respectively. During this time period only about 20% of the initial oligodendrocytes were lost. They were also replaced by the same number of oligodendrocytes that were newly integrated, keeping the overall number of OLs unchanged (**Fig. 17C**). Furthermore, I also quantified the processes density of OLs to establish the remyelination capacity within the individual areas. Analyzed areas showed, on average, an increase of 60% in the total processes length and the substantial raise in processes length per OL on c-MS d16 in compare to day 3 after cytokines injection (**Fig. 17D**).

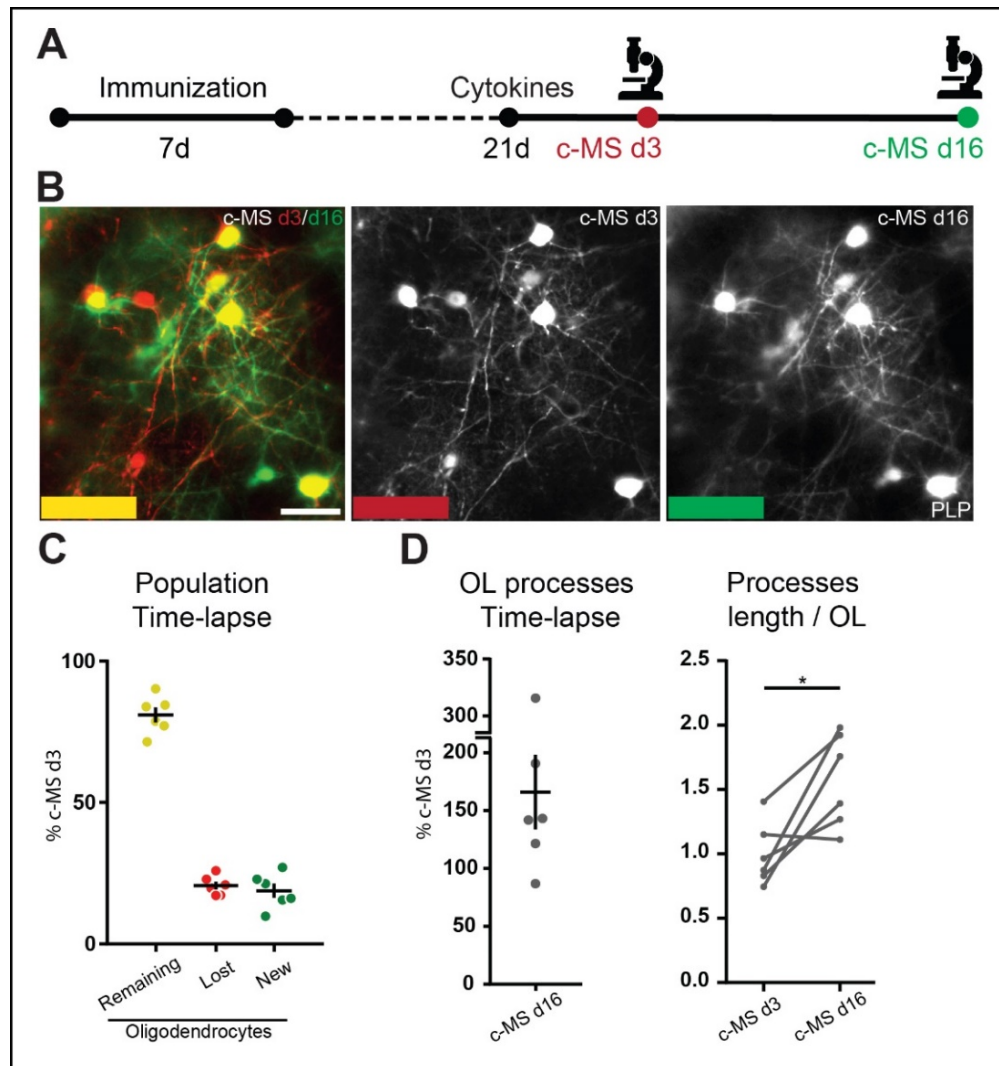


**Figure 17. *In vivo* time lapse imaging of cortical lesion.** (A) Experimental design to study OL turnover and processes length during the course of disease in c-MS model. (B) Time-lapse images of the top 80µm of layer 1 somatosensory cortex in *Plp:eGFP/C57BL6 x BiozziABH* mice with cortical MS model, obtained from 2PM imaging sessions of day 3 and 16 after cytokines injection (B, middle and right respectively). Left image: Overlay of two time points, c-MS d3 (red) and c-MS d16 (green); changes in OLs and processes within the same area are color coded with yellow for remaining, red for lost and green for new cells and processes. (C) Quantification of the oligodendrocyte cell bodies during the course of c-MS. Total number of the cells stays unchanged; 80% of the cells (yellow) remains until c-MS d16, 20% is lost (red) and almost the same in new (green) in compare to c-MS d3. (D) Quantification of oligodendrocytes processes length density (left) and processes length per OL (right) in the same area, on c-MS d16 in compare to c-MS d3. Values are normalized to c-MS d3. n= 6 mice; imaged 3-7 areas/mouse. Scale bar in B 50µm. One-way ANOVA followed by Tukey's multiple comparisons test has been performed in D (right). \*P<0.05.

These *in vivo* findings confirm that cortical lesions can be efficiently remyelinated and majority of mature oligodendrocytes, even when presented at amputated-state, remain stable during the disease course. Moreover, because of the large number of remaining OLs and the relatively small amount of new OLs, it is still elusive, which of these population mainly contributes to the myelin sheaths restoration.

Remyelination can be conducted by newly integrated OLs, which would mean they can form longer and larger processes in comparison to the processes established during development or both of the populations - pre-existing cells and newly integrated OLs - contribute to efficient remyelination. To support this hypothesis, I observed few, newly generated or extended processes, which belonged to the pre-existing oligodendrocytes. Unfortunately, GFP labelling in *Plp:eGFP/C57BL6* strain is too dense for visualization of single cells with 2P microscopy. Additionally, the GFP signal is relatively dim in the distal internodal parts and thus cannot be used to assess the compaction status of newly restored myelin sheaths regardless of their origin.

## 2.5. Compact myelin in remyelinated cortical lesion

To achieve a labelling of the entire processes and internodes of individual oligodendrocytes as well as their cell bodies, I designed and cloned a viral vector, in which first 1.3kB of MBP promoter drives the expression of membrane-targeted tdTomato protein (AAV-*Mbp:mem-tdTomato*). This virus was further characterized in *Plp:eGFP/C57BL6* mice. Single injection of high-titer ( $10^{13}$ ) viral solution into the somatosensory cortex resulted in relatively sparse, bright tdTomato signal, co-localized with transgenically driven GFP (Fig. 18). Decreased AAV-delivered tdTomato signal density facilitates tracing and reconstructing individual oligodendrocytes in the cortical MS model. TdTomato was mainly detected in the cell's membrane 18 days after injection, and repetitive imaging did not cause photo-bleaching. In addition, no virus-induced damage was observed up to 55 days after the virus administration.

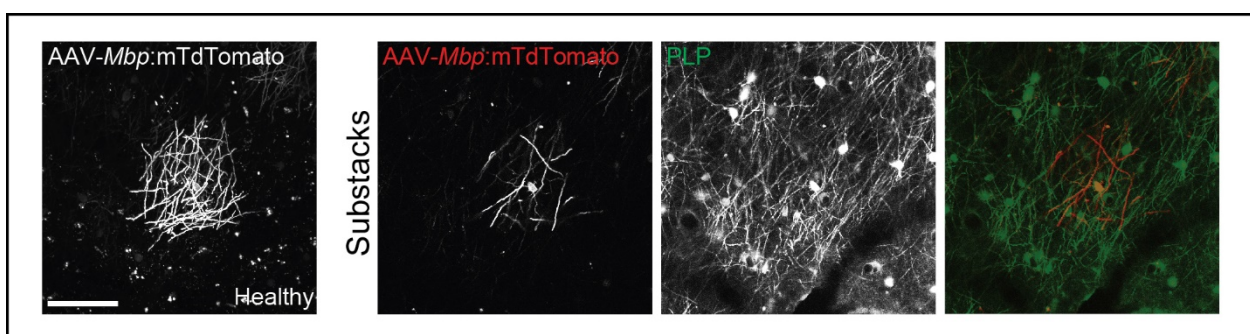


**Figure 18. AAV-*Mbp:mem-tdTomato* characterization.** (Left) Two-photon microscopy, representative stack projection of the somatosensory cortex (top 30 $\mu$ m of the layer 1), 3 weeks after the virus injection. (Right) Substack projections of the same area acquired with 1040 nm wavelength (MBP-tdTomato, red) and 800 nm wavelength (PLP-GFP, green); overlay image shows membrane localization of the tdTomato protein and sparser than the GFP signal. Scale bar 150 $\mu$ m.

Sparse tdTomato signal is still present in the fixed brains after perfusion. This feature can be used to identify *in vivo* 2PM imaged areas and assess the compaction status of their newly synthesized myelin sheaths by spectral confocal reflectance microscopy technique (SCoRe). Only multilayered compact myelin generates reflections, which give rise to a positive SCoRe signal (Schain et al., 2014).

In the interest of characterizing the remyelination at a single OL level and determine myelin compaction, I used the following experimental design: at the day of initial MOG<sub>1-125</sub> immunization, C57BL6 x BiozziABH mice received a single injection of AAV-*Mbp*:mem-tdTomato into the layer 1 of the somatosensory cortex, ipsilateral to the later cytokines injection site. With the already established *in vivo* imaging approach (Chapter IV – Results, section 2.4), I then traced the same areas with single-cell resolution over the course of the cortical MS model (Fig. 19A) and compared the presence of the internodes at the demyelination peak on c-MS d3 and during the recovery phase imaged on c-MS d16. By reconstructing the morphology of the same oligodendrocytes on both time points, I was able to trace internodes that persisted over time and new internodes which were detected only at the later time point (Fig. 19B left-middle; yellow arrowheads – remaining, green arrowheads – new internode). Immediately after the last imaging session on c-MS d16, mice were perfused, brains dissected and placed under the confocal microscope to obtain SCoRe signal from the selected areas (Fig. 19B, right). Sparse tdTomato labelling allowed the easy identification of intravital examined lesions by brief, superficial confocal scans of the somatosensory cortex region, above which, cortical window was placed before. Then, I correlated the generated SCoRe signal with the tdTomato signal obtained on c-MS d16, to assess the compaction status of newly synthesized myelin. In each evaluated area, three randomly chosen remaining internodes were used as a control for SCoRe accuracy, as they should be composed of compact myelin and therefore produce light reflection. Our findings suggested that this technique had relatively high sensitivity because 80% of reference-remaining internodes were SCoRe+. Next, the analysis of eight OL's areas from five mice showed that 75% of newly synthesized myelin sheaths also generated SCoRe signal, which indicated that grey matter OLs could form a compact myelin in the lesions (Fig. 19C).

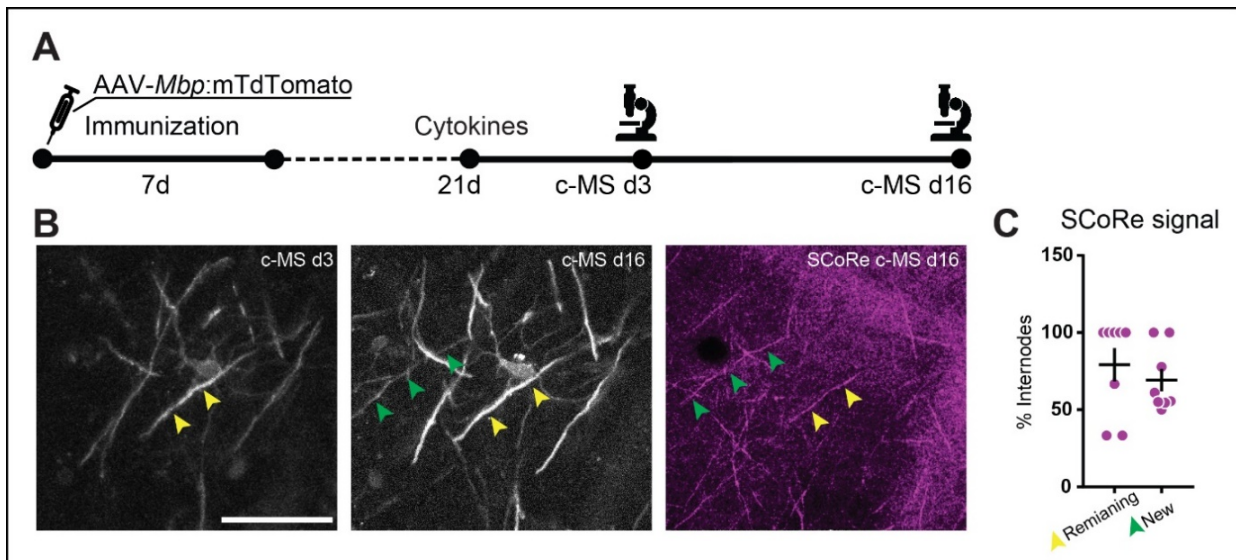


**Figure 19.** Myelin detection by *in vivo* 2PM imaging and SCoRe technique. (A) Schematic experimental diagram with indicated time points to study remyelination and myelin compaction in c-MS model. (B **left, middle**) Area with tdTomato+ oligodendrocyte was imaged intravital on c-MS d3 (left) and c-MS d16 (middle). After immediate mouse perfusion, intact dissected brain was imaged with confocal microscopy and SCoRe signal of the same area was generated (B, **right**). (C) Percentage of SCoRe-signal+/ TdTomato+ new internodes in relation to all new tdTomato+ internodes (new, green arrowheads). Internodes present on both days (remaining, yellow arrowheads) serve as referring internodes to assess SCoRe signal accuracy. n=8 OL areas from 5 mice. Values normalized per OL area. Scale bar in B 50 $\mu$ m.

Preliminary *in vivo* findings also suggested that mature oligodendrocytes could contribute to the remyelination. Near single-OL viral labelling allowed reconstruction of individual cells during the peak of the demyelination and in the recovery phase (Fig. 19). By comparing morphological changes between these time points, I could mark new internodes, which were connected to the *old* oligodendrocytes. Yet, to investigate this process and exclude the possibility that these OLs were integrated after cortical lesion induction and were early myelinating cells, I modified the experimental design to follow individual OL throughout the whole cortical lesion development, including the pre c-MS induction stage. This additional imaging session ensured investigating cellular changes only in pre-existing, mature OLs. Obtained results are described below.

## 2.6. *In vivo* imaging of mature, pre-existing oligodendrocytes in the cortical MS model

### Longitudinal *in vivo* imaging of the pre-existing OLs

Using the established sparse labeling approach of OLs and a modified timeline of the cortical MS model, I imaged the individual pre-existing OLs (1) under healthy condition, (2) in their amputated-state at the demyelination peak and (3) during the remyelination phase, in C57BL6 x BiozziABH mice (**Fig.20A**). Because TNF- $\alpha$  and IFN- $\gamma$  administration may cause some damage even without systemic EAE induction, I also investigated changes of OLs morphology in control non-immunized animals, injected with the cytokines (**Fig. 21**). For both groups, I reconstructed individual oligodendrocytes and their processes by tracing at first each of the primary processes then all branching points and further processes until reaching the final internodes. The comparison of the 3-D rendering of a single OL at all three time points allowed me to detect processes and internodes that were lost during the initial demyelination period (pre c-MS/ c-MS d3) or in the later phase (c-MS d3/ c-MS d16) as well as new or extended OL's parts, which appeared between the selected time points (**Fig. 20B-C; Fig. 21B-C**). Using this approach, I quantified the total processes length of individual cell and average changes of the processes length, at the given stage of the cortical MS model and in control animals. First, results showed that single, mature oligodendrocytes differed in generated total processes length under healthy conditions (from 3000 $\mu$ m to 6000 $\mu$ m). It is consistent with the data that during development OLs localized in the cortex generate different number of internodes, which depends on the diameter of axonal fibers they are myelinating (Chong et al., 2012; Bechler et al., 2015). Variance in OLs processes length was similar among experimental and control animals and was a consequence of random selection of imaged oligodendrocytes during the initial 2PM recordings. Secondly, in the cortical-MS model, the vast majority of process loss took place up to three days after cytokines injection and the extent of this pathology varied between individual OLs ranging from modest to severe damage in which up to 70% of the initial processes were destroyed. Furthermore, our analysis showed that the same oligodendrocyte could survive in such an amputated-state and later form new processes and internodes. Mild effect of cytokines administration on OL morphology was also visible in control animals, however these cells seldom develop or extended new processes (**Fig. 20D-F; Fig. 21D-E**).

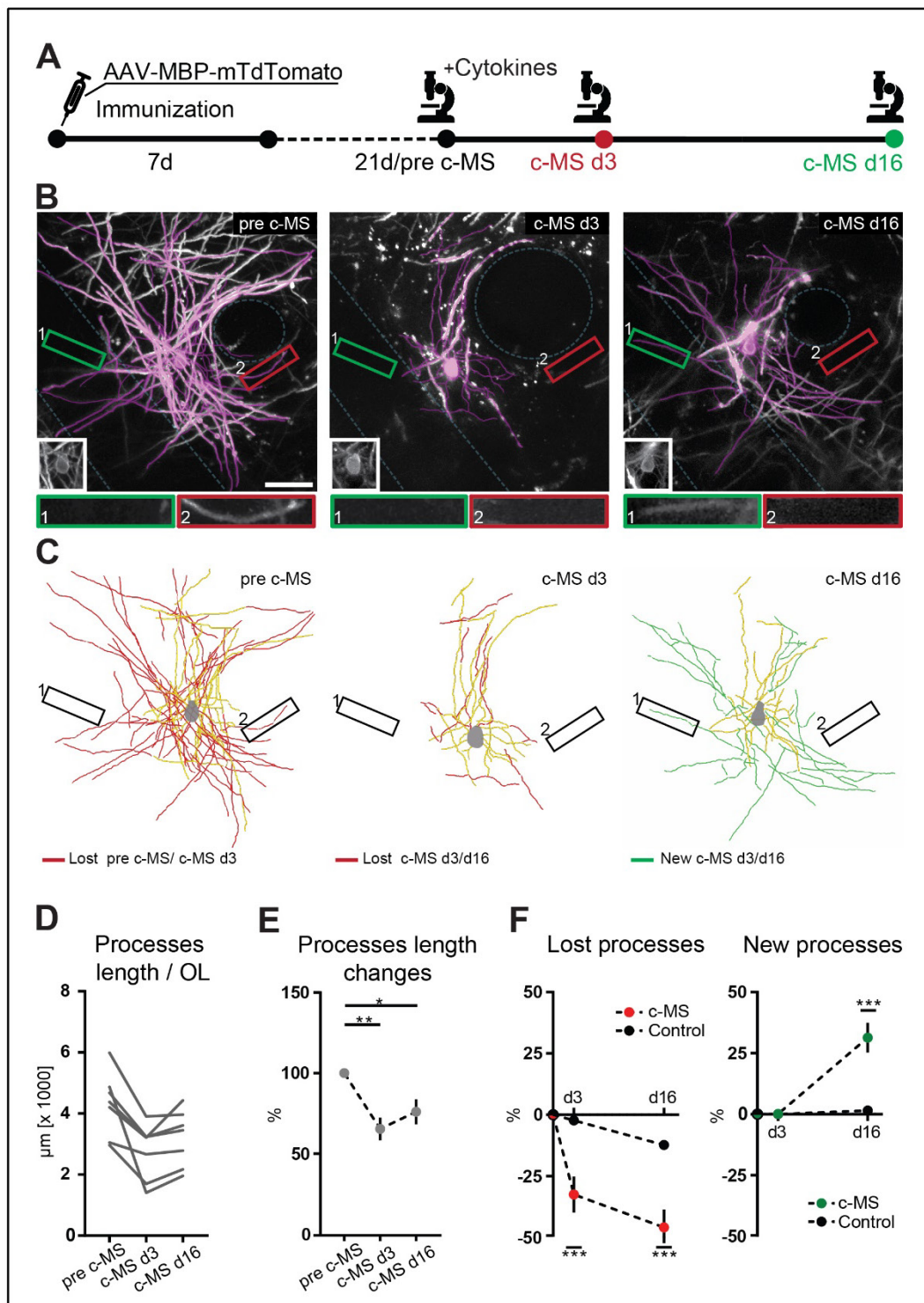


**Figure 20. Longitudinal *in vivo* imaging of pre-existing OL and its myelin in c-MS model.** (A) Experimental time line to study changes of pre-existing OLs before cortical lesion, at the peak of the myelin loss and during recovery phase, by implementing viral vector OL labelling approach (AAV-*Mbp*:mem-tdTomato). (B) Representative 2PM *in vivo* image projections of the same OL traced over time. Reconstructed processes (magenta) overlaid on tdTomato signal. Green rectangles mark area with new internode, red rectangles with the lost internode. Insets show OL soma. (C) 3-D reconstruction of the same OL (from B) during different time points. Changes in processes between time points (indicated below reconstruction) are color-coded: remaining in yellow, lost in red, new in green, OL cell body highlighted with grey. (D-E) Quantification of individual OL's processes length and average percentage changes in processes length/OL during the course of c-MS model. (F) Quantification of the lost and new processes in pre-existing OLs in c-MS model in compare

---

to cytokine-injected control animals. All values are normalized to pre c-MS/cytokine-injection condition in E and F. c-MS: n=7 OL from 3 mice, control animals: n=8 OLs from 3 mice. Scale bars in B 50µm. One-way ANOVA followed by Tukey's multiple comparisons test has been performed in E, *t*-test has been performed in F. \*\*\*P<0.001, \*\*P<0.01, \*P<0.05.

Our *in vivo* data however also revealed that on c-MS d16, newly generated tdTomato+ (dim) OLs became visible in the field of view. Although they were separated in depth, the tracing accuracy, especially of the more distal internodal parts of individual OL might be less precise (Fig. 23). Therefore, in order to validate the findings obtained by light microscopy techniques, selected example of pre-existing oligodendrocyte was used for ultrastructural electron microscopy analysis. High resolution EM images allow to reconstruct cellular and subcellular compartments with nearly native view (Snaidero et al., 2014). Correlated light and electron microscopy (CLEM) study was performed in Electron Microscopy Hub (SyNergy, German Center for Neurodegenerative Diseases) with the help of Dr. Nicolas Snaidero and Dr. Martina Schifferer.

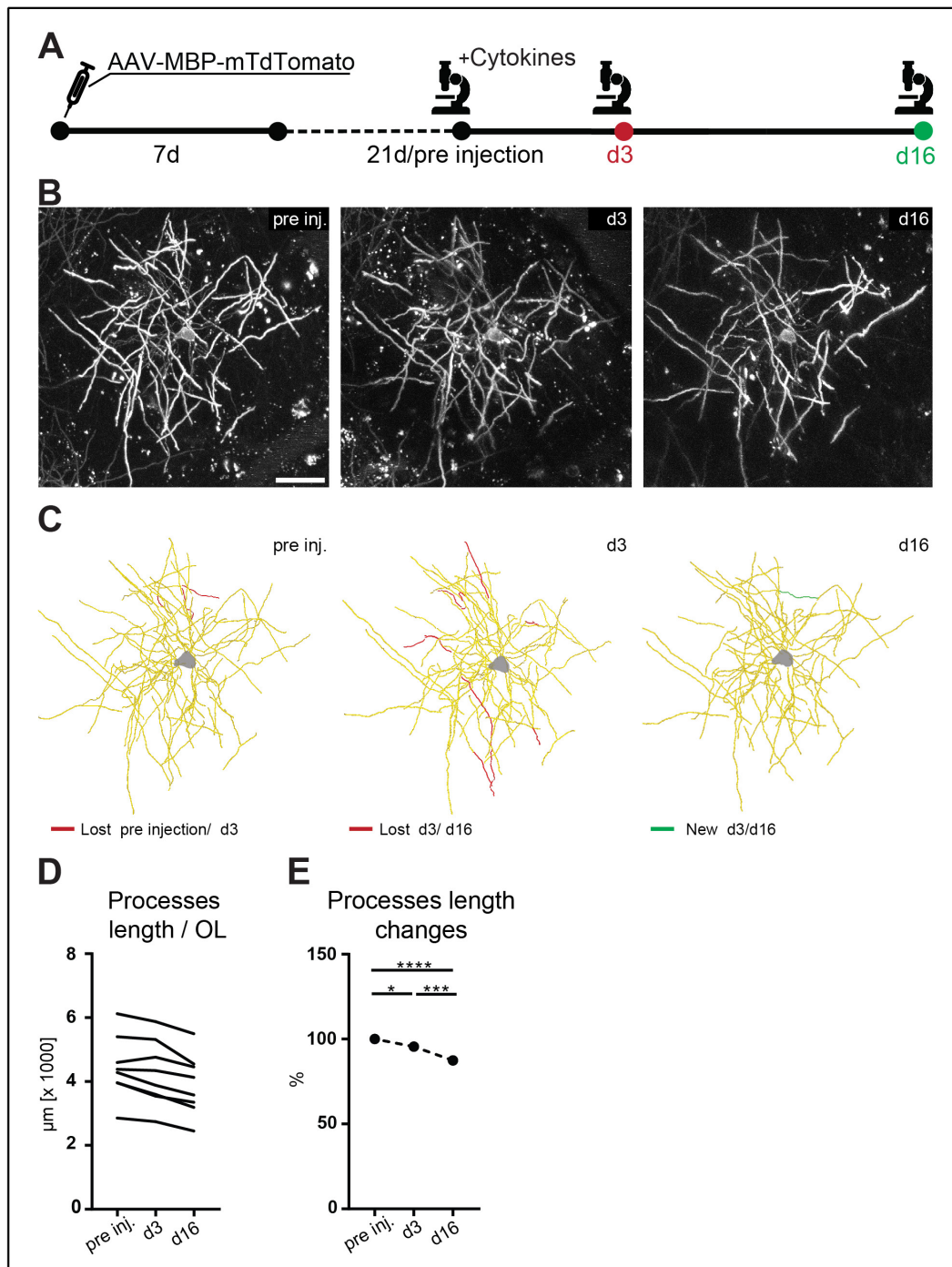


**Figure 21.** Longitudinal *in vivo* imaging of mature OLs and their myelin in cytokines injected control mice. (A) Experimental time line to detect OLs changes in control animals injected with cytokines. (B) Representative 2PM *in vivo* image projections of the same OL traced over time. (C) 3-D reconstruction of the same OL (from B) during different time points. Changes in OL morphology are color-coded: yellow-remaining, red-lost, green-new processes; OL soma in grey. (D-E) Quantification of the individual pre-existing OL's processes length and the same quantification at the OL population level in control animals. n=8 OLs from 3 mice. Scale bars in B 50µm. One-way ANOVA followed by Tukey's multiple comparisons test has been performed in E. \*\*\*\*P<0.0001, \*\*\*P<0.001, \* P<0.05.

### Correlated light and electron microscopy of individual OL

To enable identification of a specific oligodendrocyte in serial ultrathin sections, asymmetric near-infrared brandings (NIRB; Bishop et al., 2011) were performed in the intact fixed brain, around intravital imaged area, after the last imaging session on c-MS d16 (detailed protocol in Chapter III- Methods, section 3.11.) (Fig. 22A, left). Based on the NIRB and angioarchitecture, low-resolution electron microscopy images were acquired to identify region of interest (Fig. 22A, right). Next, high-resolution images were taken of the preselected area (Fig. 22B), which allowed further 3-D reconstruction of *in vivo* traced OL (Fig. 23A). We traced the selected internodes among the EM sections and determined the site where OL distal process was connected to the myelin sheath. From that place, we followed such *connector* to the OL soma (Fig. 23B). Unfortunately, we could not link the selected, newly restored myelin sheathes to pre-existing OL either because of inability to continuously track the connectors to the soma or because the internode belonged to the another cell (likely derived from an OPC). Our CLEM analysis revealed two possible obstacles in explicit reconstruction of cell morphology based only on the fluorescence signal. At first, tdTomato signal might overlapped between 2 different OLs processes. As indicated in Fig. 23A by solid white arrowhead, the ending point of the process from pre-existing OL overlaid with the another OL's process, primarily running perpendicularly to the surface of the imaged area. Secondly, the resolution in the depth direction was also limited (as depicted by open white arrowhead in Fig. 23A); this led to the impression that a connector was linked to the internode in LM image while the EM analysis revealed 3 $\mu$ m distance between these structures.

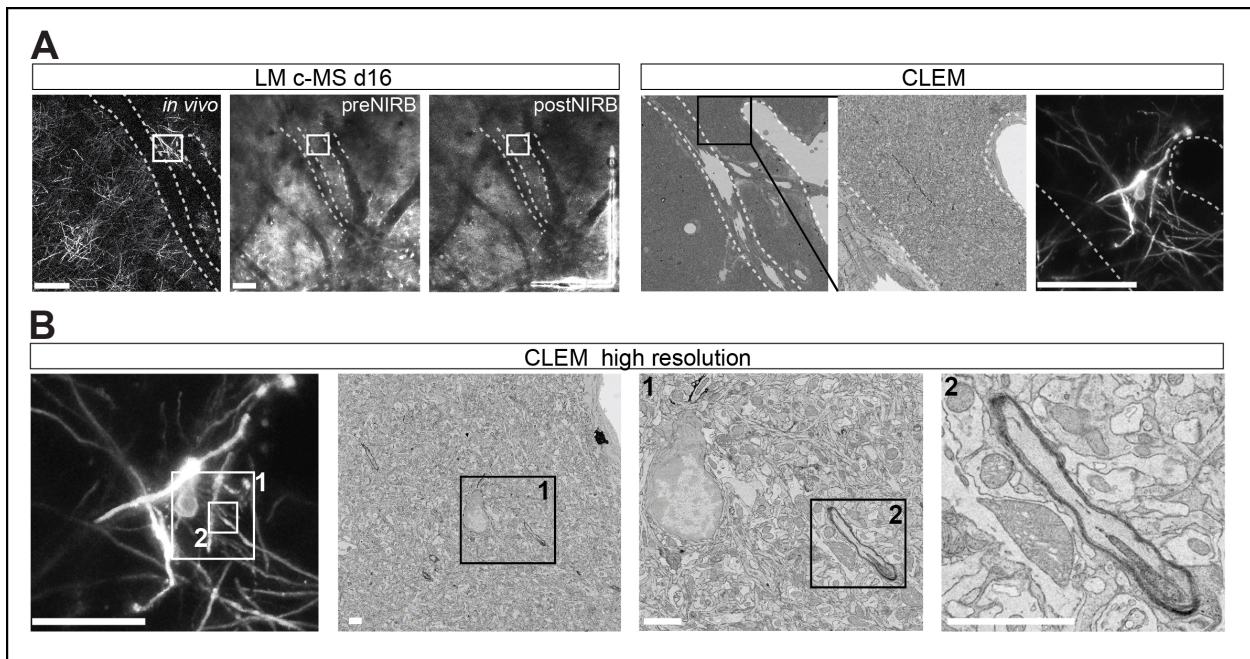


**Figure 22. Correlative *in vivo* imaging with high-resolution volume electron microscopy. (A)** A workflow allowing the identification of *in vivo* imaged OL in the EM sections. Area of interest can be identified based on NIRB and angioarchitecture. **(B)** High-resolution correlative EM of pre-existing OL, imaged on c-MS d16. Ultrastructure of marked areas in B (left) are shown with higher magnification on EM section. Scale bars in A 100 $\mu$ m (LM), B 50 $\mu$ m (LM) and 2 $\mu$ m (EM).

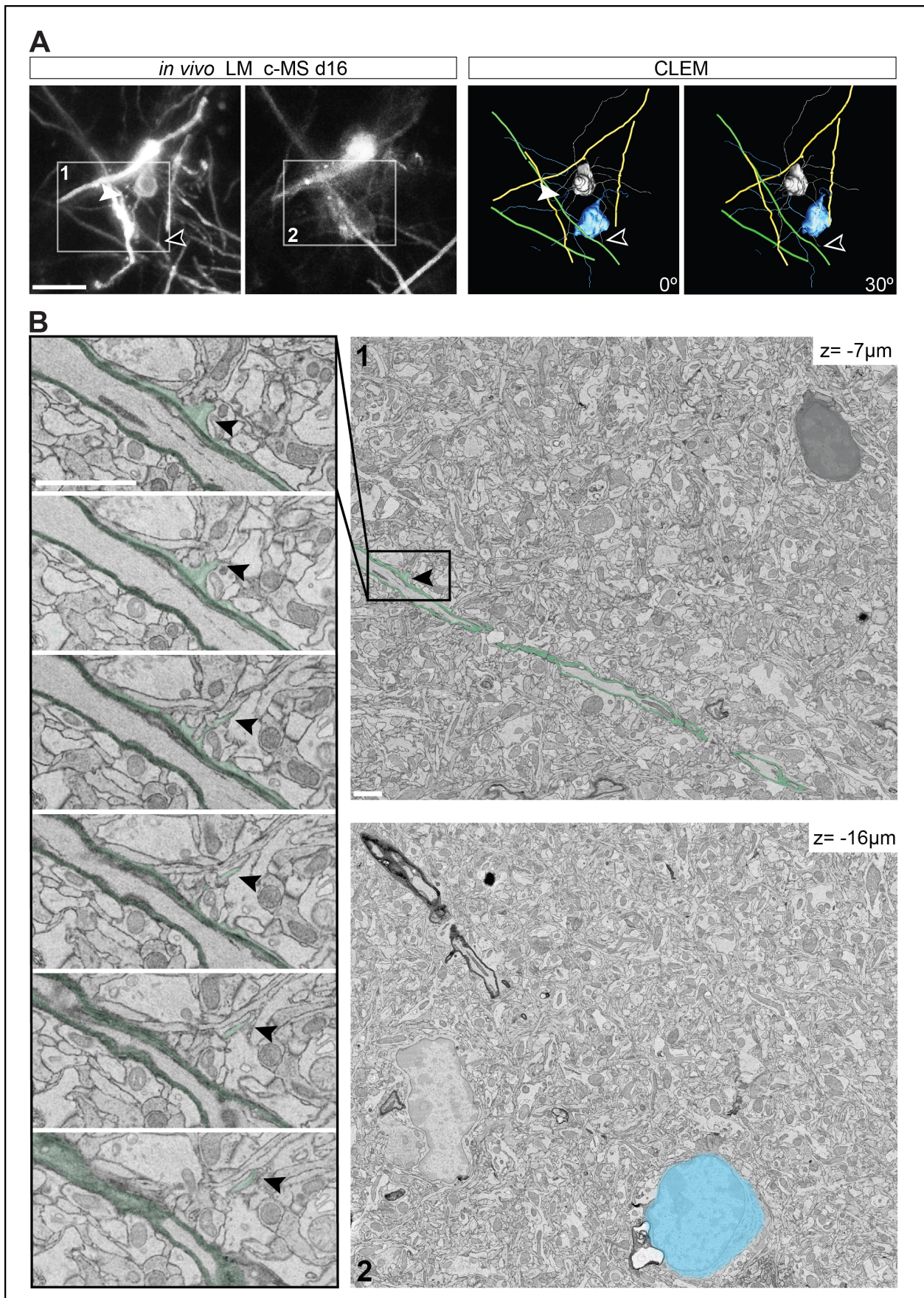
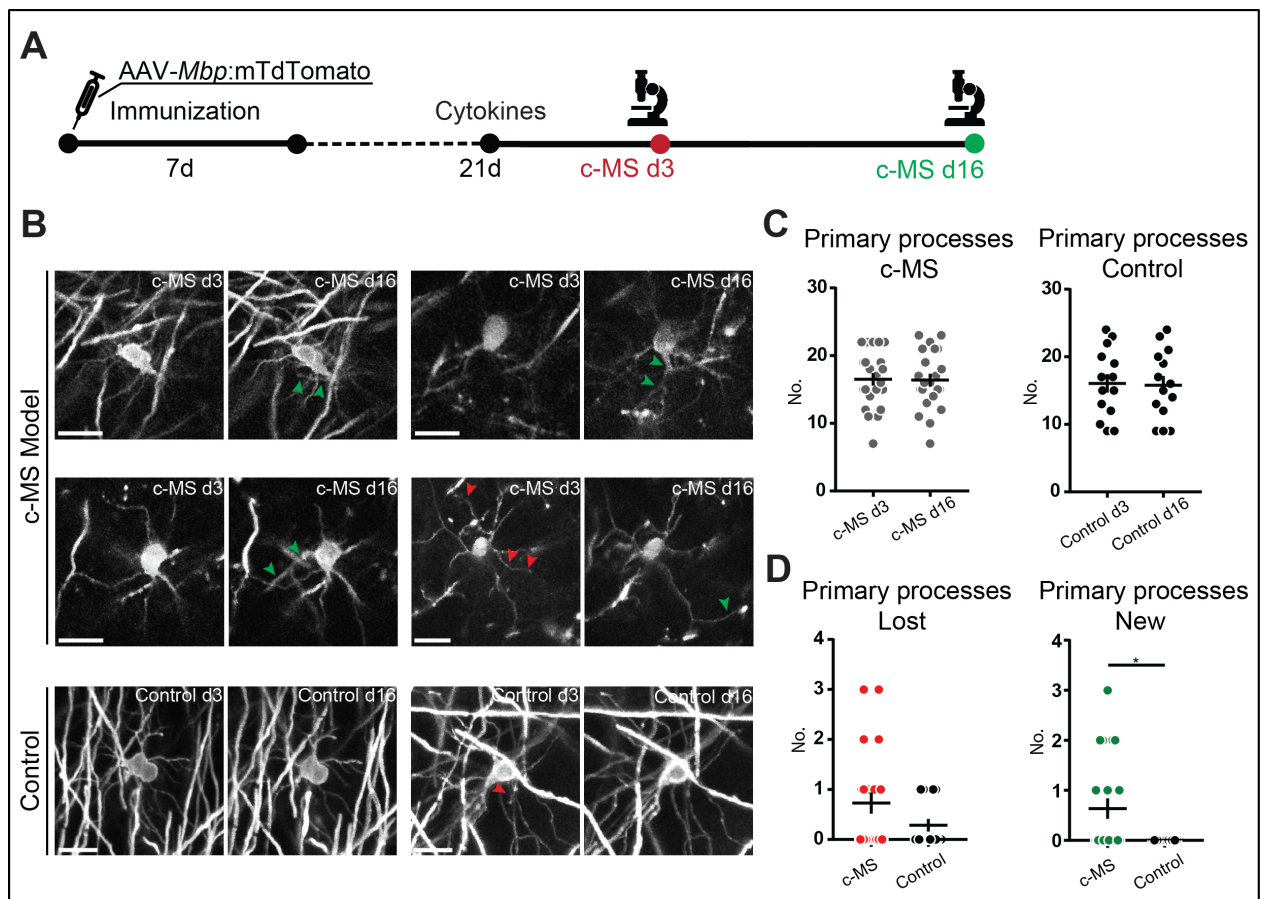


Figure 23. Correlative light and electron microscopy analysis of the pre-existing OL in c-MS model. (A) CLEM 3-D reconstructions of pre-existing OL (grey soma) and new OL (blue soma) with their belonging processes

and selected internodes. (B) High-resolution electron micrographs of areas marked in A. Z-spacing between cells is indicated in the right top corners. Connection between myelin sheath and OL's process as well as further tracing is shown in sequential EM sections of region depicted in 1. Scale bars in A 20 $\mu$ m, B 1 $\mu$ m.

### Analysis of primary processes formation by pre-existing OLs

Although EM revealed that it can be difficult to judge the distal processes architecture based on our 2PM imaging approach, it did confirm that primary processes (processes exiting the somata) can be reliably assigned to individual oligodendrocytes. Indeed, all primary processes identified with EM ultrastructural analysis were also correctly assigned and reconstructed based on the light microscopy signal (n=2 OLs) (Fig. 23A). Moreover, during the longitudinal *in vivo* imaging, comprised of three-time-points 2PM sessions, I did not detect any newly integrated OLs nor newly established processes or internodes on the c-MS d3. Therefore, it could be assumed that cells imaged at the demyelination peak are rather mature, old OLs than newly differentiating and integrating cells, which initially extend their processes towards the demyelinated axons. Taking all of above into consideration, I aimed to answer the question if pre-existing OLs can form new primary processes during the course of c-MS model. To do this, AAV-*Mbp*:mem-tdTomato was injected into C57BL6 x BiozziABH mice which were imaged on day 3 and 16 after cortical lesion induction as already described before. Three weeks after virus administration, control non-immunized animals also received cytokine injections and were imaged 3 and 16 days later (Fig. 24A). I compared the presence of primary (or most proximal) processes of the individual OLs between c-MS d3 and d16 in the model animals as well as in the cytokine-injected controls. Even under inflamed conditions, which leads also to tissue swellings, OL processes morphology remained stable therefore allowing their time-lapse tracing and identification (Fig. 24B). Analysis of *in vivo* 2PM data obtained from 22 OLs from 6 c-MS model mice and 14 OLs from 5 control mice uncovered the high variability in the number of processes existing the soma, ranging from 7 to 24 per OL, regardless of the inflammatory conditions. Further quantification showed that the total number of primary processes stayed unchanged between the time points in both of the groups. However, the loss of the OLs primary processes was more frequently detected in c-MS model mice in comparison to control animals. Importantly, I observed a formation of new primary processes only by pre-existing OLs present in grey matter with induced cortical lesion (Fig. 24C-D).



**Figure 24. Primary processes formation in pre-existing OLs in c-MS model.** (A) Schematic diagram to study changes in primary processes in pre-existing OLs in cortical lesion. (B) High magnification, intravital 2PM images of OLs labelled with AAV-*Mbp:mem-tdTomato*, recorded at the two time points (3 and 16 days after cytokines injection). Four c-MS model OLs examples with new (or extended) and lost primary processes (B, upper and middle panel); two control animal OLs examples of unchanged and lost primary processes (B, lower panel). Green arrowheads points to new processes, red arrowheads indicate lost processes. (C) Quantification of total number of primary processes in c-MS model and control animals no statistically significant differences were detected between time points and groups. (D) Quantification of the number of lost and new primary processes in c-MS model and control animals. Statistical significance detected only in 'new processes' evaluation. c-MS model n= 22 OLs from 6 mice; controls n= 14 OLs from 5 mice. Scale bars in B 20 $\mu$ m. T-test has been performed in C and Mann-Whitney test has been performed in D. \*P<0.05.

Our results indicate that mature OLs can form new primary processes. It is however not clear if they are also able to eventually establish stable axoglial *connection* and contribute to remyelination. Therefore, I have been testing alternative labelling approaches, which allow me to conclusively assign internodes to individual OL cell body.

## 2.7. New approaches for spatiotemporal oligodendrocyte labelling

Since our previously used conventional AAV- labelling technique combined with 2P microscopy imaging is not sufficient for undisputed tracing of single oligodendrocytes and all their distal internodes, I explored the following new approaches for spatiotemporal resolution of these cells.

First, I tested a new AAV viral vector system, which had been modified from the previous one by addition of another fluorescent protein – paGFP; AAV-*Mbp*:mem-tdTomato-2A-paGFP. It is photoactivatable version of GFP, which upon irradiation with ~400nm (confocal microscopy) or ~750nm (2PM), becomes visible while excited by green light (Patterson and Lippincott-Schwartz, 2002). Because paGFP diffuses around the site of activation and fluorescent signal remains stable, this technique also allows to trace individual cells and cellular compartments *in vivo* (Schneider et al., 2005). As described before, membrane-targeted tdTomato expression is driven by MBP promoter in oligodendrocyte population but additionally GFP signal can be detected in the subset of oligodendrocytes only after the targeted photoactivation. After repetitive *tornado-point* photostimulation of the selected oligodendrocyte cell bodies, the GFP can be detected not only in their somata but also in the proximal processes and internodes (Fig. 25A). Unfortunately, the photoactivated signal did not spread towards the most distal internodal parts and too excessive photoactivation lead to the OL damage.

Secondly, I tried to use conditional genetics and a two virus system to ensure the selective expression of a fluorescent label only in mature (pre-existing) OLs. In this approach, fluorescent signal can only be detected after co-transduction of CreER<sup>12</sup> and DiO XFP-bearing AAV vectors, and only after tamoxifen administration. My experimental design is based on the ‘Cre-on’ system composed of *i*) AAV-*Mbp*:DiOmem-tdTomato in which fluorescent protein is inversely orientated and *ii*) AAV-*Mbp*:CreER<sup>12</sup>, which flips this inverse ‘off’ position to sense orientation by tamoxifen-inducible Cre recombinase. This system should not only decrease the density of the labelled oligodendrocytes (as it requires both AAVs to transduce single OL) but also result in time dependent tdTomato expression. Temporal resolution is achieved by tamoxifen administration, which enables iCre-recombinase translocation into the nucleus (Feil et al., 1997 and 2009). By using this approach, early treatment with tamoxifen before systemic EAE induction, would result in tdTomato expression only in OLs integrated before cortical lesion induction. Therefore, signal detected during longitudinal *in vivo* imaging of the c-MS lesion would only come from

mature, pre-existing OLs. To validate the method, oligodendrocytes were visualized under healthy conditions in the somatosensory cortex two months after the initial viral administration (**Fig. 25B**). However, this approach results in very low efficiency in OL labelling, which might be caused by single cell transduction capability. To overcome this limitation, each of the viruses can be combined separately with one of the reporter mouse lines, which is currently our ongoing experiment (some reporter mouse lines listed in Table 1, Chapter I – Introduction, section 3.2. Oligodendrocyte and myelin visualization).

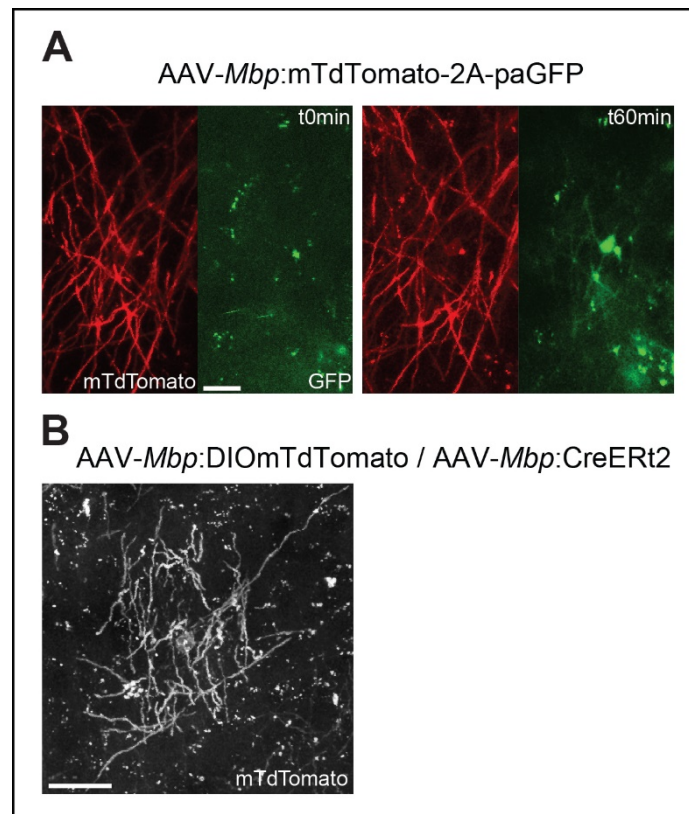


**Figure 25.** New approaches label mature OLs with spatiotemporal resolution. (A) AAV-*Mbp*:mem-tdTomato-2A-paGFP approach: *in vivo* 2PM photoactivation of GFP in selected tdTomato+ OL. 2PM images of the same area acquired with 1040nm wavelength (MBP-TdTomato, red) and 800nm wavelength (PLP-GFP, green) prior the photoactivation (**left**) and 60 minutes after photoactivation (**right**) (B) AAV-*Mbp*:CreER<sup>2</sup>/AAV-*Mbp*:DiOmem-tdTomato approach: confocal image of the single tdTomato+ OL in the somatosensory cortex (layer 2/3) observed in the test animal. Scale bar in **A** 20 $\mu$ m in **B** 50 $\mu$ m.

## Chapter V – Discussion

Demyelination followed by remyelination are the key histopathological features of multiple sclerosis lesions. Unfortunately, myelin sheaths restoration is frequently impaired in MS patients (Chang et al., 2002; Kuhlmann et al., 2008; Gruchot et al., 2019). As a result, damaged oligodendrocytes and myelin sheaths are receiving more and more interest as potential therapeutic targets in MS (Baxi et al., 2014; Green et al., 2017; Schwartzbach et al., 2017; Preston et al., 2019). Thus, it is very important to better understand mechanisms underlying remyelination. Conventional concept predicts that it is mediated by OPCs, which can differentiate into mature, myelinating cells (Gensert and Goldman, 1997; Wolswijk, 1998; Zawadzka et al., 2010). However, recent findings led to the speculations that adult, lesioned oligodendrocytes might contribute to remyelination as well (Duncan et al., 2018; Yeung et al., 2019; Jäkel et al., 2019). To investigate this possibility, I assessed the cellular sequence of demyelination and remyelination in neuroinflammatory lesions. Based on the results presented in this thesis, it can be concluded that OL damage follows an outside-to-inside pattern leading to the oligodendrocytes with shorter and fewer processes. Notably OLs can survive in such amputated-state over extended periods of time. Further, compact myelin sheaths can be restored with relatively high efficiency and results from longitudinal *in vivo* imaging suggest that pre-existing OLs can form the new processes thus possibly taking part in the remyelination process.

### 1. Demyelination pattern and oligodendrocyte loss in the MS-like lesions

The sequence of pathological changes in oligodendrocyte morphology is still not fully understood and different hypothesis of the initial site of the immune attack on OLs in MS lesions have been proposed: myelin and its proteins, distal parts of OL's processes or cell body itself (Bradl and Lassmann, 2010). In this thesis, I investigated the cellular sequence of demyelinating events in a MS model induced in mice on a BiozziABH background. The peculiar properties of this strain make the mice highly susceptible to EAE induction, which follows a relapsing-remitting course of the disease. The resulting EAE lesions are characterized by mononuclear cell infiltration, antibody deposition and extensive myelin loss (Biozzi et al., 1972; Baker et al., 1990) and show histopathological features that resemble the most frequently

occurring *Pattern II* of demyelination in MS patients (Lucchinetti et al., 2000). Using this EAE model, I showed that oligodendrocyte damage spread in a centripetal pattern, i.e. from the internodal parts towards the cell soma. During the course of the disease, myelin loss exceeded the oligodendrocyte loss, even at the initial steps of the lesion development (Fig. 7). Furthermore, at the peak of the demyelination (onset of clinical symptoms + 2 days) myelin was almost entirely gone in the lesion center and substantially decreased at the lesion border, while only a mild loss of OL cell bodies was detected in the lesion center (Fig. 8). These results are consistent with the analysis of brain biopsies from MS patients, which show that actively demyelinating MS lesions are characterized by the same gradient of myelin density, which is almost completely lost in the lesion center and significantly reduced at the rim of the lesion. In contrary, number of oligodendrocytes remain comparable between the lesion area and NAWM. Additionally, in EAE and MS samples, the extent of demyelination is not correlated with the oligodendrocyte death but rather with the density of infiltrating immune cells (Brück et al., 1994; Romanelli et al., 2016).

I also induced demyelination by ethidium bromide injection into the lumbar white matter of the spinal cord. Here, the oligodendrocyte soma is expected to be the primary site of the injury and thus, this model mimics *Pattern IV* of demyelination in MS patients (Lucchinetti et al., 2000) or the pathology observed in viral-induced diseases like progressive multifocal leukoencephalopathy (Richardson-Bruns et al., 2002). I could confirm this centrifugal pattern of myelin damage and show that vast majority of OLs is lost, leaving the myelin sheaths unsupported (Fig. 9). Thus, despite of the advantages of this model like the short experimental time line and well-defined lesion site, it is not well suited to study the fate of affected oligodendrocytes during the disease course since most of them follow necrosis pathway almost immediately after toxin administration (Sim et al., 2002). According to heterogeneity model of MS pathology, our EB model mimics rather rarely occurring MS lesions with demyelination spreading in the inside-to-outside gradient (Lucchinetti et al., 2000; Lassmann et al., 2001) but is consistent with the other suggested demyelination concept, in which initial stages of lesion formation always include OLs death and microglia activation and only later myelin alterations, suggesting only time-dependent immunopathological lesion differences (Barnett and Prineas, 2004). However, more recent findings continue to support the hypothesis of rather patient-specific MS heterogeneity (Lucchinetti et al., 2000),

as longitudinal examination of active lesions shows that they preserve their distinct immunopatterns with the disease duration (Metz et al., 2014).

Our results from the two MS models point to a significantly higher OLs survival rate in EAE lesions compared to those induced by EB-mediated demyelination. Persistence of OLs in the EAE model is in line with the findings that mature, pre-existing oligodendrocytes survive immune attack and can be found in the shadow plaques (Yeung et al., 2019). Moreover, as reported before, oligodendrocytes albeit stripped of their myelin, can survive over longer period in MS lesions (Wolswijk, 2000). Additionally, demyelination in EAE mice is induced by autoantibodies against myelin proteins (Rivers et al., 1933; Stromnes and Goverman, 2006a; Miller et al., 2007), which are also detected in the subset of MS patients (Pröbstel et al., 2011; Quintana et al., 2012; Prineas et al., 2018). Giving above, to resemble the sequence of demyelinating events and investigate the OLs fate as accurate as possible in MS-like lesions, I continued my research on oligodendrocytes dynamics in EAE model, which mimics the conditions occurring in the majority of the MS cases.

Single-cell labelling with rabies virus SAD  $\Delta$ G mcherry allowed tracing and 3-D reconstruction of the individual oligodendrocytes in the EAE settings and under healthy conditions (Wickersham et al., 2007; Romanelli et al., 2016). *In vivo* time-lapse imaging of these single OLs during the different stages of the disease course confirmed that the demyelination follows an outside-to-inside pattern and revealed that oligodendrocytes in inflammatory lesions present shorter and fewer processes as well as they exhibit more severe morphological changes with the disease progression (Fig. 10). Interestingly, during the several hours of time-lapse imaging, I observed almost no changes even among severely damaged OLs. I also did not detect any cell death during the 2PM recordings at the single-cell level nor at the population level, assessed by staining the sections with an apoptotic marker, caspase-3 (Porter and Jänicke, 1999; Hisahara et al., 2000). These results provide evidence that mature oligodendrocyte, which lost substantial number of their processes are not immediately stepping towards cell death. Thus, we speculated what would be the fate of these amputated OLs at later time points and, in particular, we wondered whether they can potentially reform their myelin sheaths as it has been recently suggested (Nave and Ehrenreich, 2019).

*In vivo*, longitudinal tracing of individual oligodendrocytes in the 'classic', active EAE model remains challenging because most of the lesions are localized in the white matter of the lumbar spinal cord

(Constantinescu et al., 2011). There are spinal cord chambers for chronic multiphoton imaging but they are rather suited to implement in the thoracic SC division (Farrar et al., 2012; Sekiguchi et al., 2016). Removal of few adjacent lumbar lamina allows only for the acute intravital imaging over several hours (Nikić et al., 2011; Sorbara et al., 2014), which restricts tracing of the same cell days later, in the recovery phase of the disease. Importantly, also high density of oligodendrocytes in the spinal cord causes difficulties in precise 3-D reconstructions of individual cells (Romanelli et al., 2016). Thus, we decided to investigate the fate of surviving oligodendrocytes in a MS mouse model of cortical MS pathology, in which a cranial window allows longitudinal *in vivo* imaging of the same area (Jafari et al., 2019) and OLs are distributed sparser in the first cortical layers in comparison to spinal cord WM (Bahney and von Bartheld, 2018). Additionally, cortical grey matter pathology is an important aspect in progressive MS but due to the lack of experimental tools has not been extensively studied (Peterson et al., 2001; Bø et al., 2003; Caramanos et al., 2003; Geurts et al., 2005; Vercellino et al., 2005).

## 2. MS model of targeted cortical demyelination

In order to study oligodendrocyte and myelin damage in the mouse cerebral grey matter lesions, we adapted previously established rat models of cortical MS pathology (Merkler et al., 2006; Gardner et al., 2013; Jafari et al., 2019). After MOG immunization, a single intracerebral injection of proinflammatory cytokines TNF- $\alpha$  and IFN- $\gamma$  leads to the targeted, focal demyelination in the cortical GM in mice on a BiozziABH x C57Bl6 background. Both cytokines are considered to play an important role in the lesion formation in MS patients as they are frequently found in actively demyelinating areas (Beck, 1988; Hofman et al., 1989; Martins et al., 2011). In conventional active EAE models, an increase in peripheral TNF- $\alpha$  leads to the instability of the synaptic connections detected before clinical symptoms onset (Yang et al., 2013). In general, by disruption of endothelial cells, cytokines facilitate encephalitogenic T cell migration across the BBB and further recruitment of other inflammatory cells leading to the CNS demyelination (Kerschensteiner et al., 2004). In our cortical MS model, lesion formation is mainly triggered in the subpial area and around the vessels, in a highly reproducible and temporally well-defined manner, which in comparison to toxin-induced lesions, however maintains the immunopathological origin of the disease. Such targeted grey matter inflammation favors the precise *in vivo* investigation of GM lesion formation

and the ensuing recovery process, which is often difficult in active EAE, where cortical pathology, if at all present, is randomly distributed (Rasmussen et al., 2007; Girolamo et al., 2011; Mangiardi et al., 2011). The administration of the proinflammatory cytokines into a predefined cortical area results in extensive phagocyte activation, T cell infiltration and substantial myelin loss spreading laterally on both hemispheres, hence mimicking the most common Type III of cortical demyelination in MS patients (Peterson et al., 2001; Lucchinetti et al., 2011). Furthermore, GM inflammation resolves around two weeks after the cortical lesion induction and is accompanied by ongoing remyelination (Jafari et al., 2019; Fig. 11). These findings are consistent with the data obtained from previously described rat models (Merkler et al., 2006; Gardner et al., 2013).

### 3. Demyelination pattern and remyelination capacity in the cortical lesion

As discussed in the *Introduction Chapter*, MS pathophysiology may differ in a region-specific manner and therefore, one could hypothesize that the sequence of demyelinating events might also depend on the lesion localization in white or grey matter (Kutzelnigg et al., 2005; Bø et al., 2007). Here, I showed that in MS models, GM oligodendrocytes followed the same pattern of pathology as observed in the WM lesions (Fig. 7,8,10). Furthermore, by utilizing the same quantification criteria, I demonstrated that oligodendrocytes number remained remarkably stable over the course of cortical MS, while myelin, almost entirely gone at the peak of the disease was restored with high efficiency two weeks later (Fig. 12). However, this aspect is in contrast to the situation observed in MS patients, who often present rather limited remyelination of cortical lesion (Kutzelnigg et al., 2005; Chang et al., 2012). A possible explanation for this discrepancy can be the fact that standard experimental animals (3 to 5 months) correspond to young human adults in their late twenties (Flurkey et al., 2007). GM pathology is however mainly associated with more progressive stages of the disease, when lesions accumulation and the increasing age of the affected patients may be the limiting factors for efficient remyelination (Sim et al., 2002; Rist and Franklin, 2008; Crawford et al., 2016a; Cantuti-Castelvetri et al., 2018). Indeed, time course analysis of cortical MS pathology in aged animals (9 to 11 months) showed that 4 weeks after lesion induction, mice presented, at best, only a minimal myelin restoration (Fig. 13). This declined recovery could be due to the decreased number of the OPCs in the lesion, however data from EAE studies and MS autopsies indicates that OPCs are still present in the demyelinated areas but often fail to complete differentiation (Chang et

al., 2002; Kuhlmann et al., 2008; Boyd et al., 2013). This failure of OPC differentiation can be explained by aging-associated dysregulated epigenetic mechanisms involved in OPC differentiation and lack of their responsiveness to the intrinsic and extrinsic signals (Shen et al., 2008; Neumann et al., 2019). However, the same pathways might be dysfunctional in pre-existing, affected OLs restricting their regenerative capacity, assuming that they can contribute to the remyelination (see below).

Our analysis revealed that OLs number remained remarkably stable in the GM lesion. However, developmental stages of these OLs cannot be assessed explicitly based only on the GFP signal, which can be relatively early present in maturing OLs in *Plp:eGFP* mouse line (Mallon et al., 2002). Thus, the oligodendrocyte population might be differently composed during the course of cortical MS, still resulting in no changes in overall cell number (Fig. 12). Considering this, I characterized OLs maturation status and showed no significant differences in the number of OPCs, OL lineage cells and mature OLs over the course of the *c*-MS model (Fig. 16). *Plp:eGFP/C57Bl6* mice present a peculiar feature in GFP intensity signal; around half of the PLP-GFP expressing cells is relatively dim, whereas the other half is very bright (Mallon et al., 2002). Because PLP expression increases with the OLs maturation, differences in GFP intensity could be an indicator for the distinct developmental stages of the cells (Patrikios et al., 2006; Marques et al., 2016). However, co-staining of the cortical sections with OL precursor's marker NG2 and mature OL's marker CC1 revealed that dim GFP cell population was almost equally composed of OPCs and old OLs. On the other hand, the vast majority of bright GFP cells could be identified as CC1+ oligodendrocytes (Fig.14). Furthermore, I detected no shifts in distribution of dim and bright GFP populations during the course of cortical lesion (Fig.15).

Because our findings in grey matter lesions of young adult mice suggest a high stability of mature oligodendrocytes and efficient remyelination that is not accompanied by an increase in OPCs at the population level, we aimed to investigate OLs turnover and myelin sheaths restoration *in vivo*, in the individual lesion areas over the course of *c*-MS. The implantation of cranial window above the somatosensory cortex, previously injected with cytokines, allowed tracing changes within the same cortical area over time course of GM pathology (Holtmaat et al., 2009; Jafari et al., 2019; Snaidero et al., 2019). Our *in vivo* analysis of OLs turnover showed that 80% of OLs survived from the initial demyelination period (*c*-MS d3) until the recovery phase two weeks later (*c*-MS d16; Fig. 17). The loss of

one fifth of the OLs was compensated by the appearance of nearly the same number of new cells. As it could be speculated that at least half of the dim GFP OLs is in fact an adult OPC population, an increase in their GFP intensity could indicate a further maturation of these cells. Interestingly, I did not detect any significant changes in fluorescent signal intensity among the same, dim GFP remaining cells, during the two imaging sessions. Furthermore, based on time-lapse imaging of the cortical MS model, I could confirm the high recovery capacity in the individual lesion areas (Fig. 17). During the remyelination phase, the total length of OLs processes increased significantly in comparison to the density detected at the peak of demyelination. Considering that there is rather little OLs turnover, it appears to be possible that mature, pre-existing OLs can contribute the remyelination (Cui et al., 2017; Duncan et al., 2018; Jäkel et al., 2018; Yeung et al., 2019). However, the extent to which this could be possible is unknown as the density of the GFP+ OLs is too high to reliably assign restored internodes to individual cells (Mallon et al., 2002; Flores et al., 2008). Another limitation of this study is the lack of the information about the compaction status of the newly produced myelin. In order to overcome these limitations, I implemented a viral labelling approach with single-cell resolution of oligodendrocytes.

#### 4. Myelin compaction in remyelinated cortical lesions

The generation of new versions of fluorophores allows precise intravital labelling of the cells and cellular components, thus enabling their *in vivo* visualization and providing the real-time information (Xiao et al., 2011; Progatky et al., 2013; Swire and French-Constant, 2018). Here, I designed, cloned and characterized a recombinant, replication deficient adeno-associated virus, in which 1.3kB of the *Mbp* promoter region drives the expression of the membrane-targeted tdTomato in OLs. Zebrafish-derived Gap43, a palmitoylated sequence of 35 amino acids is fused at its N terminal to the TdTomato, which guides the protein to the membranes – from a cell's soma to the most distal internodal parts. (Kay et al., 2004; von Jonquieres et al., 2013). Importantly, a single intracortical injection with the viral vector resulted in fluorescent labeling only in a subpopulation of the PLP-GFP+ cells about 3 weeks after injection and did not cause virally induced damage (Fig. 18). Of the note, the AAV-*Mbp*:mem-tdTomato labelling approach was also utilized in the study included in *Snaidero, Schifferer, Mezydło, (...), bioRxiv 2019* to investigate changes in myelination pattern in the OL laser ablation settings.

Sparse tdTomato signal was still present in the intact brains after 4% PFA-perfusion allowing, previously *in vivo* imaged, OL's identification with confocal microscopy. This in turn facilitated the assessment of myelin compaction with the spectral confocal reflectance microscopy technique. Only the compact myelin can be visualized by merging its simultaneous light reflections (Schain et al., 2014; Jafari et al., 2019). AAV-*Mbp*:mem-tdTomato injected and immunized C57BL6/J x Biozzi animals were imaged during the peak of the demyelination and in the recovery phase. By subtracting the pre- and post-myelin loss periods, I reconstructed the individual oligodendrocytes marking also remaining and new processes and internodes present in the cortical remyelination phase and verified if they are also SCoRe positive. Here, we demonstrated that newly restored OLs internodes, detected during the *in vivo* 2PM recordings, were in fact characterized by compact myelin (Fig. 19). These findings are in contrast to the result obtained from MS autopsies, which points out that in the MS, pre- and early myelinating OLs are not successfully integrated; regardless of the presence of their extending processes, they do not establish the stable axoglia 'connection', therefore they do not contribute to remyelination. However, these data come from rather chronic MS lesions and represent only a time-locked picture of probably more dynamic, ongoing processes (Lucchinetti et al., 1999; Chang et al., 2002; Brück et al., 2003).

Taking advantage given by longitudinal *in vivo* recordings of the cortical lesion area, I detected numerous examples of newly generated processes and internodes, which could be traced back to pre-existing oligodendrocytes. However, the *two-time-point* set up used in these experiments, in which oligodendrocytes are only imaged at the peak of the demyelination (c-MS d3) and in the remyelination phase (c-MS d16), did not allow us to exclude the unlikely possibility that these cells newly differentiated between cortical lesion induction (21 days after initial MOG<sub>1-125</sub> immunization) and the peak of the demyelination, three days later (Kotter et al., 2006; Merkler et al., 2006; Jafari et al., 2019). Therefore, experimental time line was adapted by adding the additional imaging session, before cortical lesion induction. This enabled reconstruction of morphology of pre-existing OLs also in the non-lesion conditions.

## 5. Chronic longitudinal imaging of the pre-existing oligodendrocytes in the cortical lesion

Several studies previously unveiled dynamics of cellular morphology and behavior under physiological conditions and in disease-modified settings by chronic intravital imaging of cortical areas (Hill et al., 2018;

Hughes et al., 2018; Pryazhnikov et al., 2018; Jafari et al., 2019; Snaidero et al., 2019). Here, by experimental design modification, I followed the changes of the mem-tdTomato+ individual oligodendrocytes over the entire course of MS-like grey matter pathology, covering the pre-lesion stage (pre c-MS), peak of the demyelination on c-MS d3 and remyelination phase, c-MS d16. I reconstructed the 3-D morphology of the individual cells, based on their fluorescent signal as described before (Romanelli et al., 2016; Tripathi et al., 2017; Auer et al., 2018; Hill et al., 2018; Hughes et al., 2018; Snaidero et al., 2019) and simultaneously analyzed obtained reconstructions from all the three time points, marking the remaining, lost and new processes and internodes. The major results of this analysis are as follows. First, there was a high variability in the degree to which the mature oligodendrocytes are affected during the peak of demyelination. Noteworthy, even the cells, which lost around 70% of their myelin, thereby presenting a severely amputated-state were able to survive. Secondly, in the remyelination phase, I detected many cases, in which these surviving but amputated OLs were connected to newly resorted myelin sheaths indicating that they were able not only to survive but also to recover (**Fig. 20, 21**). Unfortunately, we were not able yet to confirm these *in vivo* results by electron microscopy technique due to our limited ability to trace very thin connectors in a 3-D volume that emerged as follows. Based on NIRB marks (Bishop et al., 2011), we identified the oligodendrocyte of interest (*in vivo* followed over the entire course of GM lesion) in the EM ultrathin sections and reconstructed the morphology as shown recently (**Fig. 22, 23**; Snaidero et al., 2019). Correlated light and electron microscopy of the one, selected oligodendrocyte exposed some limitations in 3-D OL's rendering based only on the fluorescent signal. Although tdTomato+ cells density was clearly decreased in comparison to transgenically driven GFP expression in PLP-eGFP/C57bL6 strain (Mallon et al., 2002), the occupied territories of the pre-existing and newly integrated OLs can still overlap leading to the possible misdirection in tracing of the OL's processes (as shown by solid arrowhead in box 1, **Fig. 23**). Moreover, even though tissue excitation volume in multiphoton microscopy is well-defined, the fluorescent signal is collected also from few microns above and below the actual structure position (Denk et al., 1990; Bishop et al., 2011), which resulted in tdTomato-based, false-positive connection of processes and internodes that were actually spatially separated (as depicted by open arrowhead in the box 1, **Fig. 23**). Nonetheless, EM reconstruction of OL cell body and its proximal processes overlapped with the tdTomato-based reconstructions obtained from intravital imaging. Thus, light microscopy can be

---

considered as a trustworthy method to correctly assign those primary and proximal processes to the single OL's soma. Based on the reconstructions of OLs cell bodies with their most proximal field, I showed that only amputated-state, pre-existing oligodendrocytes can indeed extend new primary processes in neuroinflammatory lesions (Fig. 24). I did not observe similar changes of OL morphology in non-immunized, cytokines-injected control animals, suggesting that the mechanisms behind this process are likely driven by the loss of myelin rather than by direct effects of the injected pro-inflammatory cytokines.

We believe that it is important to further investigate the dynamics of pre-existing OLs and thus a major next step of this line of research will be to establish a relatively easy to implement experimental set up to selectively label and follow these cells over time. Despite of the fact that EM can help not only to clarify the light microscopy results but also to better characterize the restored myelin sheaths, it is also time-consuming and thus cannot be used for the first-line screening experiments or analysis of higher cell numbers. For that reason, I investigated new viral approaches, which can overcome spatio- and/or temporal resolution limitation in OLs labelling for intravital imaging (Fig. 25). Selective *switching-on* the fluorescent signal in response to irradiation with light allows visualization of the single-cell and its constituents. For example, in the viral vector in which *Mbp* promoter drives the expression of membrane-targeted tdTomato and photoactivatable GFP (AAV-*Mbp*:mem-tdTomato-2A-paGFP) all transduced oligodendrocytes can be detected *in vivo* only in the 'red channel' with the wavelength of 1020-1040nm. Only after photostimulation directed in the cell body, GFP changes its spectral properties and by spreading into the different cellular compartments become visible in the green light wavelength range (Ando et al., 2002; Schneider et al. 2005; Lippincott-Schwartz and Patterson, 2009). In this system, spatial resolution is achieved by *switching-on* the GFP in the pool of tdTomato-visualized oligodendrocytes. Unfortunately, GFP does not spread towards the distal internodes, which could be explained by relatively small diameter of the OL's processes therefore preventing efficient transport of the fluorescent protein. Another approach takes advantage of time-specific transgene expression resolved by multistep cell labelling in a tamoxifen inducible-Cre/DiO strategy (Sjulson et al., 2016). In the Cre-activated DiO switch system, the initially inactive transgene, due to its inverted orientation, is flipped back only in the presence of Cre recombinase. This strategy overcomes the unwanted effect of the transgene's leaky expression often observed with floxed stop cassette (Atasoy et al., 2008; Sohal et al., 2009). When Cre recombinase is fused to the modified ligand-

binding domain of estrogen receptor, its activity is therefore regulated by tamoxifen administration (Feil et al., 1997; Hayashi and McMahon, 2002). By injecting two viruses, AAV-*Mbp*:CreER<sup>12</sup> and AAV-*Mbp*:DiOmem-tdTomato, into the somatosensory cortex and intraperitoneal tamoxifen administration, I detected the tdTomato signal in the small subpopulation of oligodendrocytes. Furthermore, both of the viruses can be also separately used in combination with distinct reporter mouse strains. Time-defined, tamoxifen dependent oligodendrocytes labelling can be achieved by injecting AAV-*Mbp*:CreER<sup>12</sup> into the Rosa26<sup>mT/mG</sup> [Gt(ROSA)26Sortm4(ACTB-tdTomato,-EGFP)Luo/J] (Muzumdar et al., 2007; Powers et al., 2013), which results in a switch from tdTomato to GFP signal only in the successfully transduced cells. Similar outcome can be obtained with AAV-*Mbp*:DiOmem-tdTomato injection into the Opalin-iCreER<sup>12</sup> [Opalin<sup>tm1(cre)Pfw</sup>] (Tripathi et al., 2017).

## 5. Concluding remarks

Taken together the results of my PhD work, I characterize OL changes at the single-cell level during demyelination and remyelination. They reveal a centripetal spread of OL's damage during demyelination followed by recovery phase, in which mature OLs can reform primary and proximal processes. Furthermore, it is likely that these processes can form stable connections with axons and restore their myelin sheaths. It has been proposed in experimental models of demyelination that single OL can be characterized by the two fractions of internodes, which differ in g-ratio, thereby suggesting that some of them were established at the developmental stages and survived the initial immune attack, while the others were remyelinated after (Duncan et al., 2018). Moreover, recent findings from MS lesions also supports such a hypothesis; carbon-14 analysis revealed that partially remyelinated shadow plaques contain only OLs, which had been born before disease onset (Yeung et al., 2019). It remains unknown, what are the mechanisms, which would drive such re-extensions of OLs processes towards the naked axons. At this stage of understanding, it can be hypothesized that mature pre-existing OLs can again switch on the genes involved in the active myelination, therefore potentially taking one step back in their developmental stage (Jäkel et al., 2018; Falcão et al., 2019). Furthermore, how regrowing processes navigate to the correct axons and which molecular mechanisms regulate this regeneration process is still entirely unclear. It was recently shown that mutual involvement of two adhesive systems is required for axon ensheathment during development. However, if the same mechanisms are involved in mature CNS recovery process is still not

known (Djannatian et al., 2019). Interestingly, myelination pattern in the remyelinated cortex is highly preserved as most of the remyelinated axons, are the ones that had lost their myelin sheaths. Such phenomenon was observed in demyelination induced in OLs laser ablation conditions, in which 80% of the myelin was restored on previously myelinated axons (Snaidero et al., 2019).

Importantly, all of above results open a new field of regenerative therapies in which the main targets are the affected oligodendrocytes that survive in the hostile environment and are able to contribute to tissue recovery (Romanelli et al., 2016; Cui et al, 2017). By modulating the pathways involved in myelination, it may ultimately be possible to enhance remyelination capacity not only in the OPCs but also in the mature oligodendrocytes (Deshmukh et al., 2013; Najm et al., 2015; Jeffries et al., 2016; Green et al., 2017; Schwartzbach et al., 2017; Preston et al., 2019). Therefore, future treatment strategy might combine immunomodulation, neuroprotection as well as an efficient myelin sheaths restoration, to overcome the devastating effects of MS pathology.

## Chapter VI – References

- Allen NJ, Lyons DA. Glia as architects of central nervous system formation and function. *Science*. 2018 Oct 12;362(6411):181-185. doi: 10.1126/science.aat0473.
- Almeida RG, Pan S, Cole KLH, Williamson JM, Early JJ, Czopka T, Klingseisen A, Chan JR, Lyons DA. Myelination of Neuronal Cell Bodies when Myelin Supply Exceeds Axonal Demand. *Curr Biol*. 2018 Apr 23;28(8):1296-1305.e5. doi: 10.1016/j.cub.2018.02.068.
- Ando R, Hama H, Yamamoto-Hino M, Mizuno H, Miyawaki A. An optical marker based on the UV-induced green-to-red photoconversion of a fluorescent protein. *Proc Natl Acad Sci U S A*. 2002 Oct 1;99(20):12651-6. doi: 10.1073/pnas.202320599.
- Armulik A, Genové G, Mäe M, Nisancioglu MH, Wallgard E, Niaudet C, He L, Norlin J, Lindblom P, Strittmatter K, Johansson BR, Betsholtz C. Pericytes regulate the blood-brain barrier. *Nature*. 2010 Nov 25;468(7323):557-61. doi: 10.1038/nature09522.
- Ascherio A, Munger KL. Epidemiology of Multiple Sclerosis: From Risk Factors to Prevention-An Update. *Semin Neurol*. 2016 Apr;36(2):103-14. doi: 10.1055/s-0036-1579693.
- Atasoy D, Aponte Y, Su HH, Sternson SM. A FLEX switch targets Channelrhodopsin-2 to multiple cell types for imaging and long-range circuit mapping. *J Neurosci*. 2008 Jul 9;28(28):7025-30. doi: 10.1523/JNEUROSCI.1954-08.2008.
- Auer F, Vagionitis S, Czopka T. Evidence for Myelin Sheath Remodeling in the CNS Revealed by In Vivo Imaging. *Curr Biol*. 2018 Feb 19;28(4):549-559.e3. doi: 10.1016/j.cub.2018.01.017.
- Bahney J, von Bartheld CS. The Cellular Composition and Glia-Neuron Ratio in the Spinal Cord of a Human and a Nonhuman Primate: Comparison With Other Species and Brain Regions. *Anat Rec (Hoboken)*. 2018 Apr;301(4):697-710. doi: 10.1002/ar.23728.
- Baker D, O'Neill JK, Gschmeissner SE, Wilcox CE, Butter C, Turk JL. Induction of chronic relapsing experimental allergic encephalomyelitis in Biozzi mice. *J Neuroimmunol*. 1990 Aug;28(3):261-70. doi: 10.1016/0165-5728(90)90019-j.
- Barnett MH, Prineas JW. Relapsing and remitting multiple sclerosis: pathology of the newly forming lesion. *Ann Neurol*. 2004 Apr;55(4):458-68. doi: 10.1002/ana.20016.
- Baxi EG, DeBruin J, Jin J, Strasburger HJ, Smith MD, Orthmann-Murphy JL, Schott JT, Fairchild AN, Bergles DE, Calabresi PA. Lineage tracing reveals dynamic changes in oligodendrocyte precursor cells following cuprizone-induced demyelination. *Glia*. 2017 Dec;65(12):2087-2098. doi: 10.1002/glia.23229.
- Bechler ME, Byrne L, Ffrench-Constant C. CNS Myelin Sheath Lengths Are an Intrinsic Property of Oligodendrocytes. *Curr Biol*. 2015 Sep 21;25(18):2411-6. doi: 10.1016/j.cub.2015.07.056.
- Beck, J., Rondot, P., Catinot, L., Falcoff, E., Kirchner, H., & Wietzerbin, J. (1988). Increased production of interferon gamma and tumor necrosis factor precedes clinical manifestation in multiple sclerosis: Do

cytokines trigger off exacerbations? *Acta Neurologica Scandinavica*, 78(4), 318–323. doi:10.1111/j.1600-0404.1988.tb03663.x

Beecham AH et al., International Multiple Sclerosis Genetics Consortium. Analysis of immune-related loci identifies 48 new susceptibility variants for multiple sclerosis. *Nat Genet*. 2013 Nov;45(11):1353-60. doi: 10.1038/ng.2770.

Beltrán E, Gerdes LA, Hansen J, Flierl-Hecht A, Krebs S, Blum H, Ertl-Wagner B, Barkhof F, Kümpfel T, Hohlfeld R, Dornmair K. Early adaptive immune activation detected in monozygotic twins with prodromal multiple sclerosis. *J Clin Invest*. 2019 Nov 1;129(11):4758-4768. doi: 10.1172/JCI128475.

Bergles DE, Roberts JD, Somogyi P, Jahr CE. Glutamatergic synapses on oligodendrocyte precursor cells in the hippocampus. *Nature*. 2000 May 11;405(6783):187-91. doi: 10.1038/35012083.

Billiau A, Matthys P. Modes of action of Freund's adjuvants in experimental models of autoimmune diseases. *J Leukoc Biol*. 2001 Dec;70(6):849-60.

Biozzi G, Stiffel C, Mouton D, Bouthillier Y, Decreusefond C. Cytodynamics of the immune response in two lines of mice genetically selected for "high" and "low" antibody synthesis. *J Exp Med*. 1972 May 1;135(5):1071-94. doi: 10.1084/jem.135.5.1071.

Bishop D, Nikić I, Brinkoetter M, Knecht S, Potz S, Kerschensteiner M, Misgeld T. Near-infrared branding efficiently correlates light and electron microscopy. *Nat Methods*. 2011 Jun 5;8(7):568-70. doi: 10.1038/nmeth.1622.

Bitsch A, Kuhlmann T, Da Costa C, Bunkowski S, Polak T, Brück W. Tumour necrosis factor alpha mRNA expression in early multiple sclerosis lesions: correlation with demyelinating activity and oligodendrocyte pathology. *Glia*. 2000 Feb 15;29(4):366-75.

Bø L, Geurts JJ, van der Valk P, Polman C, Barkhof F. Lack of correlation between cortical demyelination and white matter pathologic changes in multiple sclerosis. *Arch Neurol*. 2007 Jan;64(1):76-80. doi: 10.1001/archneur.64.1.76.

Bø L, Vedeler CA, Nyland HI, Trapp BD, Mørk SJ. Subpial demyelination in the cerebral cortex of multiple sclerosis patients. *J Neuropathol Exp Neurol*. 2003 Jul;62(7):723-32. doi: 10.1093/jnen/62.7.723.

Boyd A, Zhang H, Williams A. Insufficient OPC migration into demyelinated lesions is a cause of poor remyelination in MS and mouse models. *Acta Neuropathol*. 2013 Jun;125(6):841-59. doi: 10.1007/s00401-013-1112-y.

Bradl M, Lassmann H. Oligodendrocytes: biology and pathology. *Acta Neuropathol*. 2010 Jan;119(1):37-53. doi: 10.1007/s00401-009-0601-5.

Brink BP, Veerhuis R, Breij EC, van der Valk P, Dijkstra CD, Bö L. The pathology of multiple sclerosis is location-dependent: no significant complement activation is detected in purely cortical lesions. *J Neuropathol Exp Neurol*. 2005 Feb;64(2):147-55. doi: 10.1093/jnen/64.2.147.

Brønnum-Hansen H, Koch-Henriksen N, Stenager E. Trends in survival and cause of death in Danish patients with multiple sclerosis. *Brain*. 2004 Apr;127(Pt 4):844-50. doi: 10.1093/brain/awh104.

- Browne P, Chandraratna D, Angood C, Tremlett H, Baker C, Taylor BV, Thompson AJ. Atlas of Multiple Sclerosis 2013: A growing global problem with widespread inequity. *Neurology*. 2014 Sep 9;83(11):1022-4. doi: 10.1212/WNL.0000000000000768.
- Brownell B, Hughes JT. The distribution of plaques in the cerebrum in multiple sclerosis. *J Neurol Neurosurg Psychiatry*. 1962 Nov;25:315-20. doi: 10.1136/jnnp.25.4.315.
- Brück W, Kuhlmann T, Stadelmann C. Remyelination in multiple sclerosis. *J Neurol Sci*. 2003 Feb 15;206(2):181-5. doi: 10.1016/s0022-510x(02)00191-0.
- Brück W, Schmied M, Suchanek G, Brück Y, Breitschopf H, Poser S, Piddlesden S, Lassmann H. Oligodendrocytes in the early course of multiple sclerosis. *Ann Neurol*. 1994 Jan;35(1):65-73. doi: 10.1002/ana.410350111.
- Burrows DJ, McGown A, Jain SA, De Felice M, Ramesh TM, Sharrack B, Majid A. Animal models of multiple sclerosis: From rodents to zebrafish. *Mult Scler*. 2019 Mar;25(3):306-324. doi: 10.1177/1352458518805246.
- Cai J, Qi Y, Hu X, Tan M, Liu Z, Zhang J, Li Q, Sander M, Qiu M. Generation of oligodendrocyte precursor cells from mouse dorsal spinal cord independent of Nkx6 regulation and Shh signaling. *Neuron*. 2005 Jan 6;45(1):41-53. doi: 10.1016/j.neuron.2004.12.028.
- Caillava C, Vandenbosch R, Jablonska B, Deboux C, Spigoni G, Gallo V, Malgrange B, Baron-Van Evercooren A. Cdk2 loss accelerates precursor differentiation and remyelination in the adult central nervous system. *J Cell Biol*. 2011 Apr 18;193(2):397-407. doi: 10.1083/jcb.201004146.
- Cantuti-Castelvetri L, Fitzner D, Bosch-Queralt M, Weil MT, Su M, Sen P, Ruhwedel T, Mitkovski M, Trendelenburg G, Lütjohann D, Möbius W, Simons M. Defective cholesterol clearance limits remyelination in the aged central nervous system. *Science*. 2018 Feb 9;359(6376):684-688. doi: 10.1126/science.aan4183.
- Caramanos Z, Carlos Santos A, Arnold DL. Magnetic resonance imaging and spectroscopy: Insights into the pathology and pathophysiology of multiple sclerosis. In: McDonald WI, Noseworthy JH, eds. *Blue Book of Practical Neurology: Multiple Sclerosis*. New York: Elsevier Science Publishing Co; 2003:139–6
- Chang A, Staugaitis SM, Dutta R, Batt CE, Easley KE, Chomyk AM, Yong VW, Fox RJ, Kidd GJ, Trapp BD. Cortical remyelination: a new target for repair therapies in multiple sclerosis. *Ann Neurol*. 2012 Dec;72(6):918-26. doi: 10.1002/ana.23693.
- Chang A, Tourtellotte WW, Rudick R, Trapp BD. Premyelinating oligodendrocytes in chronic lesions of multiple sclerosis. *N Engl J Med*. 2002 Jan 17;346(3):165-73. doi: 10.1056/NEJMoa010994.
- Chong SY, Rosenberg SS, Fancy SP, Zhao C, Shen YA, Hahn AT, McGee AW, Xu X, Zheng B, Zhang LI, Rowitch DH, Franklin RJ, Lu QR, Chan JR. Neurite outgrowth inhibitor Nogo-A establishes spatial segregation and extent of oligodendrocyte myelination. *Proc Natl Acad Sci U S A*. 2012 Jan 24;109(4):1299-304. doi: 10.1073/pnas.1113540109.

- Cohen JA, Coles AJ, Arnold DL, Confavreux C, Fox EJ, Hartung HP, Havrdova E, Selmaj KW, Weiner HL, Fisher E, Brinar VV, Giovannoni G, Stojanovic M, Ertik BI, Lake SL, Margolin DH, Panzara MA, Compston DA. Alemtuzumab versus interferon beta 1a as first-line treatment for patients with relapsing-remitting multiple sclerosis: a randomised controlled phase 3 trial. *Lancet*. 2012 Nov 24;380(9856):1819-28. doi: 10.1016/S0140-6736(12)61769-3.
- Compston A, Coles A. Multiple sclerosis. *Lancet*. 2008 Oct 25;372(9648):1502-17. doi: 10.1016/S0140-6736(08)61620-7.
- Constantinescu CS, Farooqi N, O'Brien K, Gran B. Experimental autoimmune encephalomyelitis (EAE) as a model for multiple sclerosis (MS). *Br J Pharmacol*. 2011 Oct;164(4):1079-106. doi: 10.1111/j.1476-5381.2011.01302.x.
- Cook S, Leist T, Comi G, Montalban X, Giovannoni G, Nolting A, Hicking C, Galazka A, Sylvester E. Safety of cladribine tablets in the treatment of patients with multiple sclerosis: An integrated analysis. *Mult Scler Relat Disord*. 2019 Apr;29:157-167. doi: 10.1016/j.msard.2018.11.021.
- Cramer SP, Simonsen H, Frederiksen JL, Rostrup E, Larsson HB. Abnormal blood-brain barrier permeability in normal appearing white matter in multiple sclerosis investigated by MRI. *Neuroimage Clin*. 2014;4:182-9. doi: 10.1016/j.nicl.2013.12.001.
- Crawford AH, Tripathi RB, Foerster S, McKenzie I, Kougioumtzidou E, Grist M, Richardson WD, Franklin RJ. Pre-Existing Mature Oligodendrocytes Do Not Contribute to Remyelination following Toxin-Induced Spinal Cord Demyelination. *Am J Pathol*. 2016 Mar;186(3):511-6. doi: 10.1016/j.ajpath.2015.11.005.
- Crawford AH, Tripathi RB, Richardson WD, Franklin RJM. Developmental Origin of Oligodendrocyte Lineage Cells Determines Response to Demyelination and Susceptibility to Age-Associated Functional Decline. *Cell Rep*. 2016a Apr 26;15(4):761-773. doi: 10.1016/j.celrep.2016.03.069.
- Crawford DK, Mangiardi M, Song B, Patel R, Du S, Sofroniew MV, Voskuhl RR, Tiwari-Woodruff SK. Oestrogen receptor beta ligand: a novel treatment to enhance endogenous functional remyelination. *Brain*. 2010 Oct;133(10):2999-3016. doi: 10.1093/brain/awq237.
- Crockett DP, Burshteyn M, Garcia C, Muggironi M, Casaccia-Bonnel P. Number of oligodendrocyte progenitors recruited to the lesioned spinal cord is modulated by the levels of the cell cycle regulatory protein p27Kip-1. *Glia*. 2005 Jan 15;49(2):301-8. doi: 10.1002/glia.20111.
- Cui QL, Khan D, Rone M, T S Rao V, Johnson RM, Lin YH, Bilodeau PA, Hall JA, Rodriguez M, Kennedy TE, Ludwin SK, Antel JP. Sublethal oligodendrocyte injury: A reversible condition in multiple sclerosis?. *Ann Neurol*. 2017 Jun;81(6):811-824. doi: 10.1002/ana.24944.
- Czopka T, Ffrench-Constant C, Lyons DA. Individual oligodendrocytes have only a few hours in which to generate new myelin sheaths in vivo. *Dev Cell*. 2013 Jun 24;25(6):599-609. doi: 10.1016/j.devcel.2013.05.013.

- Davalos D, Lee JK, Smith WB, Brinkman B, Ellisman MH, Zheng B, Akassoglou K. Stable in vivo imaging of densely populated glia, axons and blood vessels in the mouse spinal cord using two-photon microscopy. *J Neurosci Methods*. 2008 Mar 30;169(1):1-7. doi: 10.1016/j.jneumeth.2007.11.011.
- Dawson MR, Polito A, Levine JM, Reynolds R. NG2-expressing glial progenitor cells: an abundant and widespread population of cycling cells in the adult rat CNS. *Mol Cell Neurosci*. 2003 Oct;24(2):476-88.
- De Angelis F, John NA, Brownlee WJ. Disease-modifying therapies for multiple sclerosis. *BMJ*. 2018 Nov 27;363:k4674. doi: 10.1136/bmj.k4674.
- Denk W, Strickler JH, Webb WW. Two-photon laser scanning fluorescence microscopy. *Science*. 1990 Apr 6;248(4951):73-6. doi: 10.1126/science.2321027.
- Derfuss T, Parikh K, Velhin S, Braun M, Mathey E, Krumbholz M, Kümpfel T, Moldenhauer A, Rader C, Sonderegger P, Pöllmann W, Tiefenthaller C, Bauer J, Lassmann H, Wekerle H, Karagogeos D, Hohlfeld R, Linington C, Meinl E. Contactin-2/TAG-1-directed autoimmunity is identified in multiple sclerosis patients and mediates gray matter pathology in animals. *Proc Natl Acad Sci U S A*. 2009 May 19;106(20):8302-7. doi: 10.1073/pnas.0901496106.
- Deshmukh VA, Tardif V, Lyssiottis CA, Green CC, Kerman B, Kim HJ, Padmanabhan K, Swoboda JG, Ahmad I, Kondo T, Gage FH, Theofilopoulos AN, Lawson BR, Schultz PG, Lairson LL. A regenerative approach to the treatment of multiple sclerosis. *Nature*. 2013 Oct 17;502(7471):327-332. doi: 10.1038/nature12647.
- Dimou L, Simon C, Kirchhoff F, Takebayashi H, Götz M. Progeny of Olig2-expressing progenitors in the gray and white matter of the adult mouse cerebral cortex. *J Neurosci*. 2008 Oct 8;28(41):10434-42. doi: 10.1523/JNEUROSCI.2831-08.2008.
- Djannatian M, Timmler S, Arends M, Luckner M, Weil MT, Alexopoulos I, Snaidero N, Schmid B, Misgeld T, Möbius W, Schifferer M, Peles E, Simons M. Two adhesive systems cooperatively regulate axon ensheathment and myelin growth in the CNS. *Nat Commun*. 2019 Oct 22;10(1):4794. doi: 10.1038/s41467-019-12789-z.
- Doerflinger NH, Macklin WB, Popko B. Inducible site-specific recombination in myelinating cells. *Genesis*. 2003 Jan;35(1):63-72. doi: 10.1002/gene.10154.
- Duncan ID, Marik RL, Broman AT, Heidari M. Thin myelin sheaths as the hallmark of remyelination persist over time and preserve axon function. *Proc Natl Acad Sci U S A*. 2017 Nov 7;114(45):E9685-E9691. doi: 10.1073/pnas.1714183114.
- Duncan ID, Radcliff AB, Heidari M, Kidd G, August BK, Wierenga LA. The adult oligodendrocyte can participate in remyelination. *Proc Natl Acad Sci U S A*. 2018 Dec 11;115(50):E11807-E11816. doi: 10.1073/pnas.1808064115.
- Dutta R, Trapp BD. Pathogenesis of axonal and neuronal damage in multiple sclerosis. *Neurology*. 2007 May 29;68(22 Suppl 3):S22-31; discussion S43-54. doi: 10.1212/01.wnl.0000275229.13012.32.

- Falcão AM, van Bruggen D, Marques S, Meijer M, Jäkel S, Agirre E, Samudyata, Floriddia EM, Vanichkina DP, Ffrench-Constant C, Williams A, Guerreiro-Cacais AO, Castelo-Branco G. Disease-specific oligodendrocyte lineage cells arise in multiple sclerosis. *Nat Med*. 2018 Dec;24(12):1837-1844. doi: 10.1038/s41591-018-0236-y.
- Fard MK, van der Meer F, Sánchez P, Cantuti-Castelvetri L, Mandad S, Jäkel S, Fornasiero EF, Schmitt S, Ehrlich M, Starost L, Kuhlmann T, Sergiou C, Schultz V, Wrzos C, Brück W, Urlaub H, Dimou L, Stadelmann C, Simons M. BCAS1 expression defines a population of early myelinating oligodendrocytes in multiple sclerosis lesions. *Sci Transl Med*. 2017 Dec 6;9(419). doi: 10.1126/scitranslmed.aam7816.
- Farrar MJ, Bernstein IM, Schlafer DH, Cleland TA, Fetcho JR, Schaffer CB. Chronic in vivo imaging in the mouse spinal cord using an implanted chamber. *Nat Methods*. 2012 Jan 22;9(3):297-302. doi: 10.1038/nmeth.1856.
- Feil R, Wagner J, Metzger D, Chambon P. Regulation of Cre recombinase activity by mutated estrogen receptor ligand-binding domains. *Biochem Biophys Res Commun*. 1997 Aug 28;237(3):752-7. doi: 10.1006/bbrc.1997.7124
- Feil S, Valtcheva N, Feil R. Inducible Cre mice. *Methods Mol Biol*. 2009;530:343-63. doi: 10.1007/978-1-59745-471-1\_18
- Fields RD. White matter in learning, cognition and psychiatric disorders. *Trends Neurosci*. 2008 Jul;31(7):361-70. doi: 10.1016/j.tins.2008.04.001.
- Filippi M, Brück W, Chard D, Fazekas F, Geurts JJG, Enzinger C, Hametner S, Kuhlmann T, Preziosa P, Rovira À, Schmierer K, Stadelmann C, Rocca MA. Association between pathological and MRI findings in multiple sclerosis. *Lancet Neurol*. 2019 Feb;18(2):198-210. doi: 10.1016/S1474-4422(18)30451-4.
- Fischer MT, Wimmer I, Höftberger R, Gerlach S, Haider L, Zrzavy T, Hametner S, Mahad D, Binder CJ, Krumbholz M, Bauer J, Bradl M, Lassmann H. Disease-specific molecular events in cortical multiple sclerosis lesions. *Brain*. 2013 Jun;136(Pt 6):1799-815. doi: 10.1093/brain/awt110. Epub 2013 May 17.
- Fletcher JM, Lalor SJ, Sweeney CM, Tubridy N, Mills KH. T cells in multiple sclerosis and experimental autoimmune encephalomyelitis. *Clin Exp Immunol*. 2010 Oct;162(1):1-11. doi: 10.1111/j.1365-2249.2010.04143.x.
- Flores AI, Narayanan SP, Morse EN, Shick HE, Yin X, Kidd G, Avila RL, Kirschner DA, Macklin WB. Constitutively active Akt induces enhanced myelination in the CNS. *J Neurosci*. 2008 Jul 9;28(28):7174-83. doi: 10.1523/JNEUROSCI.0150-08.2008.
- Flurkey, Currer, Harrison. 'The mouse in biomedical research.' in James G. Fox (ed.), American College of Laboratory Animal Medicine series (Elsevier, AP: Amsterdam; Boston). 2007.
- Fox RJ, Coffey CS, Conwit R, Cudkowicz ME, Gleason T, Goodman A, Klawiter EC, Matsuda K, McGovern M, Naismith RT, Ashokkumar A, Barnes J, Ecklund D, Klingner E, Koeppe M, Long JD, Natarajan S, Thornell B, Yankey J, Bermel RA, Debbins JP, Huang X, Jagodnik P, Lowe MJ, Nakamura K, Narayanan S, Sakaie KE, Thoomukuntla B, Zhou X, Krieger S, Alvarez E, Apperson M, Bashir K, Cohen BA, Coyle PK, Delgado S, Dewitt LD, Flores A, Giesser BS, Goldman MD, Jubelt B, Lava N, Lynch SG,

- Moses H, Ontaneda D, Perumal JS, Racke M, Repovic P, Riley CS, Severson C, Shinnar S, Suski V, Weinstock-Guttman B, Yadav V, Zabeti A. Phase 2 Trial of Ibudilast in Progressive Multiple Sclerosis. *N Engl J Med*. 2018 Aug 30;379(9):846-855. doi: 10.1056/NEJMoa1803583.
- Fushimi S, Shirabe T. The reaction of glial progenitor cells in remyelination following ethidium bromide-induced demyelination in the mouse spinal cord. *Neuropathology*. 2002 Dec;22(4):233-42.
- Gao R, Asano SM, Upadhyayula S, Pisarev I, Milkie DE, Liu TL, Singh V, Graves A, Huynh GH, Zhao Y, Bogovic J, Colonell J, Ott CM, Zugates C, Tappan S, Rodriguez A, Mosaliganti KR, Sheu SH, Pasolli HA, Pang S, Xu CS, Megason SG, Hess H, Lippincott-Schwartz J, Hantman A, Rubin GM, Kirchhausen T, Saalfeld S, Aso Y, Boyden ES, Betzig E. Cortical column and whole-brain imaging with molecular contrast and nanoscale resolution. *Science*. 2019 Jan 18;363(6424). doi: 10.1126/science.aau8302
- Gardner C, Magliozzi R, Durrenberger PF, Howell OW, Rundle J, Reynolds R. Cortical grey matter demyelination can be induced by elevated pro-inflammatory cytokines in the subarachnoid space of MOG-immunized rats. *Brain*. 2013 Dec;136(Pt 12):3596-608. doi: 10.1093/brain/awt279.
- Gensert JM, Goldman JE. Endogenous progenitors remyelinate demyelinated axons in the adult CNS. *Neuron*. 1997 Jul;19(1):197-203. doi: 10.1016/s0896-6273(00)80359-1
- Geurts JJ, Barkhof F. Grey matter pathology in multiple sclerosis. *Lancet Neurol*. 2008 Sep;7(9):841-51. doi: 10.1016/S1474-4422(08)70191-1.
- Geurts JJ, Bö L, Pouwels PJ, Castelijns JA, Polman CH, Barkhof F. Cortical lesions in multiple sclerosis: combined postmortem MR imaging and histopathology. *AJNR Am J Neuroradiol*. 2005 Mar; 26(3):572-7.
- Gibson EM, Purger D, Mount CW, Goldstein AK, Lin GL, Wood LS, Inema I, Miller SE, Bieri G, Zuchero JB, Barres BA, Woo PJ, Vogel H, Monje M. Neuronal activity promotes oligodendrogenesis and adaptive myelination in the mammalian brain. *Science*. 2014 May 2;344(6183):1252304. doi: 10.1126/science.1252304.
- Girolamo F, Ferrara G, Strippoli M, Rizzi M, Errede M, Trojano M, Perris R, Roncali L, Svelto M, Mennini T, Virgintino D. Cerebral cortex demyelination and oligodendrocyte precursor response to experimental autoimmune encephalomyelitis. *Neurobiol Dis*. 2011 Sep;43(3):678-89. doi: 10.1016/j.nbd.2011.05.021.
- Green AJ, Gelfand JM, Cree BA, Bevan C, Boscardin WJ, Mei F, Inman J, Arnow S, Devereux M, Abounasr A, Nobuta H, Zhu A, Friessen M, Gerona R, von Büdingen HC, Henry RG, Hauser SL, Chan JR. Clemastine fumarate as a remyelinating therapy for multiple sclerosis (ReBUILD): a randomised, controlled, double-blind, crossover trial. *Lancet*. 2017 Dec 2;390(10111):2481-2489. doi: 10.1016/S0140-6736(17)32346-2.
- Greer JM, McCombe PA. Role of gender in multiple sclerosis: clinical effects and potential molecular mechanisms. *J Neuroimmunol*. 2011 May;234(1-2):7-18. doi: 10.1016/j.jneuroim.2011.03.003.
- Groves AK, Barnett SC, Franklin RJ, Crang AJ, Mayer M, Blakemore WF, Noble M. Repair of demyelinated lesions by transplantation of purified O-2A progenitor cells. *Nature*. 1993 Apr 1;362(6419):453-5. doi: 10.1038/362453a0.

- Gruchot J, Weyers V, Göttle P, Förster M, Hartung HP, Küry P, Kremer D. The Molecular Basis for Remyelination Failure in Multiple Sclerosis. *Cells*. 2019 Aug 3;8(8). doi: 10.3390/cells8080825.
- Grutzendler J, Kasthuri N, Gan WB. Long-term dendritic spine stability in the adult cortex. *Nature*. 2002 Dec 19-26;420(6917):812-6. doi: 10.1038/nature01276.
- Hajihosseini M, Tham TN, Dubois-Dalcq M. Origin of oligodendrocytes within the human spinal cord. *J Neurosci*. 1996 Dec 15;16(24):7981-94.
- Hampton DW, Anderson J, Pryce G, Irvine KA, Giovannoni G, Fawcett JW, Compston A, Franklin RJ, Baker D, Chandran S. An experimental model of secondary progressive multiple sclerosis that shows regional variation in gliosis, remyelination, axonal and neuronal loss. *J Neuroimmunol*. 2008 Sep 15;201-202:200-11. doi: 10.1016/j.jneuroim.2008.05.034. Epub 2008 Jul 30.
- Hayashi S, McMahon AP. Efficient recombination in diverse tissues by a tamoxifen-inducible form of Cre: a tool for temporally regulated gene activation/inactivation in the mouse. *Dev Biol*. 2002 Apr 15;244(2):305-18. doi: 10.1006/dbio.2002.0597.
- Häusser-Kinzel S, Weber MS. The Role of B Cells and Antibodies in Multiple Sclerosis, Neuromyelitis Optica, and Related Disorders. *Front Immunol*. 2019;10:201. doi: 10.3389/fimmu.2019.00201.
- Hemmer B, Kerschensteiner M, Korn T. Role of the innate and adaptive immune responses in the course of multiple sclerosis. *Lancet Neurol*. 2015 Apr;14(4):406-19. doi: 10.1016/S1474-4422(14)70305-9.
- Henderson AP, Barnett MH, Parratt JD, Prineas JW. Multiple sclerosis: distribution of inflammatory cells in newly forming lesions. *Ann Neurol*. 2009 Dec;66(6):739-53. doi: 10.1002/ana.21800.
- Hernán MA, Jick SS, Logroscino G, Olek MJ, Ascherio A, Jick H. Cigarette smoking and the progression of multiple sclerosis. *Brain*. 2005 Jun;128(Pt 6):1461-5. doi: 10.1093/brain/awh471.
- Hill RA, Li AM, Grutzendler J. Lifelong cortical myelin plasticity and age-related degeneration in the live mammalian brain. *Nat Neurosci*. 2018 May;21(5):683-695. doi: 10.1038/s41593-018-0120-6.
- Hines JH, Ravanelli AM, Schwindt R, Scott EK, Appel B. Neuronal activity biases axon selection for myelination in vivo. *Nat Neurosci*. 2015 May;18(5):683-9. doi: 10.1038/nn.3992.
- Hisahara S, Araki T, Sugiyama F, Yagami Ki, Suzuki M, Abe K, Yamamura K, Miyazaki J, Momoi T, Saruta T, Bernard CC, Okano H, Miura M. Targeted expression of baculovirus p35 caspase inhibitor in oligodendrocytes protects mice against autoimmune-mediated demyelination. *EMBO J*. 2000 Feb 1;19(3):341-8. doi: 10.1093/emboj/19.3.341.
- Hofman FM, Hinton DR, Johnson K, Merrill JE. Tumor necrosis factor identified in multiple sclerosis brain. *J Exp Med*. 1989 Aug 1;170(2):607-12. doi: 10.1084/jem.170.2.607.
- Hohlfeld R, Dornmair K, Meinl E, Wekerle H. The search for the target antigens of multiple sclerosis, part 1: autoreactive CD4+ T lymphocytes as pathogenic effectors and therapeutic targets. *Lancet Neurol*. 2016a Feb;15(2):198-209. doi: 10.1016/S1474-4422(15)00334-8.

- Hohlfeld R, Dornmair K, Meinl E, Wekerle H. The search for the target antigens of multiple sclerosis, part 2: CD8+ T cells, B cells, and antibodies in the focus of reverse-translational research. *Lancet Neurol.* 2016 Mar;15(3):317-31. doi: 10.1016/S1474-4422(15)00313-0.
- Holtmaat A, Bonhoeffer T, Chow DK, Chuckowree J, De Paola V, Hofer SB, Hübener M, Keck T, Knott G, Lee WC, Mostany R, Mrcic-Flogel TD, Nedivi E, Portera-Cailliau C, Svoboda K, Trachtenberg JT, Wilbrecht L. Long-term, high-resolution imaging in the mouse neocortex through a chronic cranial window. *Nat Protoc.* 2009;4(8):1128-44. doi: 10.1038/nprot.2009.89.
- Howell OW, Reeves CA, Nicholas R, Carassiti D, Radotra B, Gentleman SM, Serafini B, Aloisi F, Roncaroli F, Magliozzi R, Reynolds R. Meningeal inflammation is widespread and linked to cortical pathology in multiple sclerosis. *Brain.* 2011 Sep;134(Pt 9):2755-71. doi: 10.1093/brain/awr182.
- Hughes EG, Kang SH, Fukaya M, Bergles DE. Oligodendrocyte progenitors balance growth with self-repulsion to achieve homeostasis in the adult brain. *Nat Neurosci.* 2013 Jun;16(6):668-76. doi: 10.1038/nn.3390. Epub 2013 Apr 28. PubMed PMID: 23624515;
- Hughes EG, Orthmann-Murphy JL, Langseth AJ, Bergles DE. Myelin remodeling through experience-dependent oligodendrogenesis in the adult somatosensory cortex. *Nat Neurosci.* 2018 May;21(5):696-706. doi: 10.1038/s41593-018-0121-5.
- Jacobsen M, Cepok S, Quak E, Happel M, Gaber R, Ziegler A, Schock S, Oertel WH, Sommer N, Hemmer B. Oligoclonal expansion of memory CD8+ T cells in cerebrospinal fluid from multiple sclerosis patients. *Brain.* 2002 Mar;125(Pt 3):538-50. doi: 10.1093/brain/awf059.
- Jafari M, Schumacher A-M, Snaidero N, Neziraj T, Ullrich Gavilanes E.M, Jürgens T, Flórez Weidinger J.D, Schmidt S.S, Beltrán E, Hagan N, Woodworth L, Ofengeim D, Gans J, Wolf F, Kreuzfeldt M, Portugues R, Merkler D, Misgeld T, Kerschensteiner M. Localized calcium accumulations prime synapses for phagocyte removal in cortical neuroinflammation. 2019 bioRxiv 758193, doi: <https://doi.org/10.1101/758193>.
- Jäkel S, Agirre E, Mendanha Falcão A, van Bruggen D, Lee KW, Knuesel I, Malhotra D, Ffrench-Constant C, Williams A, Castelo-Branco G. Altered human oligodendrocyte heterogeneity in multiple sclerosis. *Nature.* 2019 Feb;566(7745):543-547. doi: 10.1038/s41586-019-0903-2.
- Jakovcevski I, Filipovic R, Mo Z, Rakic S, Zecevic N. Oligodendrocyte development and the onset of myelination in the human fetal brain. *Front Neuroanat.* 2009;3:5. doi: 10.3389/neuro.05.005.2009.
- Jeffries MA, Urbanek K, Torres L, Wendell SG, Rubio ME, Fyffe-Maricich SL. ERK1/2 Activation in Preexisting Oligodendrocytes of Adult Mice Drives New Myelin Synthesis and Enhanced CNS Function. *J Neurosci.* 2016 Aug 31;36(35):9186-200. doi: 10.1523/JNEUROSCI.1444-16.2016.
- Jennum P, Wanscher B, Frederiksen J, Kjellberg J. The socioeconomic consequences of multiple sclerosis: a controlled national study. *Eur Neuropsychopharmacol.* 2012 Jan;22(1):36-43. doi: 10.1016/j.euroneuro.2011.05.001.

- John GR, Shankar SL, Shafit-Zagardo B, Massimi A, Lee SC, Raine CS, Brosnan CF. Multiple sclerosis: re-expression of a developmental pathway that restricts oligodendrocyte maturation. *Nat Med*. 2002 Oct;8(10):1115-21. doi: 10.1038/nm781.
- Johnson ES, Ludwin SK. The demonstration of recurrent demyelination and remyelination of axons in the central nervous system. *Acta Neuropathol*. 1981;53(2):93-8. doi: 10.1007/bf00689988.
- Johnson KP, Brooks BR, Cohen JA, Ford CC, Goldstein J, Lisak RP, Myers LW, Panitch HS, Rose JW, Schiffer RB. Copolymer 1 reduces relapse rate and improves disability in relapsing-remitting multiple sclerosis: results of a phase III multicenter, double-blind placebo-controlled trial. The Copolymer 1 Multiple Sclerosis Study Group. *Neurology*. 1995 Jul;45(7):1268-76. doi: 10.1212/wnl.45.7.1268.
- Jones MV, Nguyen TT, Deboy CA, Griffin JW, Whartenby KA, Kerr DA, Calabresi PA. Behavioral and pathological outcomes in MOG 35-55 experimental autoimmune encephalomyelitis. *J Neuroimmunol*. 2008 Aug 13;199(1-2):83-93. doi: 10.1016/j.jneuroim.2008.05.013.
- Jürgens T, Jafari M, Kreutzfeldt M, Bahn E, Brück W, Kerschensteiner M, Merkler D. Reconstruction of single cortical projection neurons reveals primary spine loss in multiple sclerosis. *Brain*. 2016 Jan;139(Pt 1):39-46. doi: 10.1093/brain/awv353.
- Kaisey M, Solomon AJ, Luu M, Giesser BS, Sicotte NL. Incidence of multiple sclerosis misdiagnosis in referrals to two academic centers. *Mult Scler Relat Disord*. 2019 May;30:51-56. doi: 10.1016/j.msard.2019.01.048.
- Kang SH, Fukaya M, Yang JK, Rothstein JD, Bergles DE. NG2+ CNS glial progenitors remain committed to the oligodendrocyte lineage in postnatal life and following neurodegeneration. *Neuron*. 2010 Nov 18;68(4):668-81. doi: 10.1016/j.neuron.2010.09.009. PubMed PMID: 21092857;
- Kappos L, Radue EW, O'Connor P, Polman C, Hohlfeld R, Calabresi P, Selmaj K, Agoropoulou C, Leyk M, Zhang-Auberson L, Burtin P. A placebo-controlled trial of oral fingolimod in relapsing multiple sclerosis. *N Engl J Med*. 2010 Feb 4;362(5):387-401. doi: 10.1056/NEJMoa0909494.
- Káradóttir R, Cavelier P, Bergersen LH, Attwell D. NMDA receptors are expressed in oligodendrocytes and activated in ischaemia. *Nature*. 2005 Dec 22;438(7071):1162-6. doi: 10.1038/nature04302.
- Kay JN, Roeser T, Mumm JS, Godinho L, Mrejeru A, Wong RO, Baier H. Transient requirement for ganglion cells during assembly of retinal synaptic layers. *Development*. 2004 Mar;131(6):1331-42. doi: 10.1242/dev.01040.
- Kerschensteiner M, Stadelmann C, Buddeberg BS, Merkler D, Bareyre FM, Anthony DC, Linington C, Brück W, Schwab ME. Targeting experimental autoimmune encephalomyelitis lesions to a predetermined axonal tract system allows for refined behavioral testing in an animal model of multiple sclerosis. *Am J Pathol*. 2004 Apr;164(4):1455-69. doi: 10.1016/S0002-9440(10)63232-4.
- Kessarlis N, Fogarty M, Iannarelli P, Grist M, Wegner M, Richardson WD. Competing waves of oligodendrocytes in the forebrain and postnatal elimination of an embryonic lineage. *Nat Neurosci*. 2006 Feb;9(2):173-9. doi: 10.1038/nn1620.

- Kirby L, Jin J, Cardona JG, Smith MD, Martin KA, Wang J, Strasburger H, Herbst L, Alexis M, Karnell J, Davidson T, Dutta R, Goverman J, Bergles D, Calabresi PA. Oligodendrocyte precursor cells present antigen and are cytotoxic targets in inflammatory demyelination. *Nat Commun*. 2019 Aug 29;10(1):3887. doi: 10.1038/s41467-019-11638-3.
- Klugmann M, Schwab MH, Pühlhofer A, Schneider A, Zimmermann F, Griffiths IR, Nave KA. Assembly of CNS myelin in the absence of proteolipid protein. *Neuron*. 1997 Jan;18(1):59-70. doi: 10.1016/s0896-6273(01)80046-5.
- Kotter MR, Li WW, Zhao C, Franklin RJ. Myelin impairs CNS remyelination by inhibiting oligodendrocyte precursor cell differentiation. *J Neurosci*. 2006 Jan 4;26(1):328-32. doi: 10.1523/JNEUROSCI.2615-05.2006.
- Kougioumtzidou E, Shimizu T, Hamilton NB, Tohyama K, Sprengel R, Monyer H, Attwell D, Richardson WD. Signalling through AMPA receptors on oligodendrocyte precursors promotes myelination by enhancing oligodendrocyte survival. *Elife*. 2017 Jun 13;6. doi: 10.7554/eLife.28080.
- Kuhlmann T, Lingfeld G, Bitsch A, Schuchardt J, Brück W. Acute axonal damage in multiple sclerosis is most extensive in early disease stages and decreases over time. *Brain*. 2002 Oct;125(Pt 10):2202-12. doi: 10.1093/brain/awf235.
- Kuhlmann T, Miron V, Cui Q, Wegner C, Antel J, Brück W. Differentiation block of oligodendroglial progenitor cells as a cause for remyelination failure in chronic multiple sclerosis. *Brain*. 2008 Jul;131(Pt 7):1749-58. doi: 10.1093/brain/awn096.
- Kutzelnigg A, Lucchinetti CF, Stadelmann C, Brück W, Rauschka H, Bergmann M, Schmidbauer M, Parisi JE, Lassmann H. Cortical demyelination and diffuse white matter injury in multiple sclerosis. *Brain*. 2005 Nov;128(Pt 11):2705-12. doi: 10.1093/brain/awh641.
- Lagumersindez-Denis N, Wrzos C, Mack M, Winkler A, van der Meer F, Reinert MC, Hollasch H, Flach A, Brühl H, Cullen E, Schlumbohm C, Fuchs E, Linington C, Barrantes-Freer A, Metz I, Wegner C, Liebetanz D, Prinz M, Brück W, Stadelmann C, Nessler S. Differential contribution of immune effector mechanisms to cortical demyelination in multiple sclerosis. *Acta Neuropathol*. 2017 Jul;134(1):15-34. doi: 10.1007/s00401-017-1706-x.
- Lappe-Siefke C, Goebbels S, Gravel M, Nicksch E, Lee J, Braun PE, Griffiths IR, Nave KA. Disruption of *Cnp1* uncouples oligodendroglial functions in axonal support and myelination. *Nat Genet*. 2003 Mar;33(3):366-74. doi: 10.1038/ng1095.
- Larson VA, Mironova Y, Vanderpool KG, Waisman A, Rash JE, Agarwal A, Bergles DE. Oligodendrocytes control potassium accumulation in white matter and seizure susceptibility. *Elife*. 2018 Mar 29;7. doi: 10.7554/eLife.34829.
- Lassmann H, Bradl M. Multiple sclerosis: experimental models and reality. *Acta Neuropathol*. 2017 Feb;133(2):223-244. doi: 10.1007/s00401-016-1631-4.
- Lassmann H, Brück W, Lucchinetti C. Heterogeneity of multiple sclerosis pathogenesis: implications for diagnosis and therapy. *Trends Mol Med*. 2001 Mar;7(3):115-21. doi: 10.1016/s1471-4914(00)01909-2.

- Lassmann H, Brück W, Lucchinetti CF. The immunopathology of multiple sclerosis: an overview. *Brain Pathol.* 2007 Apr;17(2):210-8. doi: 10.1111/j.1750-3639.2007.00064.x.
- Lassmann H. Multiple Sclerosis Pathology. *Cold Spring Harb Perspect Med.* 2018 Mar 1;8(3). doi: 10.1101/cshperspect.a028936.
- Lee S, Leach MK, Redmond SA, Chong SY, Mellon SH, Tuck SJ, Feng ZQ, Corey JM, Chan JR. A culture system to study oligodendrocyte myelination processes using engineered nanofibers. *Nat Methods.* 2012 Sep;9(9):917-22. doi: 10.1038/nmeth.2105.
- Lee Y, Morrison BM, Li Y, Lengacher S, Farah MH, Hoffman PN, Liu Y, Tsingalia A, Jin L, Zhang PW, Pellerin L, Magistretti PJ, Rothstein JD. Oligodendroglia metabolically support axons and contribute to neurodegeneration. *Nature.* 2012 Jul 26;487(7408):443-8. doi: 10.1038/nature11314.
- Levin LI, Munger KL, Rubertone MV, Peck CA, Lennette ET, Spiegelman D, Ascherio A. Temporal relationship between elevation of epstein-barr virus antibody titers and initial onset of neurological symptoms in multiple sclerosis. *JAMA.* 2005 May 25;293(20):2496-500. doi: 10.1001/jama.293.20.2496
- Lindner M, Heine S, Haastert K, Garde N, Fokuhl J, Linsmeier F, Grothe C, Baumgärtner W, Stangel M. Sequential myelin protein expression during remyelination reveals fast and efficient repair after central nervous system demyelination. *Neuropathol Appl Neurobiol.* 2008 Feb;34(1):105-14. doi: 10.1111/j.1365-2990.2007.00879.x.
- Linthicum DS, Frelinger JA. Acute autoimmune encephalomyelitis in mice. II. Susceptibility is controlled by the combination of H-2 and histamine sensitization genes. *J Exp Med.* 1982 Jul 1;156(1):31-40. doi: 10.1084/jem.156.1.31.
- Lippincott-Schwartz J, Patterson GH. Photoactivatable fluorescent proteins for diffraction-limited and super-resolution imaging. *Trends Cell Biol.* 2009 Nov;19(11):555-65. doi: 10.1016/j.tcb.2009.09.003
- Livet J, Weissman TA, Kang H, Draft RW, Lu J, Bennis RA, Sanes JR, Lichtman JW. Transgenic strategies for combinatorial expression of fluorescent proteins in the nervous system. *Nature.* 2007 Nov 1;450(7166):56-62. doi: 10.1038/nature06293.
- Locatelli G, Wörtge S, Buch T, Ingold B, Frommer F, Sobottka B, Krüger M, Karram K, Bühlmann C, Bechmann I, Heppner FL, Waisman A, Becher B. Primary oligodendrocyte death does not elicit anti-CNS immunity. *Nat Neurosci.* 2012 Feb 26;15(4):543-50. doi: 10.1038/nn.3062.
- Lu QR, Sun T, Zhu Z, Ma N, Garcia M, Stiles CD, Rowitch DH. Common developmental requirement for Olig function indicates a motor neuron/oligodendrocyte connection. *Cell.* 2002 Apr 5;109(1):75-86. doi: 10.1016/s0092-8674(02)00678-5.
- Lu QR, Yuk D, Alberta JA, Zhu Z, Pawlitzky I, Chan J, McMahon AP, Stiles CD, Rowitch DH. Sonic hedgehog--regulated oligodendrocyte lineage genes encoding bHLH proteins in the mammalian central nervous system. *Neuron.* 2000 Feb;25(2):317-29. doi: 10.1016/s0896-6273(00)80897-1.
- Lublin F. History of modern multiple sclerosis therapy. *J Neurol.* 2005 Sep;252 Suppl 3:iii3-iii9. doi: 10.1007/s00415-005-2010-6.

- Lucchinetti C, Brück W, Parisi J, Scheithauer B, Rodriguez M, Lassmann H. A quantitative analysis of oligodendrocytes in multiple sclerosis lesions. A study of 113 cases. *Brain*. 1999 Dec;122 ( Pt 12):2279-95. doi: 10.1093/brain/122.12.2279
- Lucchinetti CF, Brück W, Parisi J, Scheithauer B, Rodriguez M, Lassmann H. Heterogeneity of multiple sclerosis lesions: implications for the pathogenesis of demyelination. *Ann Neurol*. 2000 Jun;47(6):707-17.
- Lucchinetti CF, Popescu BF, Bunyan RF, Moll NMtg, Roemer SF, Lassmann H, Brück W, Parisi JE, Scheithauer BW, Giannini C, Weigand SD, Mandrekar J, Ransohoff RM. Inflammatory cortical demyelination in early multiple sclerosis. *N Engl J Med*. 2011 Dec 8;365(23):2188-97. doi: 10.1056/NEJMoa1100648.
- Lundmark F, Duvefelt K, Jacobaeus E, Kockum I, Wallström E, Khademi M, Oturai A, Ryder LP, Saarela J, Harbo HF, Celius EG, Salter H, Olsson T, Hillert J. Variation in interleukin 7 receptor alpha chain (IL7R) influences risk of multiple sclerosis. *Nat Genet*. 2007 Sep;39(9):1108-13. doi: 10.1038/ng2106.
- Macrez R, Stys PK, Vivien D, Lipton SA, Docagne F. Mechanisms of glutamate toxicity in multiple sclerosis: biomarker and therapeutic opportunities. *Lancet Neurol*. 2016 Sep;15(10):1089-102. doi: 10.1016/S1474-4422(16)30165-X.
- Magliozzi R, Howell O, Vora A, Serafini B, Nicholas R, Puopolo M, Reynolds R, Aloisi F. Meningeal B-cell follicles in secondary progressive multiple sclerosis associate with early onset of disease and severe cortical pathology. *Brain*. 2007 Apr;130(Pt 4):1089-104. doi: 10.1093/brain/awm038.
- Magliozzi R, Howell OW, Reeves C, Roncaroli F, Nicholas R, Serafini B, Aloisi F, Reynolds R. A Gradient of neuronal loss and meningeal inflammation in multiple sclerosis. *Ann Neurol*. 2010 Oct;68(4):477-93. doi: 10.1002/ana.22230.
- Mahad DH, Trapp BD, Lassmann H. Pathological mechanisms in progressive multiple sclerosis. *Lancet Neurol*. 2015 Feb;14(2):183-93. doi: 10.1016/S1474-4422(14)70256-X.
- Mallon BS, Shick HE, Kidd GJ, Macklin WB. Proteolipid promoter activity distinguishes two populations of NG2-positive cells throughout neonatal cortical development. *J Neurosci*. 2002 Feb 1;22(3):876-85.
- Mangiardi M, Crawford DK, Xia X, Du S, Simon-Freeman R, Voskuhl RR, Tiwari-Woodruff SK. An animal model of cortical and callosal pathology in multiple sclerosis. *Brain Pathol*. 2011 May;21(3):263-78. doi: 10.1111/j.1750-3639.2010.00444.x.
- Marques S, Zeisel A, Codeluppi S, van Bruggen D, Mendanha Falcão A, Xiao L, Li H, Häring M, Hochgerner H, Romanov RA, Gyllborg D, Muñoz Machado A, La Manno G, Lönnerberg P, Floriddia EM, Rezayee F, Ernfors P, Arenas E, Hjerling-Leffler J, Harkany T, Richardson WD, Linnarsson S, Castelo-Branco G. Oligodendrocyte heterogeneity in the mouse juvenile and adult central nervous system. *Science*. 2016 Jun 10;352(6291):1326-1329. doi: 10.1126/science.aaf6463.
- Marriott JJ, Miyasaki JM, Gronseth G, O'Connor PW. Evidence Report: The efficacy and safety of mitoxantrone (Novantrone) in the treatment of multiple sclerosis: Report of the Therapeutics and Technology Assessment Subcommittee of the American Academy of Neurology. *Neurology*. 2010 May 4;74(18):1463-70. doi: 10.1212/WNL.0b013e3181dc1ae0.

- Martins TB, Rose JW, Jaskowski TD, Wilson AR, Husebye D, Seraj HS, Hill HR. Analysis of proinflammatory and anti-inflammatory cytokine serum concentrations in patients with multiple sclerosis by using a multiplexed immunoassay. *Am J Clin Pathol*. 2011 Nov;136(5):696-704. doi: 10.1309/AJCP7UBK8IBVMVNR.
- Mathey EK, Derfuss T, Storch MK, Williams KR, Hales K, Woolley DR, Al-Hayani A, Davies SN, Rasband MN, Olsson T, Moldenhauer A, Velhin S, Hohlfeld R, Meinl E, Linington C. Neurofascin as a novel target for autoantibody-mediated axonal injury. *J Exp Med*. 2007 Oct 1;204(10):2363-72. doi: 10.1084/jem.20071053.
- Matsushima GK, Morell P. The neurotoxicant, cuprizone, as a model to study demyelination and remyelination in the central nervous system. *Brain Pathol*. 2001 Jan;11(1):107-16. doi: 10.1111/j.1750-3639.2001.tb00385.x.
- Matute C, Domercq M, Sánchez-Gómez MV. Glutamate-mediated glial injury: mechanisms and clinical importance. *Glia*. 2006 Jan 15;53(2):212-24. doi: 10.1002/glia.20275.
- Matute C, Torre I, Pérez-Cerdá F, Pérez-Samartín A, Alberdi E, Etxebarria E, Arranz AM, Ravid R, Rodríguez-Antigüedad A, Sánchez-Gómez M, Domercq M. P2X(7) receptor blockade prevents ATP excitotoxicity in oligodendrocytes and ameliorates experimental autoimmune encephalomyelitis. *J Neurosci*. 2007 Aug 29;27(35):9525-33. doi: 10.1523/JNEUROSCI.0579-07.2007.
- Medaer R. Does the history of multiple sclerosis go back as far as the 14th century?. *Acta Neurol Scand*. 1979 Sep;60(3):189-92. doi: 10.1111/j.1600-0404.1979.tb02968.x.
- Mei F, Fancy SPJ, Shen YA, Niu J, Zhao C, Presley B, Miao E, Lee S, Mayoral SR, Redmond SA, Etxebarria A, Xiao L, Franklin RJM, Green A, Hauser SL, Chan JR. Micropillar arrays as a high-throughput screening platform for therapeutics in multiple sclerosis. *Nat Med*. 2014 Aug;20(8):954-960. doi: 10.1038/nm.3618.
- Merkler D, Ernsting T, Kerschensteiner M, Brück W, Stadelmann C. A new focal EAE model of cortical demyelination: multiple sclerosis-like lesions with rapid resolution of inflammation and extensive remyelination. *Brain*. 2006 Aug;129(Pt 8):1972-83. doi: 10.1093/brain/awl135.
- Metz I, Weigand SD, Popescu BF, Frischer JM, Parisi JE, Guo Y, Lassmann H, Brück W, Lucchinetti CF. Pathologic heterogeneity persists in early active multiple sclerosis lesions. *Ann Neurol*. 2014 May;75(5):728-38. doi: 10.1002/ana.24163
- Meyer N, Richter N, Fan Z, Siemonsmeier G, Pivneva T, Jordan P, Steinhäuser C, Semtner M, Nolte C, Kettenmann H. Oligodendrocytes in the Mouse Corpus Callosum Maintain Axonal Function by Delivery of Glucose. *Cell Rep*. 2018 Feb 27;22(9):2383-2394. doi: 10.1016/j.celrep.2018.02.022.
- Mi S, Hu B, Hahm K, Luo Y, Kam Hui ES, Yuan Q, Wong WM, Wang L, Su H, Chu TH, Guo J, Zhang W, So KF, Pepinsky B, Shao Z, Graff C, Garber E, Jung V, Wu EX, Wu W. LINGO-1 antagonist promotes spinal cord remyelination and axonal integrity in MOG-induced experimental autoimmune encephalomyelitis. *Nat Med*. 2007 Oct;13(10):1228-33. doi: 10.1038/nm1664.
- Miller AE, Rhoades RW. Treatment of relapsing-remitting multiple sclerosis: current approaches and unmet needs. *Curr Opin Neurol*. 2012 Feb;25 Suppl:S4-10. doi: 10.1097/01.wco.0000413319.87092.19.

- Miller SD, Karpus WJ. Experimental autoimmune encephalomyelitis in the mouse. *Curr Protoc Immunol*. 2007 May;Chapter 15:Unit 15.1. doi: 10.1002/0471142735.im1501s77.
- Miron VE, Boyd A, Zhao JW, Yuen TJ, Ruckh JM, Shadrach JL, van Wijngaarden P, Wagers AJ, Williams A, Franklin RJM, Ffrench-Constant C. M2 microglia and macrophages drive oligodendrocyte differentiation during CNS remyelination. *Nat Neurosci*. 2013 Sep;16(9):1211-1218. doi: 10.1038/nn.3469.
- Misu T, Höftberger R, Fujihara K, Wimmer I, Takai Y, Nishiyama S, Nakashima I, Konno H, Bradl M, Garzuly F, Itoyama Y, Aoki M, Lassmann H. Presence of six different lesion types suggests diverse mechanisms of tissue injury in neuromyelitis optica. *Acta Neuropathol*. 2013 Jun;125(6):815-27. doi: 10.1007/s00401-013-1116-7.
- Montalban X, Hauser SL, Kappos L, Arnold DL, Bar-Or A, Comi G, de Seze J, Giovannoni G, Hartung HP, Hemmer B, Lublin F, Rammohan KW, Selmaj K, Traboulsee A, Sauter A, Masterman D, Fontoura P, Belachew S, Garren H, Mairon N, Chin P, Wolinsky JS. Ocrelizumab versus Placebo in Primary Progressive Multiple Sclerosis. *N Engl J Med*. 2017 Jan 19;376(3):209-220. doi: 10.1056/NEJMoa1606468.
- Munger KL, Bentzen J, Laursen B, Stenager E, Koch-Henriksen N, Sørensen TI, Baker JL. Childhood body mass index and multiple sclerosis risk: a long-term cohort study. *Mult Scler*. 2013 Sep;19(10):1323-9. doi: 10.1177/1352458513483889.
- Murtie JC, Macklin WB, Corfas G. Morphometric analysis of oligodendrocytes in the adult mouse frontal cortex. *J Neurosci Res*. 2007 Aug 1;85(10):2080-6. doi: 10.1002/jnr.21339.
- Muzumdar MD, Tasic B, Miyamichi K, Li L, Luo L. A global double-fluorescent Cre reporter mouse. *Genesis*. 2007 Sep;45(9):593-605. doi: 10.1002/dvg.20335.
- Najm FJ, Madhavan M, Zaremba A, Shick E, Karl RT, Factor DC, Miller TE, Nevin ZS, Kantor C, Sargent A, Quick KL, Schlatzer DM, Tang H, Papoian R, Brimacombe KR, Shen M, Boxer MB, Jadhav A, Robinson AP, Podojil JR, Miller SD, Miller RH, Tesar PJ. Drug-based modulation of endogenous stem cells promotes functional remyelination in vivo. *Nature*. 2015 Jun 11;522(7555):216-20. doi: 10.1038/nature14335.
- Nave KA, Ehrenreich H. Time to revisit oligodendrocytes in multiple sclerosis. *Nat Med*. 2019 Mar;25(3):364-366. doi: 10.1038/s41591-019-0388-4.
- Neumann B, Baror R, Zhao C, Segel M, Dietmann S, Rawji KS, Foerster S, McClain CR, Chalut K, van Wijngaarden P, Franklin RJM. Metformin Restores CNS Remyelination Capacity by Rejuvenating Aged Stem Cells. *Cell Stem Cell*. 2019 Oct 3;25(4):473-485.e8. doi: 10.1016/j.stem.2019.08.015.
- Nielsen AS, Kinkel RP, Madigan N, Tinelli E, Benner T, Mainero C. Contribution of cortical lesion subtypes at 7T MRI to physical and cognitive performance in MS. *Neurology*. 2013 Aug 13;81(7):641-9. doi: 10.1212/WNL.0b013e3182a08ce8.
- Nikić I, Merkler D, Sorbara C, Brinkoetter M, Kreutzfeldt M, Bareyre FM, Brück W, Bishop D, Misgeld T, Kerschensteiner M. A reversible form of axon damage in experimental autoimmune encephalomyelitis and multiple sclerosis. *Nat Med*. 2011 Apr;17(4):495-9. doi: 10.1038/nm.2324.

- Nishiyama A, Chang A, Trapp BD. NG2+ glial cells: a novel glial cell population in the adult brain. *J Neuropathol Exp Neurol*. 1999 Nov;58(11):1113-24. doi: 10.1097/00005072-199911000-00001.
- Nowogrodzki A. The world's strongest MRI machines are pushing human imaging to new limits. *Nature*. 2018 Nov;563(7729):24-26. doi: 10.1038/d41586-018-07182-7.
- Okuda DT, Siva A, Kantarci O, Inglese M, Katz I, Tutuncu M, Keegan BM, Donlon S, Hua le H, Vidal-Jordana A, Montalban X, Rovira A, Tintoré M, Amato MP, Brochet B, de Seze J, Brassat D, Vermersch P, De Stefano N, Sormani MP, Pelletier D, Lebrun C. Radiologically isolated syndrome: 5-year risk for an initial clinical event. *PLoS One*. 2014;9(3):e90509. doi: 10.1371/journal.pone.0090509.
- Olsson T, Zhi WW, Höjeberg B, Kostulas V, Jiang YP, Anderson G, Ekre HP, Link H. Autoreactive T lymphocytes in multiple sclerosis determined by antigen-induced secretion of interferon-gamma. *J Clin Invest*. 1990 Sep;86(3):981-5. doi: 10.1172/JCI114800.
- Orton SM, Herrera BM, Yee IM, Valdar W, Ramagopalan SV, Sadovnick AD, Ebers GC. Sex ratio of multiple sclerosis in Canada: a longitudinal study. *Lancet Neurol*. 2006 Nov;5(11):932-6. doi: 10.1016/S1474-4422(06)70581-6.
- Patrikios P, Stadelmann C, Kutzelnigg A, Rauschka H, Schmidbauer M, Laursen H, Sorensen PS, Brück W, Lucchinetti C, Lassmann H. Remyelination is extensive in a subset of multiple sclerosis patients. *Brain*. 2006 Dec;129(Pt 12):3165-72. doi: 10.1093/brain/awl217.
- Patterson GH, Lippincott-Schwartz J. A photoactivatable GFP for selective photolabeling of proteins and cells. *Science*. 2002 Sep 13;297(5588):1873-7. doi: 10.1126/science.1074952.
- Paty DW, Li DK. Interferon beta-1b is effective in relapsing-remitting multiple sclerosis. II. MRI analysis results of a multicenter, randomized, double-blind, placebo-controlled trial. UBC MS/MRI Study Group and the IFNB Multiple Sclerosis Study Group. *Neurology*. 1993 Apr;43(4):662-7. doi: 10.1212/wnl.43.4.662.
- Pearce JM. Historical descriptions of multiple sclerosis. *Eur Neurol*. 2005;54(1):49-53. doi: 10.1159/000087387.
- Peferoen LA, Breur M, van de Berg S, Peferoen-Baert R, Boddeke EH, van der Valk P, Pryce G, van Noort JM, Baker D, Amor S. Ageing and recurrent episodes of neuroinflammation promote progressive experimental autoimmune encephalomyelitis in Biozzi ABH mice. *Immunology*. 2016 Oct;149(2):146-56. doi: 10.1111/imm.12644.
- Peterson JW, Bö L, Mörk S, Chang A, Trapp BD. Transected neurites, apoptotic neurons, and reduced inflammation in cortical multiple sclerosis lesions. *Ann Neurol*. 2001 Sep;50(3):389-400.
- Porter AG, Jänicke RU. Emerging roles of caspase-3 in apoptosis. *Cell Death Differ*. 1999 Feb;6(2):99-104. doi: 10.1038/sj.cdd.4400476.
- Powers BE, Sellers DL, Lovelett EA, Cheung W, Aalami SP, Zapertov N, Maris DO, Horner PJ. Remyelination reporter reveals prolonged refinement of spontaneously regenerated myelin. *Proc Natl Acad Sci U S A*. 2013 Mar 5;110(10):4075-80. doi: 10.1073/pnas.1210293110.

- Prat A, Biernacki K, Lavoie JF, Poirier J, Duquette P, Antel JP. Migration of multiple sclerosis lymphocytes through brain endothelium. *Arch Neurol*. 2002 Mar;59(3):391-7. doi: 10.1001/archneur.59.3.391.
- Preston MA, Finseth LT, Bourne JN, Macklin WB. A novel myelin protein zero transgenic zebrafish designed for rapid readout of in vivo myelination. *Glia*. 2019 Apr;67(4):650-667. doi: 10.1002/glia.23559.
- Prineas JW, Parratt JDE. Multiple sclerosis: Serum anti-CNS autoantibodies. *Mult Scler*. 2018 Apr;24(5):610-622. doi: 10.1177/1352458517706037.
- Pröbstel AK, Dornmair K, Bittner R, Sperl P, Jenne D, Magalhaes S, Villalobos A, Breithaupt C, Weissert R, Jacob U, Krumbholz M, Kuempfel T, Blaschek A, Stark W, Gärtner J, Pohl D, Rostasy K, Weber F, Forne I, Khademi M, Olsson T, Brilot F, Tantsis E, Dale RC, Wekerle H, Hohlfeld R, Banwell B, Bar-Or A, Meinl E, Derfuss T. Antibodies to MOG are transient in childhood acute disseminated encephalomyelitis. *Neurology*. 2011 Aug 9;77(6):580-8. doi: 10.1212/WNL.0b013e318228c0b1.
- Progzatzky F, Dallman MJ, Lo Celso C. From seeing to believing: labelling strategies for in vivo cell-tracking experiments. *Interface Focus*. 2013 Jun 6;3(3):20130001. doi: 10.1098/rsfs.2013.0001.
- Pryazhnikov E, Mugantseva E, Casarotto P, Kolikova J, Fred SM, Toptunov D, Afzalov R, Hotulainen P, Voikar V, Terry-Lorenzo R, Engel S, Kirov S, Castren E, Khiroug L. Longitudinal two-photon imaging in somatosensory cortex of behaving mice reveals dendritic spine formation enhancement by subchronic administration of low-dose ketamine. *Sci Rep*. 2018 Apr 24;8(1):6464. doi: 10.1038/s41598-018-24933-8.
- Pugliatti M, Sotgiu S, Solinas G, Castiglia P, Pirastru MI, Murgia B, Mannu L, Sanna G, Rosati G. Multiple sclerosis epidemiology in Sardinia: evidence for a true increasing risk. *Acta Neurol Scand*. 2001 Jan;103(1):20-6. doi: 10.1034/j.1600-0404.2001.00207.x.
- Quintana FJ, Farez MF, Izquierdo G, Lucas M, Cohen IR, Weiner HL. Antigen microarrays identify CNS-produced autoantibodies in RRMS. *Neurology*. 2012 Feb 21;78(8):532-9. doi: 10.1212/WNL.0b013e318247f9f3.
- Raff MC, Barres BA, Burne JF, Coles HS, Ishizaki Y, Jacobson MD. Programmed cell death and the control of cell survival: lessons from the nervous system. *Science*. 1993 Oct 29;262(5134):695-700. doi: 10.1126/science.8235590.
- Rasmussen S, Wang Y, Kivisäkk P, Bronson RT, Meyer M, Imitola J, Khoury SJ. Persistent activation of microglia is associated with neuronal dysfunction of callosal projecting pathways and multiple sclerosis-like lesions in relapsing--remitting experimental autoimmune encephalomyelitis. *Brain*. 2007 Nov;130(Pt 11):2816-29. doi: 10.1093/brain/awm219.
- Richardson-Burns SM, Kleinschmidt-DeMasters BK, DeBiasi RL, Tyler KL. Progressive multifocal leukoencephalopathy and apoptosis of infected oligodendrocytes in the central nervous system of patients with and without AIDS. *Arch Neurol*. 2002 Dec;59(12):1930-6. doi: 10.1001/archneur.59.12.1930.
- Rieckmann P. Concepts of induction and escalation therapy in multiple sclerosis. *J Neurol Sci*. 2009 Feb 1;277 Suppl 1:S42-5. doi: 10.1016/S0022-510X(09)70012-7.

- Rist JM, Franklin RJ. Taking ageing into account in remyelination-based therapies for multiple sclerosis. *J Neurol Sci.* 2008 Nov 15;274(1-2):64-7. doi: 10.1016/j.jns.2008.04.027.
- Rivers, T., Sprunt, D., and Berry, G. (1933). Observations on attempts to produce acute disseminated encephalomyelitis in monkeys. *The Journal of Experimental Medicine* 58, 39–53.
- Rodriguez EG, Wegner C, Kreutzfeldt M, Neid K, Thal DR, Jürgens T, Brück W, Stadelmann C, Merkler D. Oligodendroglia in cortical multiple sclerosis lesions decrease with disease progression, but regenerate after repeated experimental demyelination. *Acta Neuropathol.* 2014 Aug;128(2):231-46. doi: 10.1007/s00401-014-1260-8.
- Romanelli E, Merkler D, Mezydło A, Weil MT, Weber MS, Nikić I, Potz S, Meinel E, Matznick FE, Kreutzfeldt M, Ghanem A, Conzelmann KK, Metz I, Brück W, Routh M, Simons M, Bishop D, Misgeld T, Kerschensteiner M. Myelinosome formation represents an early stage of oligodendrocyte damage in multiple sclerosis and its animal model. *Nat Commun.* 2016 Nov 16;7:13275. doi: 10.1038/ncomms13275.
- Rosenberg, 2012, *Molecular Physiology and Metabolism of the Nervous System: A Clinical Perspective*, ISBN-13: 978-0195394276 (book)
- Rudick RA, Stuart WH, Calabresi PA, Confavreux C, Galetta SL, Radue EW, Lublin FD, Weinstock-Guttman B, Wynn DR, Lynn F, Panzara MA, Sandrock AW. Natalizumab plus interferon beta-1a for relapsing multiple sclerosis. *N Engl J Med.* 2006 Mar 2;354(9):911-23. doi: 10.1056/NEJMoa044396.
- Saab AS, Tzvetavona ID, Trevisiol A, Baltan S, Dibaj P, Kusch K, Möbius W, Goetze B, Jahn HM, Huang W, Steffens H, Schomburg ED, Pérez-Samartín A, Pérez-Cerdá F, Bakhtiari D, Matute C, Löwel S, Griesinger C, Hirrlinger J, Kirchhoff F, Nave KA. Oligodendroglial NMDA Receptors Regulate Glucose Import and Axonal Energy Metabolism. *Neuron.* 2016 Jul 6;91(1):119-32. doi: 10.1016/j.neuron.2016.05.016.
- Salzer J, Hallmans G, Nyström M, Stenlund H, Wadell G, Sundström P. Vitamin D as a protective factor in multiple sclerosis. *Neurology.* 2012 Nov 20;79(21):2140-5. doi: 10.1212/WNL.0b013e3182752ea8.
- Salzer J, Svenningsson R, Alping P, Novakova L, Björck A, Fink K, Islam-Jakobsson P, Malmström C, Axelsson M, Vågberg M, Sundström P, Lycke J, Piehl F, Svenningsson A. Rituximab in multiple sclerosis: A retrospective observational study on safety and efficacy. *Neurology.* 2016 Nov 15;87(20):2074-2081. doi: 10.1212/WNL.0000000000003331.
- Sawcer S et al., International Multiple Sclerosis Genetics Consortium; Wellcome Trust Case Control Consortium 2, Genetic risk and a primary role for cell-mediated immune mechanisms in multiple sclerosis. *Nature.* 2011 Aug 10;476(7359):214-9. doi: 10.1038/nature10251.
- Sawcer S, Franklin RJ, Ban M. Multiple sclerosis genetics. *Lancet Neurol.* 2014 Jul;13(7):700-9. doi: 10.1016/S1474-4422(14)70041-9.
- Schain AJ, Hill RA, Grutzendler J. Label-free in vivo imaging of myelinated axons in health and disease with spectral confocal reflectance microscopy. *Nat Med.* 2014 Apr;20(4):443-9. doi: 10.1038/nm.3495.

- Schirmer L, Velmeshev D, Holmqvist S, Kaufmann M, Werneburg S, Jung D, Vistnes S, Stockley JH, Young A, Steindel M, Tung B, Goyal N, Bhaduri A, Mayer S, Engler JB, Bayraktar OA, Franklin RJM, Haeussler M, Reynolds R, Schafer DP, Friese MA, Shioh LR, Kriegstein AR, Rowitch DH. Neuronal vulnerability and multilineage diversity in multiple sclerosis. *Nature*. 2019 Sep;573(7772):75-82. doi: 10.1038/s41586-019-1404-z.
- Schneider M, Barozzi S, Testa I, Faretta M, Diaspro A. Two-photon activation and excitation properties of PA-GFP in the 720-920-nm region. *Biophys J*. 2005 Aug;89(2):1346-52. doi: 10.1529/biophysj.104.054502
- Scholz J, Klein MC, Behrens TE, Johansen-Berg H. Training induces changes in white-matter architecture. *Nat Neurosci*. 2009 Nov;12(11):1370-1. doi: 10.1038/nn.2412.
- Schwartzbach CJ, Grove RA, Brown R, Tompson D, Then Bergh F, Arnold DL. Lesion remyelinating activity of GSK239512 versus placebo in patients with relapsing-remitting multiple sclerosis: a randomised, single-blind, phase II study. *J Neurol*. 2017 Feb;264(2):304-315. doi: 10.1007/s00415-016-8341-7.
- Serafini B, Rosicarelli B, Magliozzi R, Stigliano E, Aloisi F. Detection of ectopic B-cell follicles with germinal centers in the meninges of patients with secondary progressive multiple sclerosis. *Brain Pathol*. 2004 Apr;14(2):164-74.
- Shen S, Sandoval J, Swiss VA, Li J, Dupree J, Franklin RJ, Casaccia-Bonnel P. Age-dependent epigenetic control of differentiation inhibitors is critical for remyelination efficiency. *Nat Neurosci*. 2008 Sep;11(9):1024-34. doi: 10.1038/nn.2172.
- Shibata S, Yasuda A, Renault-Mihara F, Suyama S, Katoh H, Inoue T, Inoue YU, Nagoshi N, Sato M, Nakamura M, Akazawa C, Okano H. Sox10-Venus mice: a new tool for real-time labeling of neural crest lineage cells and oligodendrocytes. *Mol Brain*. 2010 Oct 31;3:31. doi: 10.1186/1756-6606-3-31.
- Shields SA, Gilson JM, Blakemore WF, Franklin RJ. Remyelination occurs as extensively but more slowly in old rats compared to young rats following gliotoxin-induced CNS demyelination. *Glia*. 1999 Oct;28(1):77-83.
- Sim FJ, McClain CR, Schanz SJ, Protack TL, Windrem MS, Goldman SA. CD140a identifies a population of highly myelinogenic, migration-competent and efficiently engrafting human oligodendrocyte progenitor cells. *Nat Biotechnol*. 2011 Sep 25;29(10):934-41. doi: 10.1038/nbt.1972.
- Sim FJ, Zhao C, Penderis J, Franklin RJ. The age-related decrease in CNS remyelination efficiency is attributable to an impairment of both oligodendrocyte progenitor recruitment and differentiation. *J Neurosci*. 2002 Apr 1;22(7):2451-9. doi: 20026217.
- Simon C, Lickert H, Götz M, Dimou L. Sox10-iCreERT2 : a mouse line to inducibly trace the neural crest and oligodendrocyte lineage. *Genesis*. 2012 Jun;50(6):506-15. doi: 10.1002/dvg.22003.
- Simons M, Misgeld T, Kerschensteiner M. A unified cell biological perspective on axon-myelin injury. *J Cell Biol*. 2014 Aug 4;206(3):335-45. doi: 10.1083/jcb.201404154.

- Sjulson L, Cassataro D, DasGupta S, Miesenböck G. Cell-Specific Targeting of Genetically Encoded Tools for Neuroscience. *Annu Rev Genet.* 2016 Nov 23;50:571-594. doi: 10.1146/annurev-genet-120215-035011.
- Skripuletz T, Lindner M, Kotsiari A, Garde N, Fokuhl J, Linsmeier F, Trebst C, Stangel M. Cortical demyelination is prominent in the murine cuprizone model and is strain-dependent. *Am J Pathol.* 2008 Apr;172(4):1053-61. doi: 10.2353/ajpath.2008.070850.
- Skulina C, Schmidt S, Dornmair K, Babbe H, Roers A, Rajewsky K, Wekerle H, Hohlfeld R, Goebels N. Multiple sclerosis: brain-infiltrating CD8+ T cells persist as clonal expansions in the cerebrospinal fluid and blood. *Proc Natl Acad Sci U S A.* 2004 Feb 24;101(8):2428-33. doi: 10.1073/pnas.0308689100.
- Smith KJ, Blakemore WF, McDonald WI. Central remyelination restores secure conduction. *Nature.* 1979 Aug 2;280(5721):395-6. doi: 10.1038/280395a0.
- Snaidero N, Möbius W, Czopka T, Hekking LH, Mathisen C, Verkleij D, Goebbels S, Edgar J, Merkler D, Lyons DA, Nave KA, Simons M. Myelin membrane wrapping of CNS axons by PI(3,4,5)P3-dependent polarized growth at the inner tongue. *Cell.* 2014 Jan 16;156(1-2):277-90. doi: 10.1016/j.cell.2013.11.044.
- Snaidero N, Simons M. The logistics of myelin biogenesis in the central nervous system. *Glia.* 2017 Jul;65(7):1021-1031. doi: 10.1002/glia.23116.
- Snippert HJ, van der Flier LG, Sato T, van Es JH, van den Born M, Kroon-Veenboer C, Barker N, Klein AM, van Rheenen J, Simons BD, Clevers H. Intestinal crypt homeostasis results from neutral competition between symmetrically dividing Lgr5 stem cells. *Cell.* 2010 Oct 1;143(1):134-44. doi: 10.1016/j.cell.2010.09.016.
- Sohal VS, Zhang F, Yizhar O, Deisseroth K. Parvalbumin neurons and gamma rhythms enhance cortical circuit performance. *Nature.* 2009 Jun 4;459(7247):698-702. doi: 10.1038/nature07991.
- Sorbara CD, Wagner NE, Ladwig A, Nikić I, Merkler D, Kleele T, Marinković P, Naumann R, Godinho L, Bareyre FM, Bishop D, Misgeld T, Kerschensteiner M. Pervasive axonal transport deficits in multiple sclerosis models. *Neuron.* 2014 Dec 17;84(6):1183-90. doi: 10.1016/j.neuron.2014.11.006.
- Spassky N, Goujet-Zalc C, Parmantier E, Olivier C, Martinez S, Ivanova A, Ikenaka K, Macklin W, Cerruti I, Zalc B, Thomas JL. Multiple restricted origin of oligodendrocytes. *J Neurosci.* 1998 Oct 15;18(20):8331-43.
- Stadelmann C, Albert M, Wegner C, Brück W. Cortical pathology in multiple sclerosis. *Curr Opin Neurol.* 2008 Jun;21(3):229-34. doi: 10.1097/01.wco.0000318863.65635.9a.
- Stromnes IM, Goverman JM. Active induction of experimental allergic encephalomyelitis. *Nat Protoc.* 2006;1(4):1810-9. doi: 10.1038/nprot.2006.285.
- Stromnes IM, Goverman JM. Passive induction of experimental allergic encephalomyelitis. *Nat Protoc.* 2006;1(4):1952-60. doi: 10.1038/nprot.2006.284.

- Sun LO, Mulinyawe SB, Collins HY, Ibrahim A, Li Q, Simon DJ, Tessier-Lavigne M, Barres BA. Spatiotemporal Control of CNS Myelination by Oligodendrocyte Programmed Cell Death through the TFEB-PUMA Axis. *Cell*. 2018 Dec 13;175(7):1811-1826.e21. doi: 10.1016/j.cell.2018.10.044.
- Svoboda K, Yasuda R. Principles of two-photon excitation microscopy and its applications to neuroscience. *Neuron*. 2006 Jun 15;50(6):823-39. doi: 10.1016/j.neuron.2006.05.019.
- Swire M, Ffrench-Constant C. Seeing Is Believing: Myelin Dynamics in the Adult CNS. *Neuron*. 2018 May 16;98(4):684-686. doi: 10.1016/j.neuron.2018.05.005.
- Syed YA, Zhao C, Mahad D, Möbius W, Altmann F, Foss F, González GA, Sentürk A, Acker-Palmer A, Lubec G, Lilley K, Franklin RJM, Nave KA, Kotter MRN. Antibody-mediated neutralization of myelin-associated EphrinB3 accelerates CNS remyelination. *Acta Neuropathol*. 2016 Feb;131(2):281-298. doi: 10.1007/s00401-015-1521-1.
- Thompson AJ, Banwell BL, Barkhof F, Carroll WM, Coetzee T, Comi G, Correale J, Fazekas F, Filippi M, Freedman MS, Fujihara K, Galetta SL, Hartung HP, Kappos L, Lublin FD, Marrie RA, Miller AE, Miller DH, Montalban X, Mowry EM, Sorensen PS, Tintoré M, Traboulsee AL, Trojano M, Uitdehaag BMJ, Vukusic S, Waubant E, Weinshenker BG, Reingold SC, Cohen JA. Diagnosis of multiple sclerosis: 2017 revisions of the McDonald criteria. *Lancet Neurol*. 2018 Feb;17(2):162-173. doi: 10.1016/S1474-4422(17)30470-2.
- Thorburne SK, Juurlink BH. Low glutathione and high iron govern the susceptibility of oligodendroglial precursors to oxidative stress. *J Neurochem*. 1996 Sep;67(3):1014-22. doi: 10.1046/j.1471-4159.1996.67031014.x.
- Torkildsen O, Brunborg LA, Myhr KM, Bø L. The cuprizone model for demyelination. *Acta Neurol Scand Suppl*. 2008;188:72-6. doi: 10.1111/j.1600-0404.2008.01036.x.
- Trachtenberg JT, Chen BE, Knott GW, Feng G, Sanes JR, Welker E, Svoboda K. Long-term in vivo imaging of experience-dependent synaptic plasticity in adult cortex. *Nature*. 2002 Dec 19-26;420(6917):788-94. doi: 10.1038/nature01273.
- Traka M, Podojil JR, McCarthy DP, Miller SD, Popko B. Oligodendrocyte death results in immune-mediated CNS demyelination. *Nat Neurosci*. 2016 Jan;19(1):65-74. doi: 10.1038/nn.4193.
- Tramacere I, Del Giovane C, Salanti G, D'Amico R, Filippini G. Immunomodulators and immunosuppressants for relapsing-remitting multiple sclerosis: a network meta-analysis. *Cochrane Database Syst Rev*. 2015 Sep 18;(9):CD011381. doi: 10.1002/14651858.CD011381.pub2.
- Trapp BD, Vignos M, Dudman J, Chang A, Fisher E, Staugaitis SM, Battapady H, Mork S, Ontaneda D, Jones SE, Fox RJ, Chen J, Nakamura K, Rudick RA. Cortical neuronal densities and cerebral white matter demyelination in multiple sclerosis: a retrospective study. *Lancet Neurol*. 2018 Oct;17(10):870-884. doi: 10.1016/S1474-4422(18)30245-X.
- Tripathi RB, Clarke LE, Burzomato V, Kessar N, Anderson PN, Attwell D, Richardson WD. Dorsally and ventrally derived oligodendrocytes have similar electrical properties but myelinate preferred tracts. *J Neurosci*. 2011 May 4;31(18):6809-6819. doi: 10.1523/JNEUROSCI.6474-10.2011.

- Tripathi RB, Jackiewicz M, McKenzie IA, Kougioumtzidou E, Grist M, Richardson WD. Remarkable Stability of Myelinating Oligodendrocytes in Mice. *Cell Rep.* 2017 Oct 10;21(2):316-323. doi: 10.1016/j.celrep.2017.09.050.
- Valério-Gomes B, Guimarães DM, Szczupak D, Lent R. The Absolute Number of Oligodendrocytes in the Adult Mouse Brain. *Front Neuroanat.* 2018;12:90. doi: 10.3389/fnana.2018.00090.
- van Horssen J, Brink BP, de Vries HE, van der Valk P, Bø L. The blood-brain barrier in cortical multiple sclerosis lesions. *J Neuropathol Exp Neurol.* 2007 Apr;66(4):321-8. doi: 10.1097/nen.0b013e318040b2de.
- Venturini G. Enzymic activities and sodium, potassium and copper concentrations in mouse brain and liver after cuprizone treatment in vivo. *J Neurochem.* 1973 Nov;21(5):1147-51. doi: 10.1111/j.1471-4159.1973.tb07569.x.
- Vercellino M, Plano F, Votta B, Mutani R, Giordana MT, Cavalla P. Grey matter pathology in multiple sclerosis. *J Neuropathol Exp Neurol.* 2005 Dec;64(12):1101-7. doi: 10.1097/01.jnen.0000190067.20935.42.
- von Jonquieres G, Fröhlich D, Klugmann CB, et al. Recombinant Human Myelin-Associated Glycoprotein Promoter Drives Selective AAV-Mediated Transgene Expression in Oligodendrocytes. *Front Mol Neurosci.* 2016;9:13. Published 2016 Feb 23. doi:10.3389/fnmol.2016.00013
- von Jonquieres G, Fröhlich D, Klugmann CB, Wen X, Harasta AE, Ramkumar R, Spencer ZH, Housley GD, Klugmann M. Recombinant Human Myelin-Associated Glycoprotein Promoter Drives Selective AAV-Mediated Transgene Expression in Oligodendrocytes. *Front Mol Neurosci.* 2016;9:13. doi: 10.3389/fnmol.2016.00013.
- Wang C, Popescu DC, Wu C, Zhu J, Macklin W, Wang Y. In situ fluorescence imaging of myelination. *J Histochem Cytochem.* 2010;58(7):611–621. doi:10.1369/jhc.2010.954842.
- Wegener A, Deboux C, Bachelin C, Frah M, Kerninon C, Seilhean D, Weider M, Wegner M, Nait-Oumesmar B. Gain of Olig2 function in oligodendrocyte progenitors promotes remyelination. *Brain.* 2015 Jan;138(Pt 1):120-35. doi: 10.1093/brain/awu375.
- Weil MT, Möbius W, Winkler A, Ruhwedel T, Wrzos C, Romanelli E, Bennett JL, Enz L, Goebels N, Nave KA, Kerschensteiner M, Schaeren-Wiemers N, Stadelmann C, Simons M. Loss of Myelin Basic Protein Function Triggers Myelin Breakdown in Models of Demyelinating Diseases. *Cell Rep.* 2016 Jul 12;16(2):314-322. doi: 10.1016/j.celrep.2016.06.008.
- Weiner HL. A shift from adaptive to innate immunity: a potential mechanism of disease progression in multiple sclerosis. *J Neurol.* 2008 Mar;255 Suppl 1:3-11. doi: 10.1007/s00415-008-1002-8.
- Wickersham IR, Finke S, Conzelmann KK, Callaway EM. Retrograde neuronal tracing with a deletion-mutant rabies virus. *Nat Methods.* 2007 Jan;4(1):47-9. doi: 10.1038/nmeth999.
- Wilkins A, Chandran S, Compston A. A role for oligodendrocyte-derived IGF-1 in trophic support of cortical neurons. *Glia.* 2001 Oct;36(1):48-57.

- Williams A, Piaton G, Aigrot MS, Belhadi A, Théaudin M, Petermann F, Thomas JL, Zalc B, Lubetzki C. Semaphorin 3A and 3F: key players in myelin repair in multiple sclerosis?. *Brain*. 2007 Oct;130(Pt 10):2554-65. doi: 10.1093/brain/awm202.
- Wolswijk G. Chronic stage multiple sclerosis lesions contain a relatively quiescent population of oligodendrocyte precursor cells. *J Neurosci*. 1998 Jan 15;18(2):601-9.
- Wolswijk G. Oligodendrocyte survival, loss and birth in lesions of chronic-stage multiple sclerosis. *Brain*. 2000 Jan;123 ( Pt 1):105-15. doi: 10.1093/brain/123.1.105.
- Xiao PJ, Li C, Neumann A, Samulski RJ. Quantitative 3D tracing of gene-delivery viral vectors in human cells and animal tissues. *Mol Ther*. 2012 Feb;20(2):317-28. doi: 10.1038/mt.2011.250.
- Xing YL, Röth PT, Stratton JA, Chuang BH, Danne J, Ellis SL, Ng SW, Kilpatrick TJ, Merson TD. Adult neural precursor cells from the subventricular zone contribute significantly to oligodendrocyte regeneration and remyelination. *J Neurosci*. 2014 Oct 15;34(42):14128-46. doi: 10.1523/Jneurosci.3491-13.2014.
- Yang G, Parkhurst CN, Hayes S, Gan WB. Peripheral elevation of TNF- $\alpha$  leads to early synaptic abnormalities in the mouse somatosensory cortex in experimental autoimmune encephalomyelitis. *Proc Natl Acad Sci U S A*. 2013 Jun 18;110(25):10306-11. doi:10.1073/pnas.1222895110.
- Yeung MS, Zdunek S, Bergmann O, Bernard S, Salehpour M, Alkass K, Perl S, Tisdale J, Possnert G, Brundin L, Druid H, Frisé J. Dynamics of oligodendrocyte generation and myelination in the human brain. *Cell*. 2014 Nov 6;159(4):766-74. doi: 10.1016/j.cell.2014.10.011.
- Yeung MSY, Djelloul M, Steiner E, Bernard S, Salehpour M, Possnert G, Brundin L, Frisé J. Dynamics of oligodendrocyte generation in multiple sclerosis. *Nature*. 2019 Feb;566(7745):538-542. doi: 10.1038/s41586-018-0842-3.
- Young KM, Psachoulia K, Tripathi RB, Dunn SJ, Cossell L, Attwell D, Tohyama K, Richardson WD. Oligodendrocyte dynamics in the healthy adult CNS: evidence for myelin remodeling. *Neuron*. 2013 Mar 6;77(5):873-85. doi: 10.1016/j.neuron.2013.01.006.
- Zawadzka M, Rivers LE, Fancy SP, Zhao C, Tripathi R, Jamen F, Young K, Goncharevich A, Pohl H, Rizzi M, Rowitch DH, Kessaris N, Suter U, Richardson WD, Franklin RJ. CNS-resident glial progenitor/stem cells produce Schwann cells as well as oligodendrocytes during repair of CNS demyelination. *Cell Stem Cell*. 2010 Jun 4;6(6):578-90. doi: 10.1016/j.stem.2010.04.002.
- Zhang J, Markovic-Plese S, Lacet B, Raus J, Weiner HL, Hafler DA. Increased frequency of interleukin 2-responsive T cells specific for myelin basic protein and proteolipid protein in peripheral blood and cerebrospinal fluid of patients with multiple sclerosis. *J Exp Med*. 1994 Mar 1;179(3):973-84. doi: 10.1084/jem.179.3.973.
- Zhou Q, Anderson DJ. The bHLH transcription factors OLIG2 and OLIG1 couple neuronal and glial subtype specification. *Cell*. 2002 Apr 5;109(1):61-73. doi: 10.1016/s0092-8674(02)00677-3.
- Zhu X, Hill RA, Dietrich D, Komitova M, Suzuki R, Nishiyama A. Age-dependent fate and lineage restriction of single NG2 cells. *Development*. 2011 Feb;138(4):745-53. doi: 10.1242/dev.047951.

## Acknowledgments

*This PhD thesis is the result of nearly five years of my work and would not have been possible without the support of many people in and outside the Lab. I am deeply grateful to All of you – for the endless help, hours of discussion and not letting me to resign on the way there.*

*First of all, I want to truly thank Prof. Martin Kerschensteiner, who gave me an opportunity to be a part of his outstanding team. Thank you for believing in me and encouraging me to develop my skills. Your passion and dedication to science is highly contagious ☺. Martin, you are the best supervisor I could ever wish for!*

*I extend my particular thanks to the members of my thesis advisory committee; to Prof. Thomas Misgeld for his always constructive comments and sharing his invaluable microscopy knowledge and to Prof. Mikael Simons for his important feedback during our meetings in the past years.*

*My gratitude also goes to the Graduate School of Systemic Neuroscience – I am proud that I could be part of such amazing scientific family. Thank you for giving me an opportunity not only to attend series of courses but also to get to know other graduate students during countless number of social activities.*

*Importantly, I want to say a big “thank you” to the present and former members of Kerschensteiner and Bareyre Labs. Especially, I want to thank Elisa, who taught me almost everything in the lab and guided me at the beginning of my PhD project. Many thanks also to Anja, on whose problem solving skills I could always relay on and Krisitna and Marta for the chatting time during lunches. Obviously ☺, I would like to express my warmest thanks to my Lab-Dream-Team: Paula– for everything, I could easily write a separate page for you! Yi-Heng, for providing the best cakes on Earth, Daniel – for having a premium coffee appointments and Arek, Clara and Minh for being a part of our food tasting team all over Munich restaurants!*

*I am lucky to be surrounded by friends not only in the Lab but also outside, therefore I say “thank you” to my Girls in Warsaw – Natalka, Paulina, Dominika, Asia and Maja – one day ‘I will know things, I will be informed and I will have some time’. Merci Marta for your unconditional acceptance and sisterly love; we have been through a lot and I still think it is just a beginning.*

*I would like to thank my whole family; Mum, Dad – even if I live far from home I always feel your support, Łukasz – I have to be this annoying big sister, but I still love you, Grandma and Grandpa, Babciu i Dziadku dziękuję za beztróskie dzieciństwo, które sobie przypominam jak czuję się przytłoczona [for a carefree childhood that I remember when I feel overwhelmed]. I also want to thank the best Mother and Father in-law for the support, traveling together and every joyful moment. I say thank you to Ewa, Piotr, Marcinek, Ala, Monika, Jaś, Babcia Kazia, Ciocia Marta and many others!*

*Last but not least, I want to say the biggest and the most important thank you to the person, who was always there for me and without whom all of that would not have been possible – my beloved husband Paweł. Dziękuję Kochany!*